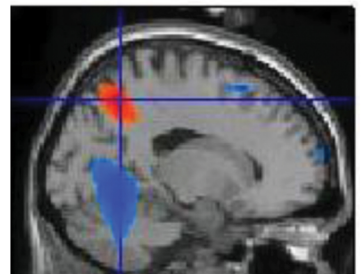
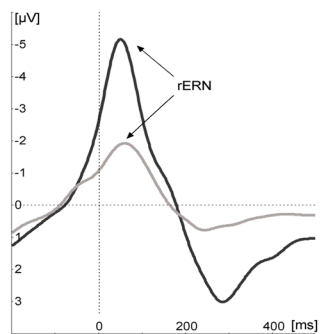
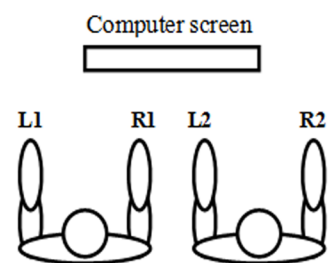
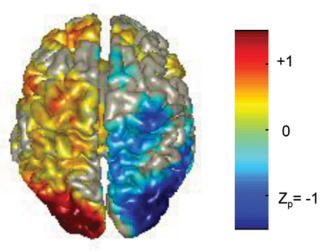


# Nijmegen CNS

Proceedings of the Cognitive Neuroscience Master of  
the Radboud University

**March 2009**  
**Volume 4**



## Table of Contents

---

<b>Editorials</b>	2
<b>Imprint</b>	4
<i>Katinka von Borries</i>	
<b>Error-related learning deficits in individuals with psychopathy: An event-related potentials study</b>	5
<i>Verena Buchholz</i>	
<b>Human oscillatory activity during spatial updating across saccades</b>	16
<i>Vivian Eijssink</i>	
<b>The action of brain-derived neurotrophic factor (BDNF) on gene expression and Ca<sup>2+</sup> signaling in melanotrope cells of <i>Xenopus laevis</i></b>	33
<i>Madelon Riem</i>	
<b>Self-other representation and differentiation in children with autism spectrum disorders</b>	45
<i>Kim Veroude</i>	
<b>Differences in resting state functional connectivity related to learning a new language</b>	59
<b>Abstracts web articles</b>	68
<b>Institutes associated with the Master's Programme in Cognitive Neuroscience</b>	76

---



## Dear readers,

With pride we present the 4th edition of the Proceedings of the Cognitive Neuroscience Master of the Radboud University. During the last four years there was not only an increase in the number of submitted theses, but also a tremendous improvement in the quality and diversity of submissions. With over twenty submitted theses the competition to be published has never been higher. Therefore, the five articles you will find in the issue in front of you is only a selection presenting the high quality research carried out by students of the master programme. Topics range from behavioural patient studies to the neurobiology of frogs, thereby reflecting the large scope of applied research methods.

In the first article von Borries describes results examined with a unique patient group, psychopaths, by means of electrophysiological (EEG) and behavioural measurements. Second, Buchholz looked at the importance of different frequencies within rhythmic brain activity using Magneto-Encephalography (MEG). Eijsink took a neurobiological approach to study the molecular mechanisms behind the ability of a specific frog species to change skin colour in accordance to differently lightened environments.

Riem analysed the behaviour of autistic children, especially with regard to social interactions. Last but not least, Veroude explored changes in brain activity when humans are exposed to a new foreign language via functional Magnetic Resonance Imaging (fMRI).

This issue has been realised by the contribution of a large number of fellow students and senior researchers writing, supporting and reviewing the theses. Furthermore, the board worked hard maintaining the high standard of the Proceedings of the Cognitive Neuroscience Master, a unique peer reviewed scientific journal run exclusively by students.

We hope you will enjoy reading the published articles and appreciate the diversity of neuroscientific research carried out at Radboud University, Nijmegen.

Maren Urner & Han Langeslag  
Editors-in-Chief



## From the Director of the Donders Centre for Cognition

I am delighted to introduce the fourth issue of the Proceedings of the Cognitive Neuroscience Master of Radboud University to anybody and everybody who is interested in up-to-date research in cognitive neuroscience; have a read, here is where it all happens!

Before writing this editorial I looked back at previous issues and came across articles on topics like motor activation during action observation, word associations in bilinguals, modulation of oscillatory neuronal synchrony in the beta band by motor set, oscillatory activity during somatosensory working memory maintenance et cetera. I stood in awe of this colourful and varied palette of cognitive neuroscience topics!

Not surprisingly, most of the articles originally printed in the student journal have found their way into respectable scientific journals like *Cerebral Cortex*, *Cortex*, *Annals of the New York Academy of Sciences*, *Journal of Cognitive Neuroscience*, *Quarterly Journal of Experimental Psychology* et cetera. Better yet, approximately 90% of all our Masters graduates have gone on to pursue PhDs in locations like Berlin, Amsterdam, Bremen and of course, Nijmegen.

From this overview it becomes clear that students in Nijmegen are trained to become the next generation top-scientists in fields like memory, language, perception and action.

Why are *our students* so great? I think a key factor is the stringent criteria we set for applicants to our Research Master Programme. We accept about 50% of all applications, but I dare to say that our selection procedure in and of itself already pre-selects only the most highly-motivated students for us to consider. If you do not mind where you study, then you probably will not end up in Nijmegen. You have to be motivated to come to us and this combination of motivated students and an excellent educational environment does make all the difference.

A second issue I would like to mention is the unique cooperative environment of our programme. Cognitive Neuroscience is an interdisciplinary area which requires students to acquire knowledge from different fields including psychology, biology, biophysics and linguistics. The fact that all these disciplines are housed in a single institute, the recently launched Donders Institute for Brain, Cognition and Behaviour, makes this multidisciplinary adventure truly possible.

I wish all our readers a pleasant journey as they share the great adventures of our authors. I hope that our students will never lose their enthusiasm for studying the mechanisms underlying human behaviour and cognition. There is still so much to discover!

Harold Bekkering  
Director Donders Centre for Cognition

## Nijmegen CNS

*Proceedings of the Cognitive Neuroscience Master of the Radboud University*

---

### Editorial Board

*Editors-in-chief*

**Maren Urner**  
**Han Langeslag**

*Section Editor Perception, Action & Consciousness*

**Maren Urner**

*Assistant Editor Perception, Action & Consciousness*

**Marius Zimmermann**

*Section Editor Neurocognition*

**Han Langeslag**

*Assistant Editor Neurocognition*

**Nathalie Buscher**

*Section Editors Psycholinguistics*

**Merel van Goch**  
**Kevin Lam**

*Layout*

**Christina Bergmann**

*Assistants Layout*

**Gabriela Garrido Rodriguez**  
**Marcella Oonk**  
**Florian Krause**

*Webmaster*

**Ioannis Zalachoras**

*Assistant Webmaster*

**Alina Lartseva**

*Public Relations*

**Marlene Meyer**

*Assistant Public Relations*

**Cecilia Maeder**

---

*Programme Director:* **Ruud Meulenbroek**  
*Senior Advisor:* **Roshan Cools**  
*Cover Image by:* **Christina Bergmann**  
*Journal Logo by:* **Guido Cavalini & Iris Grothe**

*Contact Address:*

**Journal CNS**  
**Radboud University**  
**Postbus 9104**  
**6500 HE Nijmegen**  
**The Netherlands**

# Error-related learning deficits in individuals with psychopathy: An event-related potentials study

Katinka von Borries<sup>1,3</sup>, Inti Brazil<sup>1,3</sup>, Erik Bulten<sup>3</sup>, Jan Buitelaar<sup>1</sup>, Robbert Jan Verkes<sup>1,3</sup>, Ellen de Brujin<sup>2</sup>

<sup>1</sup>Radboud University Nijmegen Medical Centre, Department of Psychiatry, Nijmegen, The Netherlands

<sup>2</sup>Donders Institute for Brain, Cognition and Behaviour, Nijmegen, The Netherlands

<sup>3</sup>Pompefichting, Nijmegen, The Netherlands

Psychopathy is associated with a performance deficit in a variety of stimulus-response and stimulus-reinforcement learning paradigms. We test the hypothesis that failures in error monitoring underlie these learning deficits. We measured electrophysiological correlates of error monitoring (error-related negativity or ERN) during a probabilistic learning task in individuals with psychopathy ( $n=13$ ) and healthy matched control subjects ( $n=18$ ). The task consisted of three graded learning conditions in which the amount of learning was manipulated by varying the degree to which the response was predictive of the value of the feedback (50%, 80%, 100%). Behaviourally, we found impaired learning and diminished accuracy in the group of individuals with psychopathy. Amplitudes of the response ERN were reduced. No differences in the feedback ERN were found. The results are interpreted in terms of a deficit in initial rule learning and subsequent generalization of these rules to new stimuli. Negative feedback is adequately processed at a neural level, but this information is not used to improve behaviour on subsequent trials. As learning is degraded, the process of error detection at the moment of the actual response is diminished. Therefore, the current study demonstrates that disturbed error-monitoring processes play a central role in the often reported learning deficits in individuals with psychopathy.

*Keywords:* Psychopathy, Error Related Negativity, Error Positivity, error monitoring, feedback learning

---

Corresponding author of thesis: A.K.L. von Borries, Pompekliniek, PO Box 31435, 6503 CK Nijmegen, The Netherlands, Email: k.v.borries@pompefichting.nl

## 1. Introduction

Individuals with psychopathy (PP) show little concern about the consequences of their actions for others and themselves. They often show poor planning skills and fail to avoid behaviours which have been punished previously (Hare, 1991). The latter is reflected in, for example, the amount and types of incidents occurring in clinical settings (Hildebrand, 2005) and in their poor response to treatment and the high relapse rates of criminal behaviour (D'Silva, Duggan, & McCarthy, 2004).

In line with these observations, psychopathic individuals show performance deficits in different stimulus-response and stimulus-reinforcement learning situations. Cleckley (1976) found individuals with PP to have a reduced capacity to learn from experience. Other studies have demonstrated abnormally low levels of aversive learning (Flor, Birbaumer, Hermann, Ziegler, & Patrick, 2002), instrumental learning (Mitchell et al., 2006), and avoidance learning (Blair et al, 2004; Newman & Kosson, 1986). The latter is the process by which one learns that omitting a certain response will result in the termination or prevention of an aversive stimulus. Additionally, impairments in decision making to rewarding and punishing stimuli have been found (Blair, Morton, Leonard, & Blair, 2006). Furthermore, studies of post-error slowing - the phenomenon of slower response times (RTs) following erroneous trials - have shown that individuals with PP fail to utilize feedback to alter future responses (Newman, 1987). Finally, recent behavioural data from a probabilistic response-reversal task indicated that individuals with PP showed learning deficits in the reversal phase only, in which the earlier learned reinforcement contingencies were suddenly reversed (Budhani, Richell, & Blair, 2006).

These findings are mainly in line with the Integrated Emotion System interpretation of PP (IES; Blair, 2005; Blair, Mitchell, & Blair, 2005) which assumes orbitofrontal and amygdala abnormalities in PP. The model predicts individuals with PP to show deficits in both stimulus-reinforcement learning involving the amygdala, and in reversal learning served by orbitofrontal areas and basal ganglia (Cools, Clark, Owen, & Robbins, 2002; Clarke, Robbins, & Roberts, 2008). Importantly, the model would not predict deficits in stimulus-response learning, a process that crucially relies on posterior medial frontal cortex (pMFC) including pre-SMA and anterior cingulate (Holroyd & Coles, 2002).

In our view, the above suggests that psychopathic

individuals have difficulties in using negative feedback or error information to adapt their behaviour. Recently, Holroyd and Coles (2002) have proposed the reinforcement-learning (RL) theory of performance monitoring. The RL theory assumes that whenever outcomes are worse than expected, an error signal is conveyed from the basal ganglia to the anterior cingulate cortex (ACC). Upon arrival of this error signal in the ACC, the error-related negativity (ERN), an ERP component measurable at the scalp, is generated (Holroyd & Coles, 2002; Carter et al, 1998; Dehaene, Posner, & Tucker, 1994; Holroyd, Dien, & Coles, 1998). The ERN not only occurs when participants make errors, but also when they receive feedback indicating that they gave an incorrect response (for an overview on ERN and performance monitoring, see Ullsperger & Falkenstien, 2003).

The onset of the ERN coincides with response initiation (rERN; Gehring & Fencsik, 2001), or with the delivery of error feedback (fERN; Holroyd & Coles, 2002). The former reflects internal error signals, the latter external error signals. Studies have demonstrated that the ERN is generated at the first moment in time when the error can be detected (Holroyd & Coles, 2002; Nieuwenhuis et al., 2002). Thus, fERNs are elicited when the negative feedback itself was not or only partly predicted by earlier events. This is for example the case when subjects are still learning the correct stimulus-response mapping by trial and error. However, as the system gradually learns the stimulus-response mapping, subjects will eventually be able to detect errors at the moment of response onset. At an electrophysiological level, this is reflected in the fERN 'propagating back in time' and 'becoming' a rERN. Consequently, while learning takes place, rERN amplitudes increase (Holroyd & Coles, 2002).

Although several studies have investigated learning in individuals with psychopathic traits at a behavioural level, learning deficits in individuals diagnosed with PP have never been studied in relation to the underlying electrophysiological markers of performance or error monitoring. Until now, most studies either focused on individuals with behavioural patterns related to PP (Dikman & Allen, 2000; Hall, Bernat, & Patrick, 2007) or investigated aspects of error monitoring unrelated to learning (Brazil et al., in press; Munro et al., 2007). An investigation of reward and avoidance learning in low socialized individuals (a concept related to PP; Kosson & Newman, 1989) has shown diminished rERN amplitudes only in the punishment condition (Dikman & Allen, 2000). Another study demonstrated

reduced rERN amplitudes in healthy individuals scoring high on externalizing psychopathology, a factor comparable to the behavioural deficit cluster in individuals with PP (Hall, Bernat, & Patrick, 2007). Only two studies investigated the rERN directly in individuals diagnosed with PP. Munro et al. (2007) used a neutral and an emotional choice-reaction task and found reduced rERNs in the emotional task only. Brazil et al. (in press) reported no differences in rERN amplitude between healthy controls and individuals with PP on a neutral task, but did demonstrate problems in the conscious evaluation and signaling of errors. Taken together these studies point towards learning deficits associated with a failure to detect and use internal and external error signals.

The present study was designed to examine the relation between error monitoring and reinforcement learning in individuals diagnosed with PP, by investigating the rERN and fERN, and the relationship between the two while learning progresses. To investigate this, a probabilistic learning task was used in which participants learned stimulus-response mappings based on feedback about their performance (trial and error learning, see e.g. Holroyd & Coles, 2002; Nieuwenhuis et al., 2002; Nieuwenhuis, Nielen, Mol, Hajcak, & Veltman, 2005). A crucial aspect of the task is that the imperative stimulus presented on each trial, differed in the degree to which the response was predictive of the value of the feedback (50%, 80%, 100%).

Compared with healthy controls, we expected individuals with PP to display learning difficulties, reflected behaviourally by reduced accuracy and electrophysiologically by smaller amplitudes of rERN, fERN and a slower propagation in time of the fERN to become a rERN.

<sup>1</sup>The Pompestichting is a “TBS-clinic” located in Nijmegen. TBS is a disposal to be treated on behalf of the state for people who committed serious criminal offences in connection with having a mental disorder. TBS is not a punishment, but an entrustment act for mentally disordered offenders (diminished responsibility). These court orders are an alternative to either long term imprisonment or confinement in psychiatric hospital, with the goal to strike a balance between security, treatment and protection.

<sup>2</sup>Exclusion criteria: Use of alcohol more than 3units/day during in the week preceding the experimental measure and use of alcohol within 24hours of the measurement. Use of cannabis or other illicit drugs within the week before measurement and use of psychotropic medication other than oxazepam during the 5 days before measurement. Use of oxazepam within 12 hours before measurement. Smoking within 3 hours before measurement. History of trauma capitis, visual and auditory disorders, neurological disorders, first degree relative with any relevant neurological disorders

## 2. Methods

### 2.1 Participants

Thirteen male violent offenders between 18 and 55 years of age (Mean age = 37, SD = 9.5) diagnosed with a psychopathy score of  $\geq 26$  according to the Hare Psychopathy Check List-Revised (PCL-R; 1) were selected from the in-patient population of a forensic psychiatric institute in The Netherlands<sup>1</sup> based on available information about clinical status and prior history (Mean PCL-R score = 31, SD = 3.4). Educational level was coded according to the Dutch educational system (1 = primary education, 2 = secondary education, 3 = higher education; mean education patients = 2.8, mean education controls = 2.3). Eighteen healthy male controls matched for age (Mean age = 37, SD = 6.5), educational level and without criminal records or a history of psychiatric disorders were recruited by advertisement. Participants in both groups were checked for drug use and for medical/neurological history<sup>2</sup>. The study was approved by the local Medical Ethical Committee.

### 2.2 Task and procedure

Participants received written information about the experiment and signed an informed consent before being screened for psychiatric exclusion criteria<sup>3</sup> by trained psychologists using the SCID-II (Groenestijn, Akkerhuis, Kupka, Schneider, & Nolen, 1999) and MINI (van Vliet, Leroy, & van Megen, 2000). Participants performed the experimental task and received a financial reimbursement. Additionally, all subjects received the bonus money earned during the experiment.

Participants performed a probabilistic learning task requiring a two-choice-decision to an imperative visual stimulus (Holroyd & Coles, 2002; see Figure 1). Following each response, a feedback stimulus representing reward information was presented informing participants whether their response was correct (green dollar signs: +2 cents), incorrect (red dollar signs: -2 cents) or too late (a cherry; - 4 cents).

The amount of learning possible was manipulated in three different conditions (50%, 80%, and 100%)

<sup>3</sup>Psychiatric exclusion criteria: Depressive Disorder, Bipolar Disorder, Schizophrenia, Schizoaffective Disorder, Schizophreniform Disorder, Delusional and other Psychotic Disorders, Schizoid or Schizotypal PD, Current Alcohol and Substance intoxication, first degree relatives with DSM IV axis I schizophrenia or schizophreniform disorder.

by varying the degree to which the response was predictive of the value of the feedback. For stimuli in the 50% control condition, the value of the feedback was uncorrelated with the selected response, making it impossible to learn stimulus-response mappings. In the 100% and 80% learning conditions, participants could learn the stimulus-response mappings to varying degrees.

In each experimental block, a new set of six different stimuli (for task and stimulus details see Cools et al., 2002) - i.e. two for each condition - was presented. The two stimuli from the 100% condition congruently mapped to either the left or the right response button throughout the entire block. For two stimuli, feedback was delivered randomly (50% condition). Of the two remaining stimuli, one required a left button press in 80% ('80% valid'), but a right button press in 20% of the trials ('80% invalid'), and vice versa for the other stimuli.

Participants started with a bonus of 2.50 Euros and were informed about the status of this bonus at the end of each block. The aim was to infer the financially most beneficial strategy by trial and error. First, participants completed a practice block of 100 trials followed by four experimental blocks of 300 trials each. The six stimuli in each block were presented randomly 50 times each (cf. Holroyd & Coles, 2002; Nieuwenhuis et al., 2002; Nieuwenhuis et al., 2005). Figure 1 depicts details about trial duration, which are identical to previous studies using the same paradigm (Holroyd & Coles, 2002; Nieuwenhuis et al., 2002; Nieuwenhuis et al., 2005).

## 2.2 Electrophysiological recording

A QuickAmp amplifier (Brainproducts, Munich, Germany) with an ActiCap system holding 32 active electrodes was used for data acquisition. EEG was recorded at a sampling rate of 500 Hz and referenced to the left ear, but was re-referenced offline to the average of both ears. Signals were filtered offline using a bandpass filter of .019-20 Hz.

## 2.3 Data analysis

Trials with RTs below 150 ms or above 700 ms were excluded from the analyses (6.06%, SD= 5.44%; Nieuwenhuis et al., 2002; Nieuwenhuis et al., 2005). For the ERP analyses, single-trial epochs were extracted relative to the presentation of the feedback stimulus for the fERNs and relative to the response for the rERN. Single trial EEG signals were corrected for EOG artifacts (Gratton, Coles,

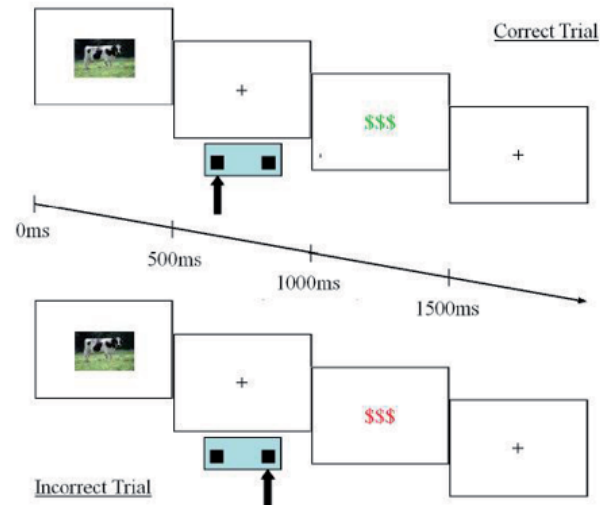


**Figure 1.** Trial details for a correct and incorrect trial: each trial started with the presentation of the imperative stimulus for 500ms, a blank screen with fixation-cross (500ms), the presentation of a feedback stimulus (500ms), and a blank screen with a fixation-cross (500ms). For each imperative stimulus one of two buttons had to be pressed with the index finger (right or left). A response deadline (1000ms) was handled to ensure that participants made enough errors in the 100% easy learning condition.

& Donchin, 1983) and averaged for each subject and condition separately using a 200 ms pre-response/feedback baseline.

In line with previous studies using the current paradigm (Holroyd & Coles, 2002; Nieuwenhuis et al., 2002; Nieuwenhuis et al., 2005), difference waves were created by subtracting the individual averages for correct responses/feedback from the individual averages for incorrect responses/feedback. The rERN amplitude was defined as the most negative peak of the response-locked difference waves at electrode Cz in a window of 0-200 ms (de Brujin, Hulstijn, Verkes, Ruigt, & Sabbe, 2004; de Brujin, Schubotz, & Ullsperger, 2007). For the fERN a window of 200-400ms (Mars, de Brujin, Hulstijn, Milter, & Coles, 2003) on the feedback-locked difference waves was chosen.

Analyses were conducted using repeated measures General Linear Models (GLMs) with Group (psychopaths, controls) as a between subject factor, and the following as possible within subject factors: Block Half (first, second), Block (1, 2, 3, 4), and Condition. Depending on the independent variable entered into the GLM, the number of levels for the factor Condition varied. First, to test the validity of our design, all four levels (100%, 80% valid, 80% invalid, 50%) were entered. Second, to investigate learning processes in more detail the two learning conditions (100% and 80%) were analyzed

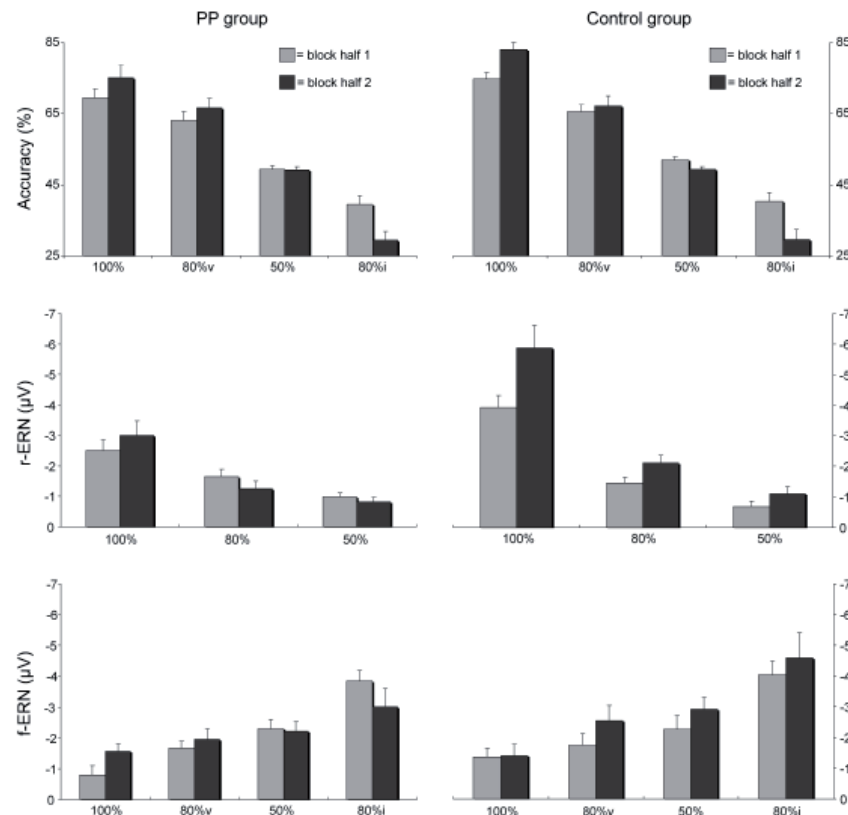


**Figure 2.** Behavioural accuracy for individuals with psychopathy (PP) and controls for each condition and the two block halves. Error bars indicate standard errors. Mean amplitudes for the rERN and fERN, for each of the two groups, each condition and the two block halves. Error bars indicate standard errors.

by means of a repeated measures GLM with Group as a between subject factor and Block Half (first, second) and Condition as within-subject factors. Because any response-locked error-related activity in the 50% condition is known to result from random fluctuations in the EEG signal (Nieuwenhuis et al., 2002; Nieuwenhuis et al., 2005) and learning cannot occur, we excluded this condition from the analyses. Note that for the rERN analyses the factor Condition includes the 80% condition but that no distinction is made between valid and invalid trials, as the actual validity of a trial in the 80% condition is unknown to the subject until the moment of feedback.

### 3. Results

#### 3.1 Behavioural results

Confirming the validity of our design, an overall analysis of Condition (100%, 80% valid, 80% invalid and 50%) revealed that accuracy was highest in the 100% conditions, followed by the 80% valid condition and lowest in the 80% invalid condition [ $F(3, 27) = 86,0, p < 0.001$ ]. Accuracy in the 50% condition was around chance level (see Figure 2 for means and SDs).

An analysis of the two learning conditions (100% and 80% valid) including Block Half revealed

**Table 1.** Mean percentage correct responses (and standard deviations) for each group, condition and both block halves separately and across block halves (total).

Condition	PP Group			Control group		
	Block Half 1	Block Half 2	Total	Block Half 1	Block Half 2	Total
	% Correct (SD)			% Correct (SD)		
100%	69 (9)	75 (13)	72 (11)	74 (7)	82 (8)	79 (8)
80% valid	63 (8)	66 (9)	65 (9)	65 (7)	67 (11)	66 (9)
50%	49 (3)	49 (2)	49 (3)	52 (3)	49 (2)	51 (2)
80% invalid	39 (9)	29 (9)	34 (8)	40 (10)	29 (12)	35 (10)

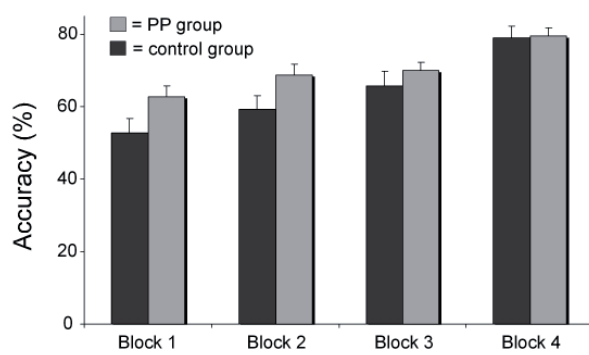


**Figure 3.** Average amount of correct responses (%) in the two learning conditions (100% and 80% valid) for control and psychopathic individuals (PP), separately for each block. Error bars indicate standard errors.

no overall group differences between psychopathic individuals and controls in accuracy [ $F(1, 29) = 1.65, p = 0.209$ ]. However, the significant interaction between Condition and Group showed that, compared to controls, psychopathic subjects were less accurate in the 100% condition, but not in the 80% valid condition [ $F(1, 29) = 6.90, p = 0.014$ ].

Planned comparisons by means of an independent t-test confirmed this (two-tailed t-test 100%:  $t(29) = 2.00, p = 0.055$ ; 80% valid:  $t(29) = 0.449, p = 0.657$ ). Accuracy was higher in the second block half than in the first [ $F(1, 29) = 23.8, p < 0.001$ ] and this was the same for both groups [ $F(1, 29) = 0.03, p = 0.87$ ]. The interaction between Condition and Block Half revealed that the increase in accuracy with block half was more pronounced for the 100% condition (6.9%) than for the 80% valid condition [2.6%;  $F(1, 29) = 14.9, p = 0.001$ ]. Most importantly, the three-way interaction between Condition, Block Half and Group showed a clear trend towards significance [ $F(1, 29) = 4.05, p = 0.054$ ]. Psychopathic individuals show less increase in accuracy between block halves for the 100% condition compared to controls, but a steeper increase between block halves in the 80% valid condition (see Table 1, Figure 2). These effects were confirmed by planned independent t-tests (two-tailed t-test 100% BH1:  $t(29) = 1.74, p = 0.093$ ; 100% BH2:  $t(29) = 2.05, p = 0.049$ ; 80% valid BH1:  $t(29) = 0.804, p = 0.428$ ;  $t(29) = 0.136, p = 0.892$ ).

To examine acquisition and generalization of

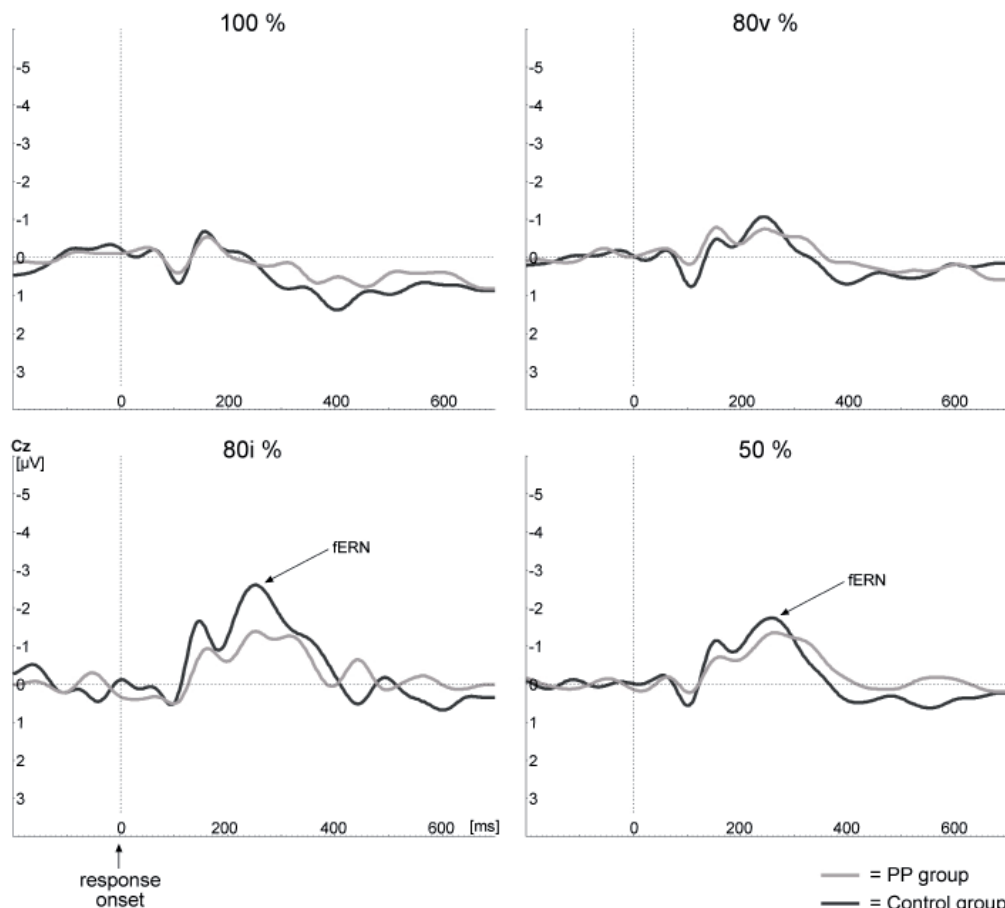


**Figure 4.** Grand average fERN difference waves (incorrect feedback minus correct feedback) for the control group (solid line) and the group of psychopaths (dashed line) for electrode site Cz and all four conditions (100%, 80% valid, 50% and 80% invalid). Feedback was given at 0ms; the fERN is indicated by the arrow.

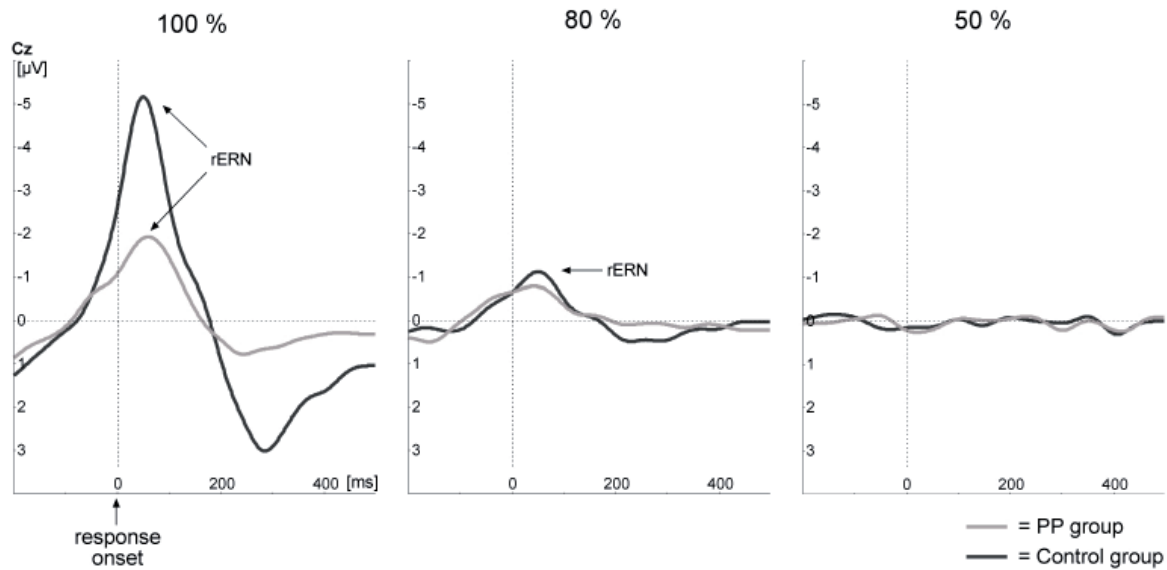


**Figure 5.** Grand average ERP difference waves (incorrect responses minus correct responses) of the 100%, 80%, and the 50% condition for the control group (solid line) and the group of psychopaths (dashed line) at electrode Cz. Responses were given at 0ms.

learning rules in the two learning conditions (100% and 80% valid), we investigated accuracy per block. Accuracy increased with each block [ $F(3, 27) = 37.2$ ,  $p < 0.001$ ; all contrasts:  $p < 0.05$ ] without an interaction between Block and Group [ $F(3, 27) = 1.78$ ,  $p = 0.175$ ]. Planned comparisons showed that individuals with PP had lower accuracy in the first block but not in the fourth [ $F(1, 29) = 5.07$ ,  $p = 0.03$ , see Figure 3].

### 3.2 ERP findings

#### 3.2.1 Feedback ERN (fERN)

In line with previous studies (Nieuwenhuis et al., 2002; Nieuwenhuis et al., 2005), comparison of fERN amplitudes between conditions revealed that amplitudes were largest in the 80% invalid condition, in which negative feedback was most unexpected, followed by the 50% condition, the 80% valid condition, and finally the 100% condition [ $F(3, 27) = 7.97$ ,  $p = 0.001$ , all contrast  $p < 0.05$ , see Figure 2 and Figure 4].

For the fERN in the learning condition (80% valid, 80% invalid and 100%) we did not find any differences in fERN amplitudes between groups or block half nor an interaction between the two (all  $p > .10$ ; see Figure 2 and Figure 4 for mean amplitudes).

#### 3.2.2 Response ERN (rERN)

Comparison of rERN amplitudes revealed a main effect of Condition ( $F(2, 28) = 42.9$ ,  $p < 0.001$ , all contrast  $p \leq 0.003$ ). Amplitudes were largest in the

100% condition, followed by the 80% condition and virtually absent in the 50% condition (see Figures 2 and 5 for mean amplitudes and SDs).

For the rERN in the learning conditions (80% and 100%) we found a main effect for Group [ $F(1, 29) = 7.94$ ,  $p = 0.009$ ] and a main effect for Block Half [ $F(1, 29) = 8.50$ ,  $p = 0.007$ ; see Figures 2 and 5 for means and SDs]. The interaction between Condition and Block Half revealed that amplitudes in the 100% condition were larger in block half 2 than in block half 1, but such a difference was present to a lesser extent or absent in the 80% condition [ $F(1, 29) = 9.03$ ,  $p = 0.005$ ]. This was confirmed by means of a paired t-test (two-tailed rERN100BH1 – rERN100BH2:  $t(30) = 3.383$ ,  $p = 0.002$ ; rERN80BH1 – rERN80BH2:  $t(30) = 1.2$ ,  $p = 0.240$ ).

The significant interaction between Group and Condition showed that while amplitudes in the 80% condition did not differ between groups, subjects with PP displayed smaller amplitudes in the 100% condition [ $F(1, 29) = 11.4$ ,  $p = 0.002$ ]. Most importantly, the interaction between Group and Block Half was significant [ $F(1, 29) = 7.29$ ,  $p = 0.011$ ], indicating that subjects with PP showed a smaller difference in amplitudes between block half 1 and 2 compared with control subjects. Finally, the three-way interaction between Group, Condition and Block Half was not significant [ $F(1, 29) = .285$ ,  $p = 0.598$ ].

## 4. Discussion

In summary, the present study revealed that individuals with PP showed lower accuracy in a probabilistic reinforcement-learning paradigm. Furthermore, diminished response ERN but normal feedback ERN amplitudes were found in psychopathic individuals.

The current study investigated the relation between error monitoring and learning in individuals with psychopathy and healthy controls. At an electrophysiological level, psychopathic individuals showed similar responses as controls to negative external feedback, reflected in the fERN. However, individuals with psychopathy did display problems in using this signal to optimize performance, which was reflected in both the behavioural and the electrophysiological data. Behaviourally, patients showed reduced accuracy in the 100% learning condition, but not in the 80% learning condition. Additionally, the PP group had a lesser increase in accuracy between block halves in the 100% learning condition and the accuracy-rate analyses over blocks demonstrated that individuals with PP had specific problems in the initial learning phase in the first block, but not in the later blocks. Importantly, diminished learning was also associated with the compromised propagation of the fERN to become a rERN. This was mainly reflected in a diminished increase in rERN amplitudes while learning progressed.

### 4.1 Behavioural findings

To master the present task, one has to learn the principle rules, and apply these to new pictures in subsequent blocks. Therefore, accuracy is expected to be low in the initial learning phase (the first block), but to increase rapidly during the generalization process (later blocks). While this pattern was found in both groups, individuals with PP showed diminished accuracy during the first block, suggesting a deficit in initial rule learning. Similar accuracy levels in the last block suggest that psychopathic individuals do reach the same performance level as healthy controls but need more time to do so. As the group of psychopathic subjects has shown abnormal error processing, this slowed learning can only be due to learning based on reward.

Interestingly, differences in accuracy were only found in the easiest learning condition and not for the more difficult 80% condition. One explanation for this finding is based on the so called low-fear hypothesis of psychopathy (Lykken, 1957), which may provide psychopathic individuals with a relative

advantage in the 80% condition compared with the 100% condition. The low-fear hypothesis assumes that psychopathic individuals are insensitive to punishment due to a low level of fear. Achieving highest performance in the 80% condition is done best by reacting as if this was a 100% condition, ignoring the 20% unpredictable trials. Control subjects are less likely to accomplish this, because they are sensitive to punishment and therefore will try to predict and avoid the invalid trials. Due to the random order, this strategy is inappropriate and will hence result in more errors in the 80% valid condition. Psychopathic individuals on the other hand are insensitive to punishment, making it easier to adopt the strategy of ignoring unpredicted negative feedback. Thus, sensitivity to punishment may lead to a less advantageous response style in this more complex condition.

Impaired learning under conditions of reward and punishment in psychopathic individuals has been shown before. For example, psychopathic individuals showed impairments in passive avoidance learning (Blair et al., 2004; Newman & Kossen, 1986) and on a differential reward/punishment task (Blair et al., 2006).

Contrary to the present results, Budhani et al. (2006) found no acquisition problems in psychopathic individuals during the initial learning phase of a probabilistic response-reversal task. However, some important differences between the response-reversal task by Budhani et al. (2006) and the present task exist that may explain the different outcomes. First of all, the current task involved more complex learning material because we included three different reinforcement contingencies, whereas Budhani et al. (2006) included only two. Furthermore, the total stimulus-response associations to be learned in our study was 24. In the response reversal task of Budhani et al. (2006) only six stimuli had to be associated with a response. Additionally, their task had no RT restriction, while the present study employed a deadline of 1000 ms. It seems plausible that these differences in complexity largely account for the divergent findings of the two studies. Moreover, the differences crucially demonstrate that possible impairments in PP may only become evident in more complex situations and might be missed in less demanding tasks.

### 4.2 Electrophysiological findings

According to the RL-theory (Holroyd & Coles, 2002), the fERN elicited by negative feedback is used to update and learn the earliest predictor of

punishment. The error signal is carried to posterior medial frontal cortex (pMFC) where it is used as a reinforcement-learning signal, guiding the adaptation of behaviour. While individuals with PP show intact processing of external negative feedback at an electrophysiological level, they do not seem to optimally use the signal to adapt behaviour and thus show diminished learning. It has been demonstrated that performance of individuals with PP in certain learning paradigms is modulated by reward but not by punishment (Blair et al., 2006). Additionally, it has been shown that low socialized individuals (a trait closely related to PP) show diminished rERNs under conditions of punishment but not reward (Dikman & Allen, 2000). With regard to the current task, individuals with PP might have learned based on reward cues, but not on punishment cues, which leads to diminished learning performance due to the fact that only part of the trials (the rewarded but not punished) are used to adapt behaviour.

An earlier investigation of the rERN in individuals diagnosed with PP outside a learning context (Munro et al, 2007) reported no indications for diminished amplitudes. Even though Brazil et al. (in press) replicated this finding at an electrophysiological level, their behavioural data demonstrated problems in error signaling in individuals with PP. This suggests that rERN amplitudes are only decreased in PP when related to explicit behavioural adaptations or learning processes but not in the context of simple error detection in a neutral task.

### 4.3 Integration

Interestingly, the currently found learning deficits in individuals with PP would not have been predicted by the Integrated Emotion System (IES; Blair, 2005; Blair et al., 2005) hypothesis of PP. The IES interpretation proposes that an underlying amygdala deficit (Blair, 2003; Pridmore, Chambers, & McArthur, 2005; Kiehl et al., 2007) leads to impairments in stimulus-reinforcement associations but not in stimulus-response associations in individuals with PP. However, while the amygdala plays a central role in the first process, other brain structures are involved in the latter process. fMRI and ERP studies using similar paradigms as the current one have demonstrated a crucial role for pMFC (including ACC and preSMA; Holroyd et al., 2004; Mars et al., 2005) and the basal ganglia (Holroyd & Coles, 2002; Ullsperger & von Cramon, 2006) in learning from errors. Currently, the IES interpretation of PP does not include these processes and brain

areas and hence does not allow for any specific predictions to be made. Therefore, we argue that for a better understanding of the learning deficits in PP, neurocognitive models should additionally focus on the areas involved in the processing of internal and external error messages and the subsequent adaptation of behaviour.

In sum, our results indicate that learning from negative feedback is compromised in PP. These results are supported by both behavioural and electrophysiological data. Deviancies in error processing may play a crucial role in the learning deficiencies associated with PP. The IES interpretation of PP predicts deficits in certain forms of learning, but does not relate these deficits to the processing of errors. Furthermore, while the model includes aspects of stimulus- response learning and stimulus-reinforcement learning, aspects of internal and external error processing relevant to trial and error learning are not included. This differentiation between learning processes also fits with a more recent model of decision making proposed by Rushworth, Behrens, Rudebeck and Walton (2007), in which the OFC, ACC and the amygdala are part of a neural network involved in learning, action monitoring and social behaviour. Our data suggests that extending the IES interpretation to include error monitoring and areas involved in error monitoring, as well as more diverse forms of learning, may lead to a broader understanding of the relationship between learning and PP.

## References

- Blair, R.J.R. (2003). Neurobiological basis of psychopathy. *British Journal of Psychiatry*, 182, 5-7.
- Blair, R.J.R.. (2005). Applying a cognitive neuroscience perspective to the disorder of psychopathy. *Development and Psychopathology*, 17, 865-891.
- Blair, R.J.R., Mitchell D.G.H., Leonard, A., Budhani, S., Peschardt, K.S. & Newman, C. (2004). Passive avoidance learning in individuals with psychopathy: modulation by reward but not by punishment. *Personality and Individual Differences*, 37, 1179-1192.
- Blair, R.J.R., Mitchell, D.G.H. & Blair, K.S. (2005). *The Psychopath - Emotion and the Brain*. Oxford, UK: Blackwell Publishing.
- Blair, K.S., Morton, J., Leonard, A. & Blair, R.J.R. (2006). Impaired decision-making on the basis of both reward and punishment information in individuals with psychopathy. *Personality and Individual Differences*, 41, 155-165.

- Brazil, I.A., de Brujin, E.R.A., Bulten, B.H., von Borries, A.K.L., van Lankveld, J.J.M., Buitelaar, J.K. & Verkes, R.J. (in press). Early and Late Components of Error-monitoring in violent offenders with Psychopathy. *Biological Psychiatry*.
- Budhani, S., Richell, R.A. & Blair, R.J.R. (2006). Impaired Reversal but Intact Acquisition: Probabilistic Response Reversal Deficits in Adult Individuals With Psychopathy. *Journal of Abnormal Psychology*, 115, 552-558.
- Carter, C.S., Braver, T.S., Barch, D.M., Botvinick, M.M., Noll, D. & Cohen, J.D. (1998). Anterior Cingulate Cortex, Error Detection, and the Online Monitoring of Performance. *Science*, 28, 747.
- Clarke, H.F., Robbins, T.W., & Roberts, A.C. (2008). Lesions of the medial striatum in monkeys produce perseverative impairments during reversal learning similar to those produced by lesions in the orbitofrontal cortex. *Journal of Neuroscience*, 28, 10972-82.
- Cleckley, H. (1976). *The Mask of sanity*, 5th edition, Mosby, St. Louis
- Cools, R., Clark, L., Owen, A.M. & Robbins, T.W. (2002). Defining the neural mechanisms of probabilistic reversal learning using event related functional magnetic resonance imaging. *Journal of Neuroscience*, 22, 4563-4562.
- de Brujin, E.R.A., Hulstijn, W., Verkes, R.J., Ruigt, Gé S.F., & Sabbe, B.G.C. (2004). Drug-induced stimulation and suppression of action monitoring in healthy volunteers. *Psychopharmacology*, 177, 151-160.
- de Brujin, E., Schubotz, R.U. & Ullsperger, M. (2007). An event-related potential study on the observation of erroneous everyday actions. *Cognitive, Affective, & Behavioral Neuroscience*, 4, 278-285.
- Dehaene, S., Posner, M.I. & Tucker, D.M. (1994). Localization of a neural system for error detection and compensation. *Psychological Science*, 5, 303-305.
- Dikman, Z.A. & Allen, J.J.B. (2000). Error monitoring during reward and avoidance learning in high- and low-socialized individuals. *Psychophysiology*, 27, 43-54.
- D'Silva, K., Duggan, C. & McCarthy, L. (2004). Does treatment really make psychopaths worse? A review of evidence. *Journal of personality disorders*, 18, 163-177.
- Flor, H., Birbaumer, N., Hermann, C., Ziegler, S. & Patrick, C.J. (2002). Aversive pavlovian conditioning in psychopath: peripheral and central correlates. *Psychophysiology*, 39, 505-518.
- Gehring, W.J. & Fencsik, D.E. (2001). Function of the Medial Frontal Cortex in the Processing of Conflict and Errors. *Journal of Neuroscience*, 21, 9430-9437
- Gratton, G., Coles, M.G.H. & Donchin, E. (1983). A new Method for off-line removal of ocular artifacts. *Electroencephalography and Clinical Neurophysiology*, 55, 468-484.
- Groenestijn, M.A.C., Akkerhuis, G.W., Kupka, R.W., Schneider, N. & Nolen, W.A. (1999). Gestureerde klinisch interview voor de vaststelling van DSM-IV As-I stoornissen (SCID-I).
- Hall, J.R., Bernat, E.M. & Patrick, C.J. (2007). Externalizing psychopathology and the error-related Negativity. *Psychological Science*, 18, 326-333.
- Hare, R. (1991). *The Hare PSychopathy Checklist – Revised*. Toronto: Multi-Health Systems.
- Hildebrand, M. (2005). Samenvatting onderzoeksrapport: Onttrekkingen tijdens verlof, ontvluchtingen en recidives tijdens de tbs-behandeling in de jaren 2000-2005. Expertisecentrum Forensische Psychiatrie.
- Holroyd, C.B. & Coles, M.G.H. (2002). The neural basis of human error processing: reinforcement learning, dopamine, and the error-related negativity. *Psychological Review*, 109, 679-709.
- Holroyd, C.B., Dien, J. & Coles, M.G.H. (1998). Error-related scalp potentials elicited by hand and foot movements: evidence for an output-independent error-processing system in humans. *Neuroscience Letters*, 242, 65-68.
- Holroyd, C.B., Nieuwenhuis, S., Yeung, N., Nystrom, L., Mars, R.B., Coles, M.G.H. & Cohen, J.D. (2004). Dorsal anterior cingulated cortex shows fMRI response to internal and external error signals. *Nature Neuroscience*, 7, 497-498.
- Kiehl, K.A., Smith, A.M., Hare, R.D., Forster, B.B., Brink, J. & Liddle, P.F. (2001). Limbic abnormalities in affective processing by criminal psychopaths as revealed by functional magnetic resonance imaging. *Biological Psychiatry*, 50, 677-684.
- Kosson, D.S. & Newman, J.P. (1989). Socialization and attentional deficits under focusing and divided attention conditions. *Journal of Personality and Social Psychology*, 57, 175-184.
- Lykken, D.T. (1957). A study of anxiety in the sociopathic personality. *Journal of Abnormal and Social Psychology*, 55, 6-10.
- Mars, R.B., Coles, M.G.H., Grol, M.J., Holroyd, C.B., Nieuwenhuis, S., Hulstijn, W. & Toni, I. (2005). Neural dynamics of error processing in medial frontal cortex. *Neuroimage*, 29, 1007-1013.
- Mars, R.B., de Brujin, E.R.A., Hulstijn, W., Milter, W.H.R. & Coles, M.G.H. (2003). What if I told you: "You were wrong"? Brain potentials and behavioral adjustments elicited by feedback in a time-estimation task. In M. Ullsperger & M. Falkenstein (Eds.), *Errors, conflict and the Brain. Current Opinions on Performance Monitoring*. Sächsisches Digitaldruck Zentrum gmbh, Dresden, Germany.
- Mitchell, D.G.V., Fine, C., Richell, R.A., Newman, C., Lumsden, J., Blair, K.S. & Blair, R.J.R. (2006). Instrumental learning and relearning in individuals with psychopathy and in patients with lesions involving the amygdala or orbitofrontal cortex. *Neuropsychology*, 20, 280-289.
- Munro, G.E., Dywan, J., Harris, G.T., McKee, S., Unsal, A. & Segalowitz, S.J. (2007). ERN varies with degree of psychopathy in an emotion discrimination task. *Biological Psychiatry*, 76, 31-42.
- Newman, J.P. (1987). Reaction to punishment in extraverts and psychopaths: implications for the impulsive behavior of disinhibited individuals. *Journal of*

- Research in Personality 21, 464–480.
- Newman, J. P. & Kossen, D. S. (1986). Passive avoidance learning in psychopathic and nonpsychopathic offenders. *Journal of Abnormal Psychology*, 95, 252-256.
- Nieuwenhuis, S., Nielen, M.M., Mol, N., Hajcak, G. & Veltman, D.J. (2005). Performance monitoring in obsessive-compulsive disorder. *Psychiatry research* 134, 111-122.
- Nieuwenhuis, S., Ridderinkhof, K.R., Talsma, D., Coles, M.G.H., Holroyd, C.B., Kok, A. & van der Molen, M.W. (2002). A computational account of altered error processing in older age: Dopamine and the error-related negativity. *Cognitive, Affective, & Behavioral Neuroscience*, 2, 19-36.
- Pridmore, S., Chambers, A. & McArthur, M. (2005). Neuroimaging in psychopathy. *Australian and New Zealand journal of psychiatry*, 39, 856-865
- Rushworth, M.F.S., Behrens, T.E.J., Rudebeck, P.H. & Walton, M.E. (2007). Contrasting roles for cingulate and orbitofrontal cortex in decisions and social behavior. *Trends in Cognitive Sciences*, 11, 168-176.
- Ullsperger, M., & Falkenstien M. (2003). MPI special Issue: Errors, Conflict, and the Brain. Current Opinions on Performance Monitoring. Dresden, Germany: Sächsisches Digitaldruck Zentrum GmbH
- Ullsperger, M. & von Cramon, D.Y. (2006). The role of intact frontostriatal circuits in error processing. *Journal of Cognitive Neuroscience*. 18, 651-664.
- van Vliet, I.M. , Leroy, H., & van Megen, H.J.G.M. (2000). M.I.N.I. Internationaal Neuropsychiatrisch Interview, Nederlandse Versie 5.0.0.

# **Human oscillatory activity during spatial updating across saccades**

Verena Buchholz<sup>1</sup>, Jurrian Van Der Werf<sup>1</sup>, Ole Jensen <sup>2</sup>, Pascal Fries<sup>1,2</sup>, Pieter Medendorp<sup>1</sup>

<sup>1</sup>Donders Institute for Brain, Cognition and Behaviour, Nijmegen, The Netherlands

<sup>2</sup>Department of Biophysics, Radboud University Nijmegen, Nijmegen, The Netherlands

Both single-unit studies in macaques and neuroimaging studies in humans indicate that the posterior parietal cortex encodes spatial working memories in dynamic, gaze-centered maps, such that each eye movement causes an internal updating of these representations. We applied MagnetoEncephaloGraphy (MEG) to investigate the dynamics of human parietal oscillatory activity in this updating process. In the experiments, participants had to remember the location of a visual goal, briefly presented to the left or right relative to a central fixation point. After a delay, participants made a saccade to a new fixation point. Then, following a second delay, they saccaded to the remembered goal location. We examined changes in spectral power during the two delay periods, excluding error trials based on EOG eye tracking. After presentation of the goal target, we observed a transient broad-band gamma band power (40-120 Hz) increase in the hemisphere contralateral to the goal location in parietal sensors. After the change of fixation point, that is during the second delay period, we found a more sustained narrow gamma band activity (55-85 Hz) in the hemisphere contralateral to the saccade goal, independent of the initial hemifield of the stimulus. The neuronal synchronization in the gamma band seems to reflect an updated eye-centered goal representation of the upcoming saccade. In the alpha band power (8-12 Hz), we found a sustained response in both delays that dynamically remapped with the change of fixation point. During the first delay period, the power increase was sustained in the hemisphere ipsilateral to the goal location. But when the remembered goal location reversed sides relative to the fixation point, increased power switched to the other hemisphere. The dynamic synchronization of the alpha band during spatial updating is consistent with an eye-centered mechanism, disengaging the hemisphere that does not encode the goal.

*Key words:* human, MEG, oscillations, parietal cortex, saccade, spatial updating, sensorimotor

---

Corresponding author of thesis: V.N. Buchholz, Donders Institute for Brain, Cognition and Behaviour, Radboud University Nijmegen, The Netherlands, Email: verena.buchholz@fcdonders.ru.nl

## 1. Introduction

Sensory information enters the brain in its natural reference frame. In vision, this reference frame is the retina and locations of objects are reported in eye-centered coordinates. These coordinates however, become obsolete as soon as the eyes move. Yet, despite movement of the eyes, the brain manages to keep track of object location by a process called spatial updating. This process is thought to operate by recomputing the object locations in a retinal frame during eye movements (Duhamel et al., 1992; Batista et al., 1999), using extraretinal information (Genovesio & Ferraina, 2004; Wurtz, 2008). As such it is an important mechanism to preserve perceptual stability as well as spatial constancy in motor control.

The posterior parietal cortex (PPC) is assumed to be a key structure in the processing and storing of spatial information in both humans and monkeys. In the monkey, the PPC is anatomically segregated into regions specialized to code space for different effectors. A well-studied region is lateral intraparietal area (LIP), which encodes target location for saccades (Gnadt & Andersen, 1988; Barash et al., 1991). LIP neurons have retinotopic receptive fields and are organized in a topographic fashion, with a preference for contralateral space (Blatt et al., 1990). Neurons in this area also show movement-related responses; movement fields generally coincide with the sensory receptive fields (Mazzoni et al., 1996). In delayed-saccade tasks, many LIP neurons also show memory-related activity (Gnadt & Andersen, 1988). There is ongoing debate whether this memory-related activity is associated with a retrospective stimulus representation or with a goal representation of the saccade (for review see Colby & Goldberg, 1999; Andersen & Buneo, 2002; Gottlieb, 2002).

Gnadt et al. (1988) trained monkeys to look from an extinguished fixation spot towards a briefly flashed target and then back towards the remembered fixation position in complete darkness (double-step saccade paradigm as defined by Mays & Sparks, 1980). They identified neurons that increased their firing rate after the monkey achieved the first target and planned the return saccade to the remembered fixation spot, the location of which was in their response fields. Because these neurons never had a stimulus physically presented in their receptive field, the response of these neurons must have been a remapped response. That is, the representation of the fixation stimulus is transferred from the group of neurons that was stimulated by it, to the group

of neurons that have their receptive fields at that location after the first saccade. Gnadt and Andersen (1988) interpreted this activity pattern as memory-related motor activity. In later years, Duhamel et al. (1992) showed that it was not necessary to make an eye movement for this remapping to occur. They found many neurons to shift their receptive fields already before the initiation of a saccade that would bring a stationary stimulus into the RF. They referred to this updated activity as predictive remapping, to be mediated by a copy of the actual motor command (Sommer & Wurtz, 2008), and regarded it as a mechanism for maintaining perceptual stability across eye movements. Recently it was discovered that also extrastriate areas V2, V3, and V3A, remap activity across saccades, but the proportion of neurons in those regions showing this behaviour is smaller than in LIP and the latency increases relative to saccade onset (Nakamura, 2002). Also more motor-related areas such as the frontal eye fields (FEF) (Umeno & Goldberg, 1997, 2001; Sommer & Wurtz, 2008) and the superior colliculus (SC) (Walker et al., 1995) have been shown to remap activity across saccades.

In humans, an area within the intraparietal sulcus (IPS) has recently been proposed as the homologue of monkey area LIP. Functional magnetic resonance imaging (fMRI) has provided evidence for contralateral, retinotopic mapping of remembered visual targets in the IPS (Sereno et al., 2001). It was further found that when eye movements reverse the remembered horizontal target location relative to the gaze fixation point, this region exchanges activity across the two hemispheres, which provides evidence for eye-centered updating (Medendorp et al., 2003; Merriam et al., 2003). Recently it was shown that transcranial magnetic stimulation (TMS) on the IPS can disrupt the process of spatial updating during a double-step saccade task. This suggests that human IPS is actually implementing the mechanism of updating across saccades (Van Donkelaar & Muri, 2002). As in the monkey, remapping of activity has also been shown in earlier visual areas, with decreasing strength towards areas lower in the hierarchy from V3A, to V4 and down to V2/V1 (Merriam et al., 2007).

Memory activity in delayed-response studies is defined as sustained activity during the delay, but which mechanism is involved in storing and updating the neuronal representation? Oscillatory activity at the population level is considered a neuronal basis for maintenance of working memory representations (Tallon-Baudry et al., 1998; Jensen et al., 2002; Pesaran et al., 2002; Howard et al., 2003; Jensen et al., 2007; Jokisch & Jensen, 2007). Gamma band

synchronization (30-90Hz) is associated with active stimulus maintenance during short-term spatial memory in both humans and monkeys (Tallon-Baudry & Bertrand, 1999; Kaiser & Lutzenberger, 2001; Pesaran et al., 2002; Tallon-Baudry et al., 2004; Kaiser & Lutzenberger, 2005; Scherberger et al., 2005; Jensen et al., 2007; Jokisch & Jensen, 2007; Kaiser et al., 2008b). Alpha band synchronization (8 -12 Hz) has been linked to inhibition of areas disengaged in a certain task (Sauseng et al., 2005a; Jokisch and Jensen, 2007; Klimesch et al., 2007; Medendorp et al., 2007; Rihs et al., 2007). Conversely, alpha band desynchronization has been related to increased processing or excitability of the respective areas (Sauseng et al., 2005a; Sauseng et al., 2005b; Yamagishi et al., 2005; Thut et al., 2006; Romei et al., 2008).

Only few studies have reported oscillatory activity during saccade tasks (Okada & Salenius, 1998; Lachaux et al., 2006). Pesaran et al. (2002) found directionally-selective gamma band power increases (25-90Hz) in monkey area LIP during the memory period in a delayed-saccade task. In humans, Medendorp et al. (2007) observed a directionally-selective synchronization in the gamma band (60-90Hz) in parietal areas during a double-step saccade task. In addition, alpha band suppression (8-12Hz) was reported in parieto-occipital cortex. Recently, Van Der Werf et al. (2008) exploited a delayed anti-saccade paradigm to distinguish sensory and motor components in oscillatory activity. Alpha band activity showed dynamics more related to the processing of the stimulus, with only modest selectivity for the goal of the saccade. They also found an increase in gamma band activity in response to stimulus presentation in the contralateral hemifield in posterior parietal cortex which remapped to the hemisphere contralateral to the direction of the saccade goal during the delay period.

In this study, we address the role of oscillatory activity in the coding and updating of spatial information across saccades. We investigate the dynamics of oscillatory activity during a delayed double saccade task, where the stimulus representation must be remapped based on the metrics of the intervening saccade to provide a veridical motor goal representation for the second saccade. We exploit the directional-selectivity of two frequency bands of interest (alpha and gamma range) to compare conditions in which the stimulus representation must be remapped between hemispheres versus conditions in which the stimulus representation remains within one hemisphere.

## 2. Methods

### 2.1 Participants

Twenty-two naïve participants (7 female/15 male; mean age 26.5 years; 4 left handed/18 right handed), free of any peripheral or central disorders (by self-report), volunteered to participate in the study. All participants provided written consent according to guidelines of the local ethics committee (CMO Committee on Research Involving Humans subjects, region Arnhem-Nijmegen, the Netherlands).

### 2.2 MEG recordings

Participants were sitting in the MEG system within a magnetically shielded room. The stimulus screen was positioned 40 cm in front of them and participants were instructed to sit comfortable without moving. An LCD video projector (SANYO PROXTRA multiverse, 60Hz refreshrate) back-projected the stimuli onto the screen using two front silvered mirrors. MEG data was recorded continuously using a whole head system with 275 axial gradiometers (CTF MEG TM Systems Inc., Port Coquitlam, Canada). Head position was continuously measured using localization coils fixed at anatomical landmarks (nasion; left/right ear). Electrooculogram (EOG) and electrocardiogram was recorded with electrodes placed below and above the left eye, the bilateral canthi, above the right clavicula and under the last left false rib. Impedance was kept below 5 and 50 kΩ, respectively. During the experiment, the EOG recordings were continuously inspected to ensure that participants were vigilant and correctly performing the task. All signals were low passed filtered at 300 Hz, sampled at 1200 Hz. The EOG signal was calibrated off-line, based on the refixations. For each participant, a full anatomical MR image was acquired using a standard inversion prepared 3D T1 weighted scan sequence (FA=15 deg; voxel size: 1.0 mm in-plane, 256 x 256, 164 slices, TR=0.76 s; TE=5.3 ms). A 1.5 T whole-body scanner (Siemens, Erlangen, Germany) was used to record the anatomical MRIs, with reference markers at the same locations as during the MEG recording, to allow alignment of the individual MEG and MRI data.

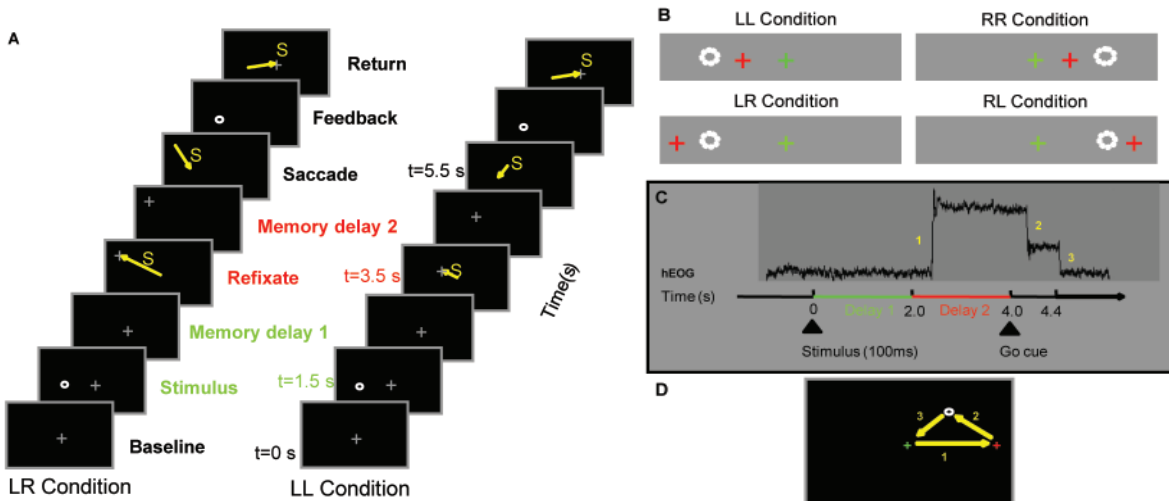
### 2.3 Experimental paradigm

Figure 1 describes the experimental paradigm. In figure 1a the trial timing is depicted. After a 1.5 s

baseline period with a central white fixation cross, a brief peripheral white dot was presented for 100 ms while the fixation cross remained, indicating the stimulus location and the start of delay 1. For the rest of delay 1, fixation was straight ahead. Then, at time  $t=2$  s, the fixation cross jumped to a new location, indicating the start of delay 2. The participant had to saccade to the new fixation cross (intervening saccade) and maintain gaze at this location for the rest of the 2 s delay. At the moment the fixation cross disappeared, the participant had to saccade to the remembered stimulus location. A blue dot was presented 400 ms later at the correct location for 300 ms, to provide the participants with feedback. Subsequently, the reappearance of the central fixation cross indicated the start of a new trial. The complete trial lasted for 6.2 s.

Delay times were chosen to maximize the number of trials (600) within one hour MEG recording time and optimize statistical power. Between blocks of trials (20 blocks of 30 trials), there was a brief rest of 10 s, during which participants could freely move their eyes. The eccentricity of the stimulus was jittered ( $\pm 2$  degrees) around either 3 or 9 degrees horizontal visual angle. The eccentricity of the refixation cross was jittered ( $\pm 2$  degrees) around either 3, 9, or 15 degrees horizontal angle. The amplitude of the saccade towards the remembered location was fixed for all conditions to 6 degrees ( $\pm 2$  degrees) horizontal visual angle to

avoid confounding factors during memory delay 2. Vertical visual angle was randomized between 0 and 2 degrees in both directions. The side of refixation for the RR and LL conditions was randomized, as were conditions, such that participants could not anticipate the direction of the refixation based on the stimulus location. Figure 1b depicts the four main conditions, two with stimulus location remaining in the same hemifield after the intervening saccade (RR and LL) and two for stimulus locations changing hemifields, due to the gaze change (RL and LR). The first letter of the condition name indicates the hemifield of the stimulus presentation, whereas the second letter indicates the side of the remembered stimulus location relative to fixation during delay 2 (hence stimulus direction in updated eye-centered coordinates). In the RL condition for example, the stimulus was presented in the right hemifield (RL) and the refixation saccade was also to the right, with a larger horizontal visual angle, shifting the remembered stimulus location to the left (RL) relative to the new fixation point. Figure 1c depicts a scheme of a typical horizontal eye-movement trace recorded during a trial in the RL condition. The numbers indicate the saccades that were made during the trial and the colours green and red on the time-line indicate delay 1 (with stimulus) and delay 2, respectively. Figure 1d depicts the respective saccades involved in that trial.



**Figure 1. A.** Trial timing. After a 1.5 s baseline period, a brief peripheral dot was presented for 100 ms. After a delay of 2 s, the fixation cross changed location for another 2 s. When it disappeared at time  $t=4$  s, the participant had to saccade toward the remembered location of the stimulus. **B.** Design. The four conditions, with fixation during delay 1 indicated by a green fixation cross and fixation during delay 2 indicated by red. In delay two, the stimulus remains either in the same hemifield (LL and RR), or changes hemifield (LR and RL), due to the new gaze direction. Note that during delay 1, stimulation is the same for conditions depicted in the upper and lower panel. **C.** A typical eye-movement-trace for the RL condition. **D.** The sequence of saccades for that respective trial.

## 2.4 Behavioural analysis

Electrooculographic (EOG) data from each subject was inspected online to ensure high vigilance levels and correct performance of the task. As shown in Figure 1c by a typical horizontal EOG trace, the participant maintains fixation during the first delay and makes an eye-movement to the new fixation cross, following the appearance of it at time  $t=2\text{s}$ . The participant maintains fixation again, until he makes an eye-movement toward the remembered stimulus location following fixation cross extinction ( $t=4\text{s}$ ), stops briefly at the remembered location waiting for feedback ( $t=4.4\text{s}$ ) and returns to the center fixation cross. Trials in which participants either broke fixation, blinked during a trial or moved too early were excluded. Moreover, based on EOG calibration, trials were excluded in which the participant did not saccade into the correct direction 50 ms after feedback onset or did not show stable fixation again at time  $t=2.65\text{s}$ . On average  $442 \pm 84$  (SD) trials per participant were accepted for further analysis. Reaction times for the final saccade did not differ between conditions of interhemispheric (RL+LR) versus intrahemispheric (RR+LL) remapping ( $p>0.05$ ), whereas reaction times for the intervening saccades did differ slightly across conditions RR/LL and RL/LR with a mean difference of 30 ms. The latter effects were ignored, because frequency and source analysis were only conducted on data from time  $t=2.85\text{s}$  onwards, with all saccades terminated at least at time  $t=2.65\text{s}$ .

Open source fieldtrip software (<http://www.ru.nl/fcdonders/fieldtrip>) was used to analyze the data, which is a Matlab toolbox developed at the F.C.Donders Centre for Cognitive Neuroimaging. After rejecting trials based on EOG recordings, data segments that contained muscle activity or jump artifacts in the SQUIDS were excluded using automatic artifact rejection routines. A planar gradient estimate was calculated from the axial gradiometer signals using information from neighbouring sensors (Bastiaansen and Knosche, 2000) to simplify the interpretation of the sensor-level data, as the maximal signal is located above the source with planar gradients (Hämäläinen et al., 1993). The sum of the calculated horizontal and vertical planar MEG field gradients was computed to obtain the power at each virtual planar gradiometer location. Time-frequency representations (TFR), estimating time-varying power values were computed based on a Fourier Approach. To optimize time-frequency resolution, we analyzed the two frequency ranges of interest separately (2-30 Hz and 40-100 Hz). For the lower

frequencies a fixed time window of 0.5s and sliding Hanning taper window was applied, resulting in a spectral smoothing of approximately 3 Hz. For the higher frequencies a multitaper approach (Percival et al., 1993) was applied, optimizing sensitivity for specific high frequency power modulation. This resulted in a fixed window length of 0.4s and 11 orthogonal Slepian tapers, with an estimated spectral smoothing of 15 Hz.

To investigate task-related changes in power in these two frequency ranges, we transformed the data into t-scores, reflecting power changes relative to baseline. T-scores were obtained by computing power over a baseline time-window centered 0.3s prior to stimulus presentation (0.5s for lower and 0.4s for higher frequencies). Using a jackknife procedure (Efron & Tibshirani, 1993) to determine the variance in power, we expressed the difference in power between the period of interest (4s following stimulus onset) and the baseline as a t-score for each participant and condition. We transformed the t-scores into z-scores to obtain values normalized for intrasubject variance (as in Medendorp et al. 2007) and averaged the resulting scores ( $Z_{\text{group}} = 1/N \sum z_i$ ; with  $z_i$  being the score of the  $i$ -th participant and  $N$  the number of subjects). Because these z-values cannot be interpreted as a statistical test outcome and only provide the input unit for the second level analysis, we call them Pseudo-Z (abbreviated  $Z_p$ ) to avoid confusion. The directional selectivity in the various frequency bands was examined by comparing these power values for stimulus locations to the right and left relative to current gaze direction. To select a group of sensors of interest for the higher frequencies, we applied a cluster-based randomization test statistic (Maris & Oostenveld, 2007), averaging over time  $t=0.1-0.6$  (initial sensory response as in Van Der Werf et al. 2008) and frequency (40-100 Hz). This analysis was done contrasting all conditions [(RR+RL)-(LL+LR)] and subtracting left minus right hemisphere and resulted in a sensor choice of 6 sensors that showed a strong response to visual stimuli. Within these channels of interest, a frequency band of interest was defined by using a cluster-based randomization test statistic on the frequency range of 40-100 Hz, for the two delays separately. For statistical analysis of the second memory delay ( $t=2.85-3.8\text{s}$  for higher frequencies;  $2.9-3.75\text{s}$  for lower frequencies), the same procedure was applied, but contrasting conditions in which the stimulus location was in the same hemifield during delay 2 [(RR+LR)-(LL+RL)] and subtracting hemispheres. For lower frequencies, the analysis was performed averaging over the

same sensors, constrained to a center frequency of 10 Hz and averaged over each delay period. With the predefined channel-frequency-time window of interest, a single pseudo z-score was computed for each participant, representing the contrast between conditions. Statistical significance was then tested by means of a non-parametric permutation test across participants. First, the significance at the group level was assessed by pooling these zp-scores over all participants and testing them against the standard normal distribution, which corresponds to a fixed effects statistic. To be able to make statistical inferences about the population, we tested the significance of this group level statistic by a randomizing procedure. Each individual zp-score was multiplied by +1 or -1, which corresponds to permutation of the original conditions in that participant. A randomization distribution was obtained by repeating this procedure 400 times. The proportion of values constituting the lower 5 percent of the randomization distribution defined the Monte Carlo significance threshold (Nichols & Holmes, 2002; Maris & Oostenveld, 2007).

To localize the neural sources of the spectral components of interest, an adaptive spatial filtering (or beamforming) technique was applied (Dynamic Imaging of Coherent Sources (DICS), Gross et al., 2001; Liljestrom et al., 2005). Each participant's brain volume was divided into an individually spaced three-dimensional grid using SPM2 (<http://www.fil.ion.ucl.ac.uk/spm>), with each location corresponding to a location in the regular 1cm grid based on a brain template (International Consortium for Brain Mapping; Montreal Neurological Institute, Montreal, Canada). Averaging over participants later on reduces the potential influence of different grid spacing per participant, as averaged locations will approach MNI grid locations. The filter was then computed from forward models with respect to dipolar sources at each individual grid point (the leadfield matrix) and the cross spectral density between all combinations of sensors at the frequency of interest (Nolte et al., 2003). This procedure has the advantage that it neither requires normalization nor interpolation. Furthermore, there is no assumption about smoothness being made. The computed spatial filter fully passes activity from the location of interest (the individual grid points), while attenuating activity from all other locations (Van Veen et al., 1997). The leadfield matrix was computed by using a single-spheric volume conductor model (Huang et al., 1999). As for the sensor data, we computed the power changes at the selected frequency bands and

calculated the z-statistic to express the power effects across participants at the source level.

### 3. Results

We investigated the changes in oscillatory activity during the processing of spatial constancy across saccades. In our tests, participants produced intervening saccades between seeing a goal target and generating an eye movement toward its remembered location. While the goal target remained stable relative to the head (and body), the remembered location of this target must be updated during the intervening saccade in order to correctly code its new location in eye-centered coordinates. In the latter case, the paradigm entailed four different conditions as to the location of the goal before and after the intervening saccade: either it remained in the same hemifield (LL and RR conditions) or it shifted into the opposite hemifield (LR and RL conditions). We exploited the directional selectivity of power in the gamma and alpha band reported during delayed saccade tasks (Medendorp et al., 2007; Van Der Werf et al., 2008) to discriminate changes in oscillatory activity in relation to eye-centered updating of the goal across hemispheres as opposed to updating within a single hemisphere.

#### 3.1 Gamma band activity reflects initial stimulus encoding and saccade planning, but not stimulus maintenance

Figure 2a shows the time-frequency representations of the higher frequency power averaged over the sensors of interest (see methods) relative to baseline for each of the four conditions. Time t=0s denotes the onset of the stimulus presentation and time t=2s indicates the relocation of the fixation cross, which prompts the first, intervening saccade. In this colour format, warmer (red) colours indicate an increase of power relative to baseline, while cooler (blue) colour reflect a power decrease. Directly following stimulus presentation, the TFRs show strong enhancements in power in response to contralateral stimuli, in the range of 40 to 120 Hz. These enhancements seem to be transient in nature, as they are already vanished completely at time t=0.6 and most probably reflect initial stimulus encoding. For the rest of memory delay 1, laterality effects seem to remain absent by first inspection. Then, in all panels, a broad-banded power increase

can be observed at time  $t=2-2.8$ s in response to the refixation cue and accompanying saccade. We cannot distinguish this activity in components related to memory retention, saccade generation and artifacts caused by a moving retina. Since we found gaze fixation to be stable again at 2.65 s, we analyzed activity in the second delay period from time  $t=2.85$ s onward (see Methods). During this delay (2.85-3.8s), Figure 2a shows increased power ( $>55$  Hz) strongest for goals that are contralateral to the new direction of gaze (see next paragraph for directional selectivity and further analysis).

### 3.2 Gamma band activity during initial encoding of stimulus

To analyze these observations in more detail, we will now focus on the laterality effects in the two memory delay periods separately. For this purpose, signal to noise ratio was increased by pooling and contrasting conditions. First, based on the similar effects in the two hemispheres, the spectrograms were pooled across conditions with respect to the goal contralateral or ipsilateral to the current

gaze direction and subtracted from each other [ $(RR+RL)-(LL+LR)$ ], resulting in Figure 2b. In this format, warmer colours indicate a preference for a stimulus presented to the right of the current gaze direction and cooler colours indicate a preference for a stimulus to the left. Both hemispheres show a clear preference for a contralateral stimulus in this frequency band, reflected by stronger gamma band activity in response to contralateral stimuli. This observation is in line with the assumption that the stimulus is processed in the contralateral hemisphere. However, after the disappearance of the stimulus at time  $t=0.1$ , these lateralization effects vanish quickly and remain absent during the rest of delay 1 ( $t=0.6-1.8$ s). There was no significant cluster found in the frequency range 40 -100 Hz during the first delay period.

### 3.3 Directional selectivity of gamma band activity during saccade planning

In the second delay period (2.85-3.8s), the same clustering method revealed a significant modulation of power in the frequency band of 55-85 Hz (center

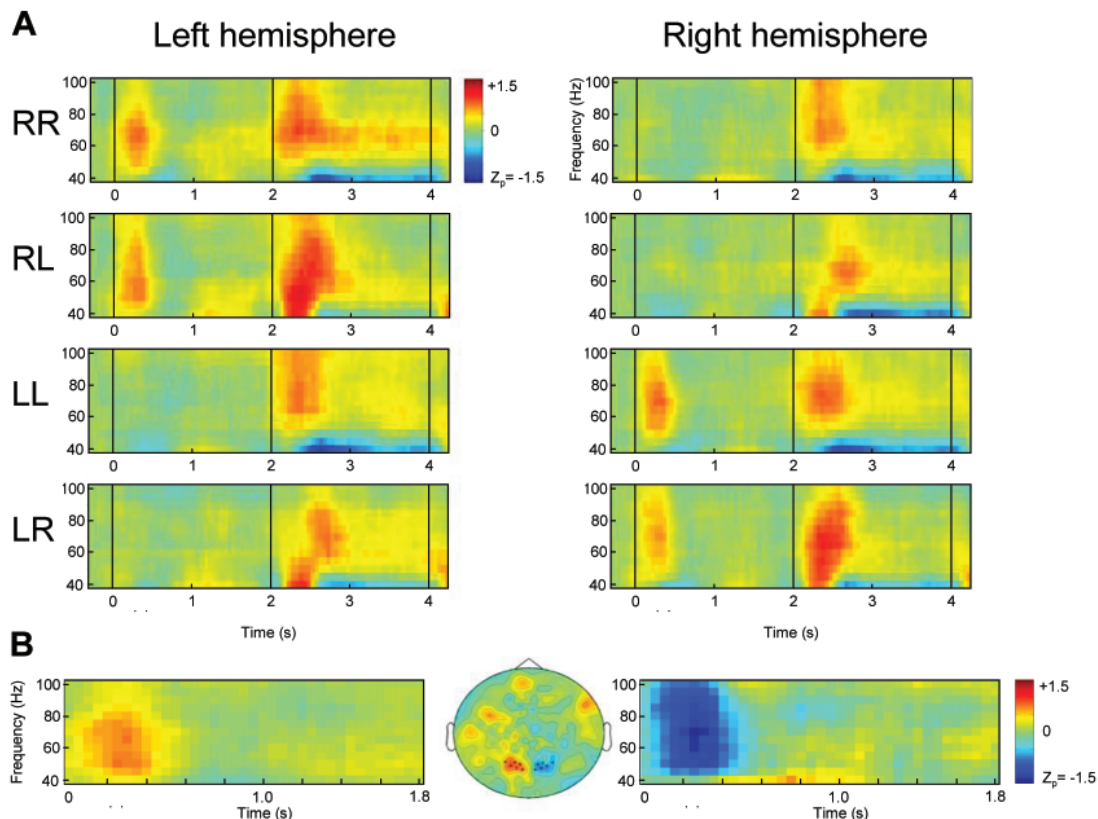


**Figure 2.** **A.** Time-frequency representations of the higher frequency power, averaged over posterior sensors relative to baseline for each of the four conditions. Time  $t=0$  s denotes the onset of the stimulus presentation and time  $t=2$  s indicates the relocation of the fixation cross, which prompts the first, intervening saccade. In this colour format, warmer (red) colours indicate an increase of power relative to baseline, while cooler (blue) colour reflect a power decrease. **B.** Spectograms pooled across conditions with respect to the hemifield of the presented stimulus and contrasted ( $RR+RL$ )-( $LL+LR$ ). Warmer colours (red) indicate a preference for a stimulus in the right hemifield, cooler colours indicate a preference for a stimulus in the left hemifield. Sensor choice is indicated in the topography plot (40-120 Hz; 0.1-0.6s).

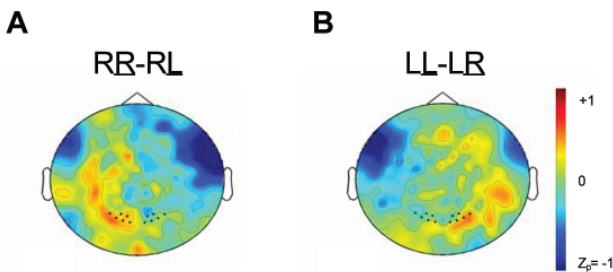


**Figure 3.** Contrasting conditions with the stimulus presented in the same hemifield, but different gaze fixation during delay 2. **A.** In this colour format warmer colours indicate a preference for a stimulus remaining in the right hemifield, whereas cooler colours indicate a preference for a stimulus that shifted into the left hemifield. **B.** In this colour format warmer colours (red) indicate a preference for a stimulus remaining in the left hemifield, whereas cooler colours (blue) indicate a preference for a stimulus that shifted into the right hemifield.

frequency 70 Hz, with 15 Hz smoothing). To further investigate the directional selectivity during the second delay period, we contrasted the conditions in which the goal remained in the same eye-centered hemifield versus conditions in which the remembered goal changed hemifields (thus: RR-RL and LL-LR). If oscillatory activity is related to the eye-centered location of the goal, then the directional selectivity of the power distributions should reverse during spatial updating. However, if the directional selectivity for the goal location as seen in memory delay 1 (Figure 2b) would be defined in a reference frame other than eye-centered, there should be no laterality effects observed in these contrasts during delay 2. Figure 3 shows the laterality effects of the higher frequencies for the specified contrasts. Note that these topographies are based on a smaller number of trials than the topography of Figure 2b (contrast of 2 conditions versus contrasting all 4 conditions). The two scalp topographies show the power distribution for the specified contrasts

averaged over the frequency range 55-85 Hz during the second delay (2.85-3.8s), while the participant is fixating at the new position. In panel A, a red colouring means a preference for saccade goals in the right visual field with cooler colours indicating a preference for goals in the left hemifield. Panel B has the opposite labeling, with red representing preference for saccade goals in the left visual field, and blue colours representing a preference for saccade goals in the right visual field. The RR-RL contrast shows a stronger gamma band response for a goal location contralateral to the current fixation point, as compared to a stimulus being presented contralateral, but now being ipsilateral to the current gaze direction. This laterality effect is in agreement with an update of the saccade goal representation in eye-centered coordinates (RR-RL). Also the LL-LR contrast shows this directional selectivity for goals remaining contralateral to gaze direction. The topographies also illustrate putative artifacts of the isometric eye-muscle contractions, i.e., keeping gaze position eccentric during the delay, primarily reflected in the fronto-temporal sensors. The topographies show that the statistical choice of posterior sensors based on the initial brain response to visual stimuli, is also sensible to our effect of interest during memory delay 2. One might wonder if these differences are driven primarily by the sustained gamma band activity in the RR and LL conditions, as compared to conditions RL and LR.

To investigate the putative differences between interhemispheric remapping and intrahemispheric remapping conditions, Figure 4 shows the TFRs of the contrasts RR-LL and RL-LR. The format of Figure 4 is the same as in Figure 2b, with warmer colours (red) for a preference of a goal presented in the right hemifield as compared to a stimulus presented in the left hemifield and cooler colours (blue) indicate a preference to the left as compared to the right, defined by the initial hemifield of stimulus presentation (the first letter of the condition name).

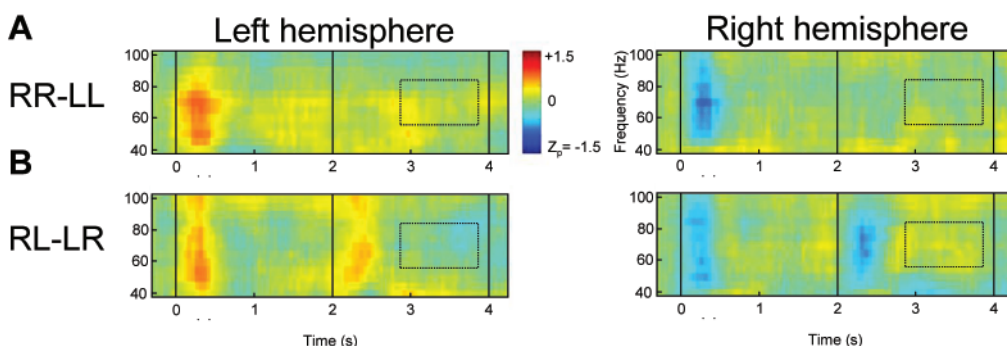


**Figure 4.** Time-frequency representation of contrasts between intrahemispheric remapping and interhemispheric remapping. Warmer colours (red) for a preference of a goal in the right hemifield, as compared to the left hemifield and cooler colours (blue) indicate a preference to the left as compared to the right, defined by the initial hemifield of stimulus presentation (the first letter of the condition name).

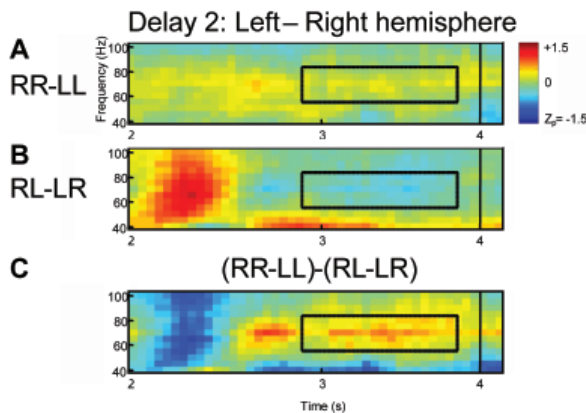


**Figure 5.** Delay 2. Change in preference for a stimulus due to eye-centered updating. Same colour format as in Figure 4. **A.** The left hemisphere still shows a clear preference to a stimulus presented in the right hemifield, whereas in **B** this preference is reversed. **C.** Preference for a remembered stimulus location contralateral to the current gaze direction during delay 2.

the right, defined by the initial hemifield of stimulus presentation. In both contrasts, the left hemisphere shows a preference for a stimulus to the right during the initial encoding of the stimulus and vice versa for the other hemisphere, as already seen in Figure 2a. Importantly, in memory delay 2 the preference changes according to the new eye-centered stimulus position. Only in the conditions where the remembered stimulus remains in the same hemifield (RR-LL contrast), the laterality effect continues in the same direction as during memory delay 1. In the RL-LR contrast however, the preference for a stimulus is reversed with the gaze change shifting to the remembered stimulus location into the opposite hemifield. When contrasting the differences observed between the RR-LL and RL-LR contrasts during memory delay 2 in Figure 5, we clearly see

a narrow gamma band (55-85 Hz) modulation, showing a directional selectivity for goal locations contralateral to the current gaze fixation point. A non-parametric randomization test (see Methods) over the predefined time-frequency window from 2.85 – 3.8s and 55-85 Hz (see Methods for the choice of the predefined window) revealed the significance of this effect ( $P < 0.05$ ).

### 3.4 Source underlying saccade goal encoding in updated eye-centered coordinates

We used a spatial filtering technique to estimate the sources underlying the transient gamma band response after stimulus presentation (0.1-0.5 s) and the sustained narrow band activity (55-85 Hz) during saccade goal encoding in updated coordinates (2.9-3.4 s). For source reconstruction we pooled the conditions according to the current hemifield of the stimulus. For delay 1 this resulted in [(RR+RL)-(LL+LR)], whereas for delay 2 we contrast [(RR+LR)-(LL+RL)]. Warmer colours (red) indicate a preference for a stimulus in the right hemifield, as compared to a stimulus presented in the left hemifield, whereas cooler colours (blue) indicate a preference for a stimulus in the left hemifield, as compared to the right hemifield. Figure 6 shows the source reconstructions for the transient response to the stimulus (A) with threshold  $|Z_p| > 0.3$  and the sustained response during saccade goal encoding (B) with threshold  $|Z_p| > 0.7$ . The broad-band gamma band activity originates from occipital and posterior parietal regions, with the peak in occipital cortex, in line with the interpretation that it reflects stimulus encoding, with information subsequently

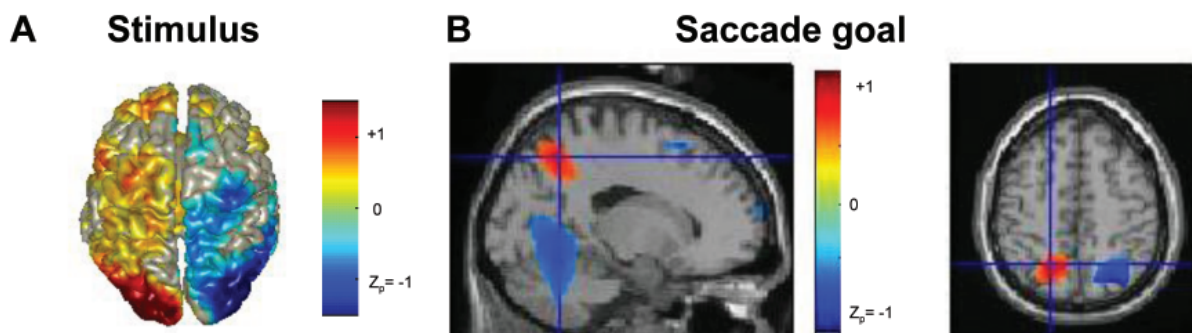


**Figure 6.** Source reconstructions of gamma band activity in CTF coordinates. Warmer colours (red) indicate a preference for a stimulus in the right hemifield, whereas cooler colours (blue) indicate a preference for a stimulus in the left hemifield. **A.** The stimulus induced response (0.1-0.6s) at the gamma frequency range (40-120 Hz). The broad-band gamma activity originates from occipital and parietal regions. **B.** The narrow gamma band delay activity (2.9-3.4s; 55-85 Hz) related to saccade planning in updated eye-centered coordinates, originates from posterior parietal cortex. Note that the conditions are pooled according to the updated stimulus coordinates, such that reversal of lateralization cannot be observed here. Cerebellar activity should be interpreted with caution, due to low reliability of source reconstruction of deeper sources in MEG.

passed from visual cortex to PPC. The sustained narrow band activity however, which appears at the moment the stimulus is updated for the intervening saccade and becomes a saccade goal, originates from posterior parietal cortex. Thus, the gamma band activity in the PPC encodes saccade goals in eye-centered coordinates.

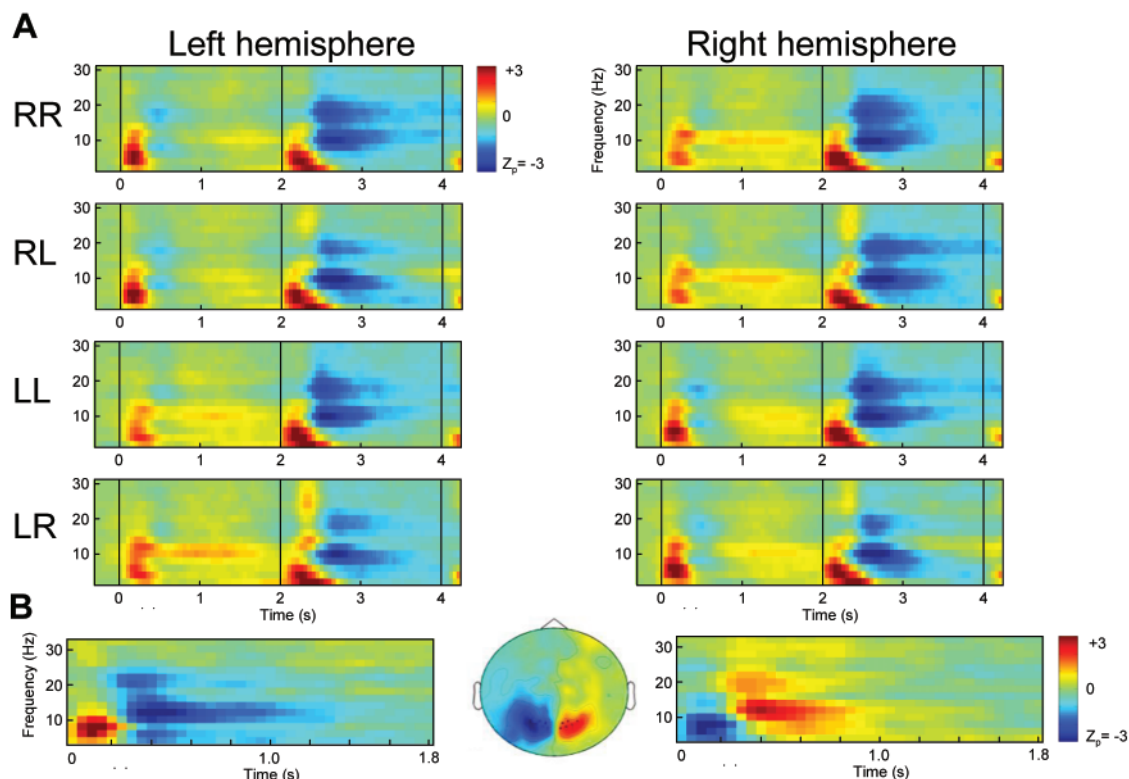
### 3.5 Sustained alpha band activity reflects interhemispheric remapping across saccades

Figure 7 shows the time-frequency representations of power of posterior sensors relative to baseline for each of the four conditions, for the lower frequencies. Time  $t=0$  s denotes the onset of the stimulus presentation and time  $t=2$  s indicates the occurrence of a refixation cue, which prompts the first, intervening saccade. In this colour format, warmer (red) colours indicate an increase of power relative to baseline, while cooler (blue) colour reflect a power decrease. The lower frequencies show a brief, transient increase in power in the theta range (4-8 Hz), which is stronger for contralateral visual cues. The alpha range (8-12 Hz) shows a sustained

power increase during the first delay interval, which is stronger in relation to ipsilateral than contralateral stimuli ( $p<0.05$ ). A clear bilateral decrease of power in the alpha band occurs at the beginning of the second delay period. This bilateral decrease is followed by a lateralization effect, showing more sustained suppression for a goal contralateral to the new direction of gaze. Similar effects can be observed in the beta band (13-25 Hz), in the second delay period.

### 3.6 Sustained alpha band activity following stimulus presentation

Again, we will focus on the laterality effects during the two memory delays separately. The data in Figure 7b was pooled across conditions in the same way as for the higher frequencies during memory delay 1 (Figure 2b). In this format, warmer colours indicate a preference for a stimulus presented to the right of the current gaze direction and cooler colours a preference for a stimulus to the left. A clear directional selectivity is observed following stimulus presentation at time  $t=0$ , with a slightly increased latency for the alpha band activity, as compared to



**Figure 7.** Activity in lower frequency bands, plotted in the same format as Figure 2. **A.** Both hemispheres initially show a preference for stimuli in the ipsilateral hemifield. Around time  $t=2.2$  s the intervening saccade is initiated, and a strong suppression is observed in alpha and beta bands. The suppression is maintained longer for remembered stimuli updated into the contralateral hemifield. **B.** In contrast to the higher frequencies, there is a sustained response during the first delay interval with more synchronization at 10 Hz for a stimulus in the ipsilateral than contralateral hemifield. The topographic plot depicts the distribution of power in the 8-12 Hz range, averaged over time  $t=0.3-0.8$ s.

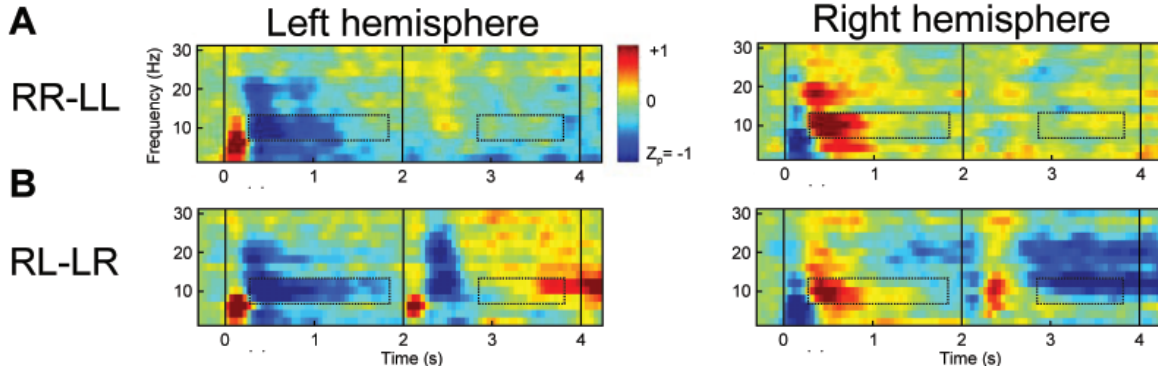


**Figure 8.** Time-frequency representation of the lower frequencies in the same format as Figure 4. In panel **A** the preference for a stimulus in the ipsilateral hemifield is preserved during delay 2. In panel **B**, the preference is reversed due to eye-centered updating of the stimulus into the opposite hemifield.

the laterality effects in the gamma band (Figure 2).

Both hemispheres show a stronger alpha band activity in response to ipsilateral stimuli. This observation is in line with the assumption that the ipsilateral hemisphere is disengaged because the stimulus is processed in the contralateral hemisphere. With the disappearance of the stimulus at time  $t=0.1$  (power effects leaking up to  $t=0.3$ ), these lateralization effects are sustained during the rest of delay 1 ( $p<0.05$ ). Note that this was not the case for gamma band power, as described above.

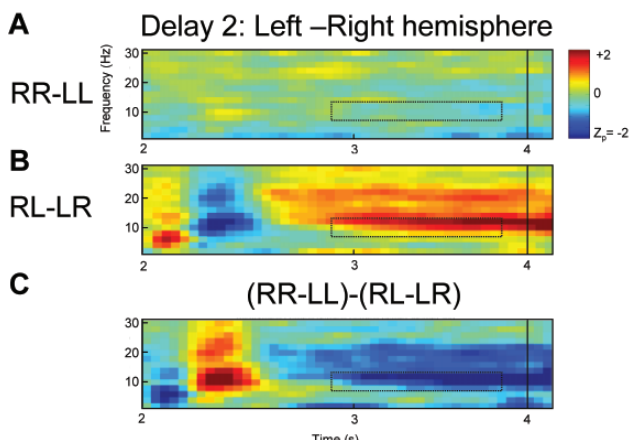
### 3.7 Alpha band activity during memory delay 2 shows a topography dependent on eye-centered coordinates

Figure 8 shows the directional selectivity of the lower frequencies in the same format as Figure 4. Initially, the left hemisphere shows an increased alpha band power in response to a left hemifield stimulus, as compared to a right hemifield stimulus, as noticed already in Figure 7A. This effect is the same in both contrasts. Importantly, in memory delay 2 the preference changes according to the new eye-centered stimulus position. Only in the conditions where the stimulus remains in the same hemifield (RR-LL contrast), the laterality effect continues in the same direction as during memory delay 1. In the RL-LR contrast however, the preference for a stimulus is reversed with the change in gaze, shifting the remembered stimulus location into the opposite hemifield. When contrasting the differences observed during memory delay 2 in Figure 9, we clearly see an alpha band (10 Hz) modulation, showing a directional selectivity for stimulus locations ipsilateral to the current gaze fixation point ( $p<0.05$  for RL-LR). Note that the center frequency of this effect seems to be slightly elevated ( $\sim 2$  Hz), as compared to

memory delay 1 and that the laterality effect increases in strength towards the saccade. To conclude, the results show an interhemispheric remapping of oscillatory activity when the goal location changes side relative to the new fixation point, indicating that the stimulus representation was updated for the intervening saccade.

### 3.8 Source reconstruction for the stimulus remapping in eye-centered coordinates

We used the same spatial filtering technique as for the higher frequency bands, with three periods of interest shown in Figure 10A/B. The pooling within Figure 10A is in the same format as for Figures 2B and 7B [(RR+RL)-(LL+LR)]. The pooling for the second delay is the same as for Figure 6B [(RR+LR)-(LL+RL)]. Thresholds for plotting the conditions were at  $|Z_p|>0.3$ . The stimulus-induced response (0.3-0.8 s) in A shows a desynchronization relative to baseline in parieto-occipital areas that is stronger in



**Figure 9.** Time-frequency representation as in Figure 5. **A.** The hemispheric preference from delay 1 is maintained during delay 2. **B.** The preference is reversed from delay 1 to delay 2, due to eye-centered updating. **C.** The difference between the responses.

response to a stimulus in the contralateral hemifield, as compared to a stimulus in the ipsilateral hemifield. The peak of the lateralization effect is observed in occipital areas. This lateralization is maintained during the entire delay interval 1 (A). The second delay (B) shows the similarities between the conditions with stimuli initially presented in opposite hemifields, but being updated into the same hemisphere during delay 2. Note that the conditions are pooled according to the updated stimulus coordinates, such that reversal of lateralization cannot be observed here.

## 4. Discussion

We studied the dynamics of oscillatory activity during spatial updating across saccades, under the assumption that oscillatory activity reflects a neuronal basis for maintenance of working memory representations (Tallon-Baudry et al., 1998; Pesaran et al., 2002; Howard et al., 2003; Jensen et al., 2007; Jokisch & Jensen, 2007). We expected a dynamic remapping of oscillatory activity patterns, when the

memory-trace of a target has to be updated due to a gaze change. Our findings show that the directional selectivity observed in two frequency bands during a delay period is actually dependent on an eye-centered reference frame and changes dynamically with updating across saccades. We found sustained high frequency gamma band activity to be selective for saccade goals contralateral to the current gaze direction, independent of the original hemifield of the visual stimulus. In the lower frequency range, alpha band lateralization is reversed when the remembered stimulus location shifts into the opposite hemifield by a saccade. These results strongly suggest that oscillatory activity at the population level reflects the remapping of activity observed in firing-rates of individual LIP neurons, providing a basis for dynamic working memory maintenance in eye-centered coordinates.

Our results are consistent with recent findings on oscillatory activity during delayed antisaccades, showing that alpha band activity related more to the visual stimulus component and gamma band activity more to the saccade goal (Van Der Werf

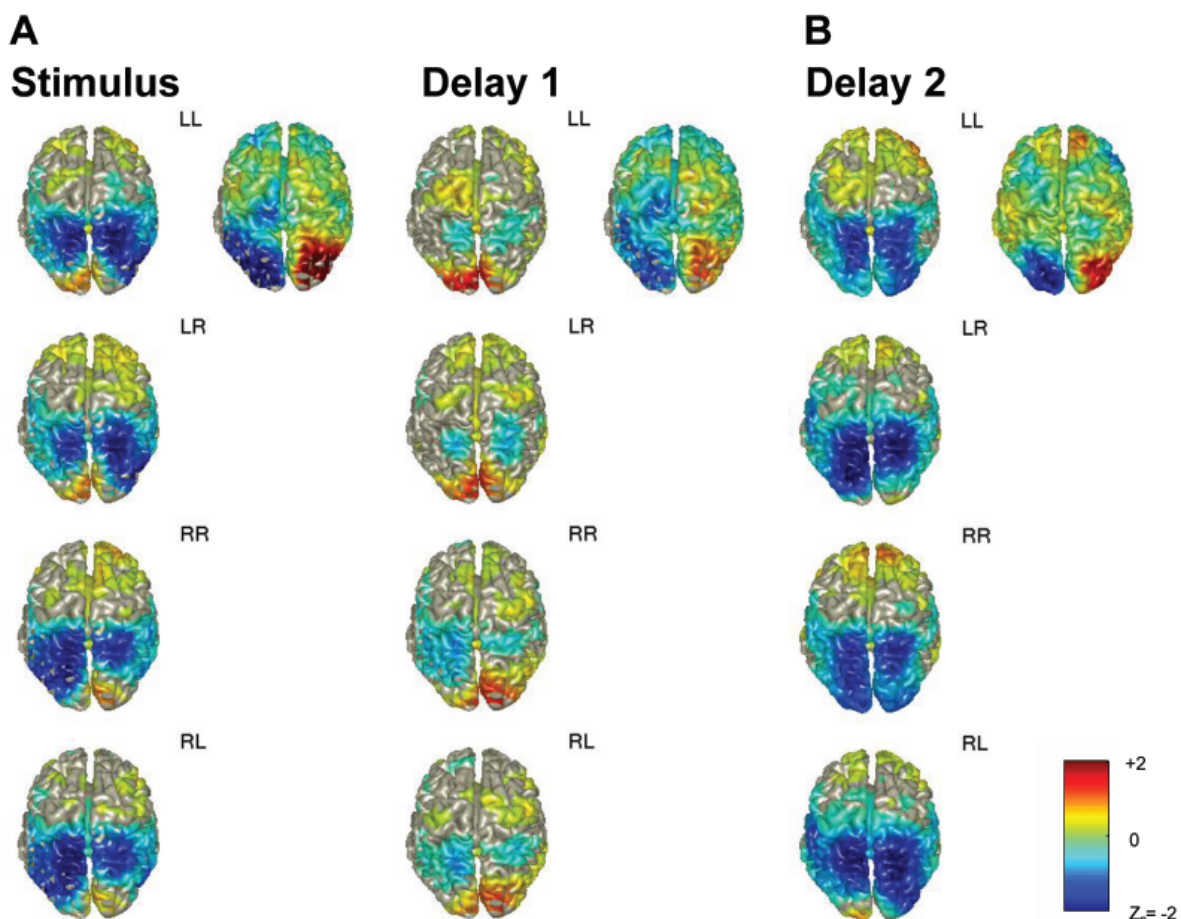


**Figure 10.** Source reconstruction for lower frequencies for three periods of interest. Pooling is the same as previously for gamma during delay 1 (RR+RL)-(LL+LR) and delay 2 (RR+LR)-(LL+RL). **A.** The initial response after stimulus presentation (0.3-0.8s) and the sustained response in delay 1(0.8-2.3s). **B.** The sustained response during delay 2, prior to the final saccade (3.5-4.0s).

et al., 2008). In other words, alpha band activity observed in that task merely remapped towards the direction of the stimulus, whereas gamma band activity showed a clear directional selectivity for the saccade goal, after the initial transient response during stimulus encoding. Yet, in the exploited anti-saccade task, participants could directly compute the goal component, as soon as they had perceived the stimulus. Therefore, it was not necessary to maintain the stimulus representation itself in working memory as soon as it was translated into a motor goal. Otherwise stated, the paradigm might not have been well suited to elicit a sustained gamma band activity reflecting stimulus maintenance in working memory. In the present study, participants did not know in advance where they had to fixate during the second delay, such that the veridical goal processing could only take place when the stimulus representation was first maintained during the delay and subsequently was spatially updated for the intervening saccade. Most probably, participants were covertly attending the stimulus location during the first memory delay, but sustained gamma band synchronization was not evident there. This null finding is probably not due to methodological issues, as we could clearly identify it during the second delay. In our view, this provides even more compelling evidence that gamma band activity originating from PPC relates to sensory-motor processing, as opposed to either stimulus maintenance or spatial attention. As already mentioned earlier, evidence from monkeys points into the same direction, as spatially elevated gamma band power (25-90 Hz) observed in local field potentials in LIP was linked to saccade planning in a delayed saccade task (Pesaran et al., 2002). Here, we observed this sustained gamma band activity at a location in the brain that corresponds to an eye-centered goal, updated for the intervening saccade.

In the lower frequencies, we observed sustained parieto-occipital alpha band synchronization in response to ipsilateral stimuli during the first delay, in line with the assumption that the stimulus is processed contralateral and this hemisphere is disengaged. These findings also support earlier reports of sustained alpha band suppression in response to contralateral stimuli (Medendorp et al., 2007), as it is probably more the relative difference in alpha band power between hemispheres reflecting processing versus disengagement and not absolute values (Linkenkaer-Hansen et al., 2004; Hanslmayr et al., 2005; Hanslmayr et al., 2007). The novel finding is that alpha band activity clearly remaps in relation to an eye-centered reference frame. Why did we observe such a clear remapping of activity, given

that alpha activity virtually not remapped during the anti-saccade task (Van Der Werf et al., 2008)? One possible explanation is that alpha band activity relates to the stimulus maintenance in working memory. As already mentioned above, the present task requires the stationary maintenance of the stimulus during the first delay and the updating of that representation for the intervening saccade before it can provide veridical stimulus information needed for the final saccade. Does the increase of the laterality effects towards the final saccade support the interpretation of this frequency band in terms of stimulus related activity? The results on the source level reveal that the lateralization effect is predominately evident in extrastriate areas, in addition to clear alpha band suppression in bilateral posterior parietal areas. The remapping of alpha band activity is in line with evidence for remapping in primate extrastriate areas (Nakamura & Colby, 2002; Merriam et al., 2007). However, from monkey data we know that remapping of activity in these areas has a longer latency and the proportion of neurons showing this behaviour is smaller, as compared to PPC, suggesting a top-down control from PPC to extrastriate cortex (Nakamura & Colby, 2002). It might be that alpha band power in visuo-motor tasks reflects recurrent processing between PPC and extrastriate areas, perhaps even V1, keeping the stimulus trace active and veridical, with PPC routing the stimulus representation across eye-movements to the corresponding location in visual cortex. In addition to dynamic visual working memory maintenance, this mechanism would increase visual cortex activity locally and therefore preparing it for input coming from the same location in space, as suggested by authors studying alpha band activity with attentional paradigms (Sauseng et al., 2005b; Rihs et al., 2007). For example, phosphene detection thresholds show a positive correlation with alpha band activity in parieto-occipital areas, which could be interpreted as increased excitability of extrastriate cortex (Romei et al., 2007). Alternatively, it could be the responsiveness of PPC to input from visual areas that varies with alpha band power and leads to lower detection thresholds. Triple-pulse TMS applied unilaterally to PPC reduces phosphene detection thresholds in the contralateral hemifield, but not when applied to both sides simultaneously, suggesting that PPC exerts at least hemisphere specific top-down control on extrastriate visual areas (Silvanto et al., 2008), if not retinotopic specific control. However, clear evidence for alpha band suppression being related to stimulus maintenance is still missing and suppression of this frequency band could rather reflect a more general allocation of

resources towards these areas, providing conditions in which higher frequency oscillations can emerge. Further investigation is required to clarify these issues.

Another potential role of alpha band activity for spatial updating is the truncation of activity in areas that should no longer maintain the stimulus representation, because it changed position in eye-centered coordinates. Active inhibition by means of synchronization in this frequency band could provide a mechanism for this truncation. Results from LIP neurons indicate that active inhibition takes place, because neurons do not slowly cease firing but activity is sharply truncated (Duhamel et al., 1992).

How do these findings relate to the decomposition of delay activity observed in multi-unit recordings of neurons in LIP? By means of intracranial recordings in monkeys, Mazzoni et al. (1996) found that 77% of the recorded neurons in LIP showed delay activity related to the next intended saccade, whereas only 16 % encoded the most recent visual stimulus independent of the saccade plan. Furthermore, there is an ongoing debate based on a huge number of intracranial recordings in monkeys about attentional modulation of area LIP and the necessity of the stimulus being a saccade goal (for reviews see Colby & Goldberg, 1999; Andersen & Buneo, 2002; Gottlieb, 2002). Here we find a clear dissociation between synchronization at the gamma band, building up at the moment of saccade planning and alpha band activity related to the stimulus in current eye-centered coordinates. How can we link these findings at the population level to the results from extra-cellular recordings?

Recent evidence suggests that only part of the information carried in firing-rates is transmitted between layers and suggestions have been made that spikes occurring during a certain phase of the oscillation carry more important information than others (Fries et al., 2007). According to this view, one could consider oscillatory activity at the population level as a read out mechanism of information being implicitly present in the firing-rates. This could also explain discrepancies between some results from intracranial recordings in monkeys about the content encoded or the reference-frames employed. With respect to reference-frames for example, oscillatory activity at the population level and the BOLD signal might reflect the actual reference frame being employed during a certain task, whereas firing rates might also reflect information necessary to transform between frames. Visuo-motor transformation requires different computational

stages and representations, which might coexist in the information encoded in spikes. However, to make rapid adjustments of trajectories and recombination of cross-modal signals possible, e.g. coordinating behaviour from several effectors within different frames simultaneously, a flexible read-out mechanism or routing is required, with shorter integration time than firing rates.

In more general terms, gamma band activity has been related to more efficient processing of sensory changes (Kaiser et al., 2006; Womelsdorf et al., 2007), accuracy in sensory tasks requiring behavioural responses (Kaiser et al., 2007; Kaiser et al., 2008a) and increased response speed in sensory-motor task (Gonzalez Andino et al., 2005; Womelsdorf et al., 2006). These findings suggest that phase synchronization at the gamma band indeed increases efficiency in sensory-motor integration networks and most probably plays an important role in movement planning, based on remembered visual input. From a neurophysiological perspective, synchronization at a frequency higher than 30 Hz leads to non-linear increases in input gain in a network (Fries et al., 2007; Womelsdorf et al., 2007). If input is provided simultaneously, it can induce a rapid change in membrane depolarization, thereby increasing the probability of a spike (Fries et al., 2007; Womelsdorf et al., 2007). If also downstream neurons fire coherently, the input arrives at times optimal for reception, thereby increasing the gain even further (Zeitler et al., 2008). This is in line with the interpretation that parietal cortex must increase its gain on downstream motor areas at the moment it provides a veridical goal representation for a subsequent saccade.

In future work, it would be interesting to investigate the dynamics of oscillatory activity during stimulus maintenance with the stimulus being presented to a different modality. For example, a spatial tactile stimulus must first be translated into an eye-centered reference frame to guide an eye-movement towards it. This would provide insight into alpha band activity being primarily related to extrastriate cortex excitability (gating mechanism for external visual stimuli) or to a more general parietal mechanism, providing specific spatial information to unisensory areas, independent of input modality. Furthermore it would be interesting to investigate modulations of gamma band activity related to movements with other effectors or multiple effectors towards visual stimuli, because one would expect this frequency band to play a similar role there, eventually with a lower center frequency when integration over larger networks is required.

## Acknowledgments

I would like to thank my three supervisors for their excellent support and enthusiasm during the course of this project. Furthermore I would like to thank Paul Gaalman for assisting me with the acquisition of the anatomical data, Bram for fixing technical problems and Ingrid, Robert and Christian for their constructive input. I enjoyed the open and informal atmosphere in Ole's group and the really funny moments in the traineeroom! Thanks!

## References

- Andersen, R. A., & Buneo, C. A. (2002). Intentional maps in posterior parietal cortex. *Annu Rev Neurosci*, 25, 189-220.
- Barash, S., Bracewell, R. M., Fogassi, L., Gnadt, J. W., & Andersen, R. A. (1991). Saccade-related activity in the lateral intraparietal area. II. Spatial properties. *J Neurophysiol*, 66, 1109-1124.
- Bastiaansen, M. C., & Knosche, T. R. (2000). Tangential derivative mapping of axial MEG applied to event-related desynchronization research. *Clin Neurophysiol*, 111, 1300-1305.
- Batista, A. P., Buneo, C. A., Snyder, L. H., & Andersen, R. A. (1999). Reach plans in eye-centered coordinates. *Science*, 285, 257-260.
- Blatt, G. J., Andersen, R. A., & Stoner, G. R. (1990). Visual receptive field organization and cortico-cortical connections of the lateral intraparietal area (area LIP) in the macaque. *J Comp Neurol*, 299, 421-445.
- Colby, C. L., Goldberg, M. E. (1999). Space and attention in parietal cortex. *Annu Rev Neurosci*, 22, 319-349.
- Duhamel, J. R., Colby, C. L., & Goldberg, M. E. (1992). The updating of the representation of visual space in parietal cortex by intended eye movements. *Science*, 255, 90-92.
- Efron, B., & Tibshirani, R. J. (1993). An introduction to the bootstrap. Boca Raton, FL: Chapman and Hall/CRC.
- Fries, P., Nikolic, D., & Singer, W. (2007). The gamma cycle. *Trends Neurosci*, 30, 309-316.
- Genovesio, A., & Ferraina, S. (2004). Integration of retinal disparity and fixation-distance related signals toward an egocentric coding of distance in the posterior parietal cortex of primates. *J Neurophysiol*, 91, 2670-2684.
- Gnadt, J. W., & Andersen, R. A. (1988). Memory related motor planning activity in posterior parietal cortex of macaque. *Exp Brain Res*, 70, 216-220.
- Gonzalez Andino, S. L., Michel, C. M., Thut, G., Landis, T., & Grave de Peralta, R. (2005). Prediction of response speed by anticipatory high-frequency (gamma band) oscillations in the human brain. *Hum Brain Mapp*, 24, 50-58.
- Gottlieb, J. (2002). Parietal mechanisms of target representation. *Curr Opin Neurobiol*, 12, 134-140.
- Gross, J., Kujala, J., Hamalainen, M., Timmermann, L., Schnitzler, A., & Salmelin, R. (2001). Dynamic imaging of coherent sources: Studying neural interactions in the human brain. *Proc Natl Acad Sci U S A*, 98, 694-699.
- Hämäläinen, M., Hari, R., Ilmoniemi, R. J., Knuutila, J., & Lounasmaa, O. V. (1993). Magnetoencephalography-theory, instrumentation, and applications to non-invasive studies of the working human brain. *Rev Mod Phys*, 65, 413-497.
- Hanslmayr, S., Aslan, A., Staudigl, T., Klimesch, W., Herrmann, C. S., & Bauml, K. H. (2007). Prestimulus oscillations predict visual perception performance between and within subjects. *Neuroimage*, 37, 1465-1473.
- Hanslmayr, S., Klimesch, W., Sauseng, P., Gruber, W., Doppelmayr, M., Freunberger, R., & Pecherstorfer, T. (2005). Visual discrimination performance is related to decreased alpha amplitude but increased phase locking. *Neurosci Lett*, 375, 64-68.
- Howard, M. W., Rizzuto, D. S., Caplan, J. B., Madsen, J. R., Lisman, J., Aschenbrenner-Scheibe, R., Schulze-Bonhage, A., & Kahana, M. J. (2003). Gamma oscillations correlate with working memory load in humans. *Cereb Cortex*, 13, 1369-1374.
- Huang, M. X., Mosher, J. C., & Leahy, R. M. (1999). A sensor-weighted overlapping-sphere head model and exhaustive head model comparison for MEG. *Phys Med Biol*, 44, 423-440.
- Jensen, O., Kaiser, J., & Lachaux, J. P. (2007). Human gamma-frequency oscillations associated with attention and memory. *Trends Neurosci*, 30, 317-324.
- Jensen, O., Gelfand, J., Kounios, J., & Lisman, J. E. (2002). Oscillations in the alpha band (9-12 Hz) increase with memory load during retention in a short-term memory task. *Cereb Cortex*, 12, 877-882.
- Jokisch, D., & Jensen, O. (2007). Modulation of gamma and alpha activity during a working memory task engaging the dorsal or ventral stream. *J Neurosci*, 27, 3244-3251.
- Kaiser, J., & Lutzenberger, W. (2001). Parietal gamma-band activity during auditory spatial precueing of motor responses. *Neuroreport*, 12, 3479-3482.
- Kaiser, J., & Lutzenberger, W. (2005). Cortical oscillatory activity and the dynamics of auditory memory processing. *Rev Neurosci*, 16, 239-254.
- Kaiser, J., Lennert, T., & Lutzenberger, W. (2007). Dynamics of oscillatory activity during auditory decision making. *Cereb Cortex*, 17, 258-2267.
- Kaiser, J., Heidegger, T., & Lutzenberger, W. (2008a). Behavioral relevance of gamma-band activity for short-term memory-based auditory decision-making. *Eur J Neurosci*, 27, 3322-3328.
- Kaiser, J., Hertrich, I., Ackermann, H., & Lutzenberger, W. (2006). Gamma-band activity over early sensory areas predicts detection of changes in audiovisual

- speech stimuli. *Neuroimage*, 30, 1376-1382.
- Kaiser, J., Heidegger, T., Wibral, M., Altmann, C. F., & Lutzenberger, W. (2008b). Distinct Gamma-Band Components Reflect the Short-Term Memory Maintenance of Different Sound Lateralization Angles. *Cereb Cortex*.
- Klimesch, W., Sauseng, P., & Hanslmayr, S. (2007). EEG alpha oscillations: the inhibition-timing hypothesis. *Brain Res Rev*, 53, 63-88.
- Lachaux, J. P., Hoffmann, D., Minotti, L., Berthoz, A., & Kahane, P. (2006). Intracerebral dynamics of saccade generation in the human frontal eye field and supplementary eye field. *Neuroimage* 30:1302-1312.
- Liljestrom, M., Kujala, J., Jensen, O., Salmelin, R. (2005). Neuromagnetic localization of rhythmic activity in the human brain: a comparison of three methods. *Neuroimage*, 25, 734-745.
- Linkenkaer-Hansen, K., Nikulin, V. V., Palva, S., Ilmoniemi, R. J., & Palva, J. M. (2004). Prestimulus oscillations enhance psychophysical performance in humans. *J Neurosci*, 24, 10186-10190.
- Maris, E., & Oostenveld, R. (2007). Nonparametric statistical testing of EEG- and MEG-data. *J Neurosci Methods*, 164, 177-190.
- Mazzoni, P., Bracewell, R. M., Barash, S., & Andersen, R. A. (1996). Motor intention activity in the macaque's lateral intraparietal area. I. Dissociation of motor plan from sensory memory. *J Neurophysiol*, 76, 1439-1456.
- Medendorp, W. P., Goltz, H. C., Vilis, T., & Crawford, J. D. (2003). Gaze-centered updating of visual space in human parietal cortex. *J Neurosci*, 23, 6209-6214.
- Medendorp, W. P., Kramer, G. F., Jensen, O., Oostenveld, R., Schoffelen, J. M., & Fries, P. (2007). Oscillatory activity in human parietal and occipital cortex shows hemispheric lateralization and memory effects in a delayed double-step saccade task. *Cereb Cortex*, 17, 2364-2374.
- Merriam, E. P., Genovese, C. R., & Colby, C. L. (2003). Spatial updating in human parietal cortex. *Neuron*, 39, 361-373.
- Merriam, E. P., Genovese, C. R., & Colby, C. L. (2007). Remapping in human visual cortex. *J Neurophysiol*, 97, 1738-1755.
- Nakamura, K., & Colby, C. L. (2002). Updating of the visual representation in monkey striate and extrastriate cortex during saccades. *Proc Natl Acad Sci U S A*, 99, 4026-4031.
- Nichols, T. E., & Holmes, A. P. (2002). Nonparametric permutation tests for functional neuroimaging: a primer with examples. *Hum Brain Mapp*, 15, 1-25.
- Nolte, K., Muller, B., & Dibbets, J. (2003). Comparison of linear measurements in cephalometric studies. *J Orofac Orthop*, 64, 265-274.
- Okada, Y. C., & Salenius, S. (1998). Roles of attention, memory, and motor preparation in modulating human brain activity in a spatial working memory task. *Cereb Cortex*, 8, 80-96.
- Percival, D. B., & Walden, A. T., (1993). Spectral analysis for physical applications: multitaper and conventional univariate techniques. Cambridge UP.
- Pesaran, B., Pezaris, J. S., Sahani, M., Mitra, P. P., & Andersen, R. A. (2002). Temporal structure in neuronal activity during working memory in macaque parietal cortex. *Nat Neurosci*, 5, 805-811.
- Rihs, T. A., Michel, C. M., & Thut, G. (2007). Mechanisms of selective inhibition in visual spatial attention are indexed by alpha-band EEG synchronization. *Eur J Neurosci*, 25, 603-610.
- Romei, V., Rihs, T., Brodbeck, V., & Thut, G. (2008). Resting electroencephalogram alpha-power over posterior sites indexes baseline visual cortex excitability. *Neuroreport*, 19, 203-208.
- Romei, V., Brodbeck, V., Michel, C., Amedi, A., Pascual-Leone, A., & Thut, G. (2007). Spontaneous Fluctuations in Posterior {alpha}-Band EEG Activity Reflect Variability in Excitability of Human Visual Areas. *Cereb Cortex*.
- Sauseng, P., Klimesch, W., Doppelmayr, M., Pecherstorfer, T., Freunberger, R., & Hanslmayr, S. (2005a). EEG alpha synchronization and functional coupling during top-down processing in a working memory task. *Hum Brain Mapp*, 26, 148-155.
- Sauseng, P., Klimesch, W., Stadler, W., Schabus, M., Doppelmayr, M., Hanslmayr, S., Gruber, W. R., & Birbaumer, N. (2005b). A shift of visual spatial attention is selectively associated with human EEG alpha activity. *Eur J Neurosci*, 22, 2917-2926.
- Scherberger, H., Jarvis, M. R., & Andersen, R. A. (2005). Cortical local field potential encodes movement intentions in the posterior parietal cortex. *Neuron*, 46, 347-354.
- Sereno, M. I., Pitzalis, S., & Martinez, A. (2001). Mapping of contralateral space in retinotopic coordinates by a parietal cortical area in humans. *Science*, 294, 1350-1354.
- Silvanto, J., Muggleton, N., Lavie, N., & Walsh, V. (2008). The Perceptual and Functional Consequences of Parietal Top-Down Modulation on the Visual Cortex. *Cereb Cortex*.
- Sommer, M. A., & Wurtz, R. H. (2008). Visual perception and corollary discharge. *Perception*, 37, 408-418.
- Tallon-Baudry, C., & Bertrand, O. (1999). Oscillatory gamma activity in humans and its role in object representation. *Trends Cogn Sci*, 3, 151-162.
- Tallon-Baudry, C., Bertrand, O., Peronnet, F., & Pernier, J. (1998). Induced gamma-band activity during the delay of a visual short-term memory task in humans. *J Neurosci*, 18, 4244-4254.
- Tallon-Baudry, C., Mandon, S., Freiwald, W. A., & Kreiter, A. K. (2004). Oscillatory synchrony in the monkey temporal lobe correlates with performance in a visual short-term memory task. *Cereb Cortex*, 14, 713-720.
- Thut, G., Nietzel, A., Brandt, S. A., & Pascual-Leone, A. (2006). Alpha-band electroencephalographic activity over occipital cortex indexes visuospatial attention bias and predicts visual target detection. *J Neurosci*, 26, 9494-9502.

- Umeno, M. M., & Goldberg, M. E. (1997). Spatial processing in the monkey frontal eye field. I. Predictive visual responses. *J Neurophysiol*, 78, 1373-1383.
- Umeno, MM, & Goldberg, M. E. (2001). Spatial processing in the monkey frontal eye field. II. Memory responses. *J Neurophysiol*, 86, 2344-2352.
- Van Der Werf, J., Jensen, O., Fries, P., & Medendorp, W. P. (2008). Gamma band activity in human posterior parietal cortex encodes the motor goal during delayed pro- and anti-saccades. *Journal of Neuroscience*, X, X.
- Van Donkelaar, P., & Muri, R. (2002). Craniotopic updating of visual space across saccades in the human posterior parietal cortex. *Proc Biol Sci*, 269, 735-739.
- Van Veen, B. D., Van Dongelen, W., Yuchtman, m., & Susuki, A. (1997). Localization of brain electrical activity via linearly constrained minimum variance spatial filtering.
- Walker, M. F., Fitzgibbon, E. J., & Goldberg, M. E. (1995). Neurons in the monkey superior colliculus predict the visual result of impending saccadic eye movements. *J Neurophysiol*, 73, 1988-2003.
- Womelsdorf, T., Fries, P., Mitra, P. P., & Desimone, R. (2006). Gamma-band synchronization in visual cortex predicts speed of change detection. *Nature*, 439, 733-736.
- Womelsdorf, T., Schöffelen, J. M., Oostenveld, R., Singer, W., Desimone, R., Engel, A. K., & Fries, P. (2007). Modulation of neuronal interactions through neuronal synchronization. *Science*, 316, 1609-1612.
- Wurtz, R. H. (2008). Neuronal mechanisms of visual stability. *Vision Res*.
- Yamagishi, N., Goda, N., Callan, D. E., Anderson, S. J., & Kawato, M. (2005). Attentional shifts towards an expected visual target alter the level of alpha-band oscillatory activity in the human calcarine cortex. *Brain Res Cogn Brain Res*, 25, 799-809.
- Zeitler, M., Fries, P., & Gielen, S. (2008). Biased competition through variations in amplitude of gamma-oscillations. *J Comput Neurosci*, 25, 89-107.

# The action of brain-derived neurotrophic factor (BDNF) on gene expression and $\text{Ca}^{2+}$ signaling in melanotrope cells of *Xenopus laevis*

Vivian Eijsink<sup>1</sup>, Wim Scheenen<sup>1</sup>, Eric Roubos<sup>1</sup>

<sup>1</sup>Department of Cellular Animal Physiology, Radboud University Nijmegen, Nijmegen, The Netherlands

Brain-derived neurotrophic factor (BDNF) is a neurotrophin that stimulates growth, survival and plasticity of neurons. It is also produced by the endocrine melanotrope cells in the pituitary pars intermedia of *Xenopus laevis*. This amphibian matches its skin colour to the ambient light situation by regulating secretion of  $\alpha$ -melanophore-stimulating hormone ( $\alpha$ -MSH) from melanotrope cells. Several inputs from hypothalamic origin converge on the melanotrope cell and affect intracellular  $\text{Ca}^{2+}$  dynamics to regulate the production and release of  $\alpha$ -MSH.  $\text{Ca}^{2+}$  plays a central role as intracellular second messenger in this model. During background adaptation, melanotrope cells undergo dramatic plasticity reflected, among others, in differential gene expression of membrane receptors such as the corticotropin-releasing hormone receptor 1 (CRHr1). Placing the animal on a black-background stimulates production of the  $\alpha$ -MSH precursor – pro-opiomelanocortin (POMC) and of BDNF, leading to secretion of  $\alpha$ -MSH and BDNF. Released BDNF likely has autocrine/paracrine actions on the cell by binding to its receptors, the tropomyosin-receptor-kinase B (TrkB) and the p75NTR, and initiating intracellular signalling pathways. In other cell types, three signalling pathways have been described for the Trk receptor, which may lead to regulation of gene expression and release of  $\text{Ca}^{2+}$  through inositol 1,4,5-trisphosphate (InsP3). InsP3 receptors are present on the endoplasmic reticulum (ER), one of the intracellular  $\text{Ca}^{2+}$  stores. The  $\text{Ca}^{2+}$  uptake into the ER usually is done through the sarco- and endoplasmic reticulum  $\text{Ca}^{2+}$ -ATPase (SERCA). The aim of the present study was to investigate first, whether BDNF affects the differential gene expression seen in this model, specifically of POMC, BDNF and CRHr1 genes; and second, whether BDNF affects the  $\text{Ca}^{2+}$  dynamics of melanotrope cells through the InsP3 pathway. Our results indicate that BDNF is regulating its transcript IV mRNA expression in the melanotrope cells, but not POMC or CRHr1 mRNA. Based on the  $\text{Ca}^{2+}$  dynamic experiments, it can be concluded that BDNF stimulates the frequency of  $\text{Ca}^{2+}$  oscillations and the release of  $\text{Ca}^{2+}$  from InsP3- and SERCA-dependent intracellular  $\text{Ca}^{2+}$  stores.

*Keywords:* BDNF, gene expression,  $\text{Ca}^{2+}$ , POMC, InsP3 pathway, melanotrope

---

Corresponding author of thesis: V.D. Eijsink, Email: viviane.eijsink@hotmail.com

## 1. Introduction

Brain-derived neurotrophic factor (BDNF) belongs to the neurotrophin family and it plays a role in neuronal survival and differentiation, plasticity, learning and memory (Bekinschtein et al., 2008; Bramham & Messaoudi, 2005; Chao, 2003; Tapia-Arancibia et al., 2004). Moreover, BDNF has been linked to numerous neurodegenerative diseases and psychiatric disorders such as depression, Alzheimer's disease and epilepsy (Chao, 2003; Tapia-Arancibia et al., 2004).

The different roles of BDNF reflect the diverse intracellular signalling pathways involved with this neurotrophic factor. These pathways may be initiated when BDNF binds to its receptors: the tropomyosin-receptor-kinase B (TrkB) and the p75NTR (Chao, 2003; Huang & Reichardt, 2001; Tapia-Arancibia et al., 2004). Known Trk pathways are the ERK/MAPK, the PI3K/Akt and the PLC pathways which may lead for example to regulation of gene expression and translation (Bramham & Messaoudi, 2005; Chao, 2003; Huang & Reichardt, 2001; Takei et al., 2001). Specifically, activation of phospholipase C (PLC) leads to the generation of the second messengers inositol 1,4,5-trisphosphate (InsP<sub>3</sub>) and diacylglycerol (DAG). Subsequently, InsP<sub>3</sub> cause release of calcium ( $\text{Ca}^{2+}$ ) from intracellular calcium stores and DAG activates the PKC pathway (Bramham & Messaoudi, 2005; Huang & Reichardt, 2001; Kovalchuk et al., 2004). In addition, TrkB receptors are able to influence the activity of membrane channels (Blum et al., 2002; Blum & Konnerth, 2005; Chao, 2003; Kovalchuk et al., 2004).

An appropriate model for studying the role of BDNF in plasticity is the neuroendocrine melanotrope cell in the pituitary pars intermedia of the amphibian *Xenopus laevis*. This amphibian matches its skin colour to the ambient light situation by regulating secretion of  $\alpha$ -melanophore-stimulating hormone ( $\alpha$ -MSH) from melanotrope cells. Secretion is stimulated by placing the animal on a black background and it is inhibited on a white background (Jenks et al., 2007; Jenks et al., 2003). BDNF is also produced by the melanotrope cells (Kramer et al., 2002) and it co-exists with  $\alpha$ -MSH in the secretory granules (Wang et al., 2004). The levels of BDNF mRNA and BDNF precursor protein (proBDNF) are up regulated in melanotrope cells of black-adapted animals (Kramer et al., 2002). Moreover, melanotrope cells express BDNF receptors TrkB (full-length and truncated) and p75NTR opening the possibility for

an autocrine/paracrine action of released BDNF on the melanotrope cell (Kidane et al., 2007). It has been shown that BDNF can stimulate biosynthesis of the  $\alpha$ -MSH precursor – pro-opiomelanocortin (POMC) (Kramer et al., 2002); and it also seems to be involved in the melanotrope cell size growth observed during black background adaptation of the animal (Kuribara and Scheenen, unpublished data).

Similar to the situation in rodents and other species (Aid et al., 2007; Heinrich & Pagtakhan, 2004; Liu et al., 2005; Timmusk et al., 1993), the *Xenopus laevis* BDNF gene has seven different transcripts that are differently regulated (Kidane et al., 2008). Transcripts I, IV, V, VI and VII5'ext are present in the neurointermediate lobe. Of these transcripts, exon VI and VII5'ext do not differ significantly between melanotrope of black- and white-adapted animals. Exon I and V expression levels are undetectable in white-adapted animals and lower than the levels of transcript IV in the black-adapted animals. Finally, transcript IV is most strongly regulated during background adaptation since its expression is drastically higher in melanotrope cells of black-adapted animals (Kidane et al., 2008).

Melanotrope cells exhibit great plasticity during the animals' background adaptation. Black background adaptation activates melanotrope cells, reflected by increased expression and production of POMC and BDNF, secretion of  $\alpha$ -MSH, increased cell size and decreased expression of the receptor for the stimulatory neuropeptide corticotropin-releasing hormone, the CRH receptor 1 (CRH<sub>1</sub>) (Jenks et al., 2007; Jenks et al., 2003; Roubos et al., 2005). CRH is one of multiple stimulatory and inhibitory inputs that converge on the melanotrope cell to regulate production and secretion of  $\alpha$ -MSH and intracellular  $\text{Ca}^{2+}$  dynamics (Jenks et al., 2007; Jenks et al., 2003; Roubos et al., 2005). In general, stimulatory inputs stimulate intracellular  $\text{Ca}^{2+}$  oscillations while inhibitory inputs inhibit them (Scheenen et al., 1994b; Shibuya & Douglas, 1993; for review, see Jenks et al., 2003). As such,  $\text{Ca}^{2+}$  plays a central role as second messenger in this model for the regulation of  $\alpha$ -MSH secretion and POMC biosynthesis (van den Hurk et al., 2005; Jenks et al., 2003). These  $\text{Ca}^{2+}$  oscillations depend on influx of extracellular  $\text{Ca}^{2+}$  through voltage-activated  $\text{Ca}^{2+}$  channels, which is followed by a cytoplasmic  $\text{Ca}^{2+}$  wave that eventually enters the nucleus (Jenks et al., 2003; Scheenen et al., 1996; Scheenen et al., 1994a). The propagation of the  $\text{Ca}^{2+}$  waves through the cytoplasm likely involves InsP<sub>3</sub>-sensitive intracellular  $\text{Ca}^{2+}$  stores (Scheenen et al., 1996).  $\text{Ca}^{2+}$  can be stored in different intracellular compartments, namely the endoplasmic reticulum

(ER), mitochondria, and the less well-described Golgi apparatus, lysosomes, secretory granules and endocytic vesicles (Clapham, 2007; Rizzuto & Pozzan, 2006). These compartments must be able to control uptake and release of  $\text{Ca}^{2+}$ . Well-studied ER channels by which  $\text{Ca}^{2+}$  can be released are the InsP3 and ryanodine receptors; uptake generally takes place through the SERCA, the sarco- and endoplasmic reticulum  $\text{Ca}^{2+}$ -ATPase (Clapham, 2007; Rizzuto & Pozzan, 2006).

The role of BDNF in the plasticity of the melanotrope cells of *Xenopus laevis* is not yet fully understood. The aim of the present study was to investigate first, whether BDNF affects the expression of genes that are differentially expressed in black- versus white-adapted animals, specifically of POMC, BDNF transcript IV and CRHr1 genes. Secondly, we investigated whether BDNF affects the  $\text{Ca}^{2+}$  dynamics of melanotrope cells through the InsP3 pathway.

## 2. Animals, materials and methods

### 2.1 Animals

Forty-two young-adults of the South African claw toad *Xenopus laevis*, aged 6 months, were reared in our laboratory under standard conditions, kept in tap water at 22 °C, 12 hours light-dark cycle, and fed beef heart and trout pellets (Touvit, Trouw, Putten, The Netherlands). Full background skin adaptation was achieved by keeping the animals on a black background under continuous light, for 3 weeks. All experiments were carried out under the guidelines of the Dutch law concerning animal welfare and are in agreement with the Declaration of Helsinki, verified by the committee for animal experimentation of the Radboud University Nijmegen.

### 2.2 Quantification of gene expression

#### 2.2.1 Neurointermediate lobe incubation

Eight fully black-adapted animals were decapitated and their neurointermediate pituitary lobes (NILs, containing melanotrope cells) collected in 1 ml *Xenopus laevis* Leibovitz culture medium (XL-L15) consisting of 67% Leibovitz culture medium (Gibco, Paisley, UK), 33% Milli Q water, 10 mg/ml kanamycin (Gibco), 10 mg/ml antibiotic/antimycotic (Gibco), 1.8 mM  $\text{CaCl}_2$  and 10 mM glucose, pH 7.4. The NILs were rinsed three times

with XL-L15 and one time with XL-L15 containing 10% foetal calf serum (FCS) (Gibco). Then NILs were individually incubated in a 48-well plate (Greiner bio-one, Germany) for three days at 22 °C, each well containing 220  $\mu\text{l}$  incubation medium that was refreshed daily. Four NILs were incubated in XL-L15 containing 10% FCS and [1:50] polyclonal rabbit anti-BDNF serum (200  $\mu\text{g}/\text{ml}$ , Santa Cruz Biotechnology Inc., CA, USA); and four NILs in 220  $\mu\text{l}$  XL-L15 containing 10% FCS. After the three-day incubation, NILs were collected for RNA extraction. This experiment was repeated independently.

We also tested whether adding antibody serum to the incubation medium had aspecific effects. For this, NILs of nine fully black-adapted animals were collected and incubated as described above. Three NILs were incubated with anti-BDNF serum, three NILs with incubation medium only and, in addition, three NILs were incubated with medium containing [1:50] rabbit anti-MSH serum (raised in house) as a control for the effect of antibody serum.

#### 2.2.2 RNA extraction and cDNA synthesis

After a three-day incubation, NILs were individually collected in 500  $\mu\text{l}$  ice-cold Trizol (Life Technologies, Paisley, UK) and homogenized by sonification. After chloroform extraction and isopropyl alcohol precipitation, RNA was dissolved in 20  $\mu\text{l}$  RNase-free  $\text{H}_2\text{O}$ . Total RNA was measured with an ND-1000 Spectrophotometer (Isogen Life Sciences, B.V.)

First strand cDNA synthesis was performed with 0.1  $\mu\text{g}$  RNA and 5 mU/ $\mu\text{l}$  random primers (Roche, Mannheim, Germany), at 70 °C for 10 minutes, followed by incubation in first strand buffer (Life Technologies), 10 mM DTT (Life technologies), 20 U Rnasin (Promega, Madison, WI, USA), 0.5 mM dNTPs (Roche) and 100 U Superscript II reverse transcriptase (Life Technologies) at 37 °C for 75 minutes, then at 95 °C for 10 minutes.

#### 2.2.3 Quantitative RT-PCR

Quantitative RT-PCR was performed in a total volume of 25  $\mu\text{l}$  in a buffer solution containing 12.5  $\mu\text{l}$  SYBR Green Master Mix (Applied Biosystems, Warrington, UK), 0.6  $\mu\text{M}$  of each primer forward and reverse; and 5  $\mu\text{l}$  [1:5] cDNA diluted in RNase-free  $\text{H}_2\text{O}$  (except for POMC that had 5  $\mu\text{l}$  [1:800] cDNA, due to its high expression levels). Primer pairs used and their respective primer efficiencies were: BDNF transcript IV, forward 5'-GCTGAGATCCCCAATACAAGTGT-3' and

reverse 5'-CATAGTAAGGAAAAGGATGGTCATCA-3' (primer efficiency 1.97); POMC, forward 5'-AGGAAACGATGGAAGCAACA-3' and reverse 5'-TGTACCTGGAGCATCTGATC-3' (primer efficiency 2.00); CRHr1, forward 5'-CAACTCITCCTGCAGTCCITC-3' and reverse 5'-ATTGAAATGCTTGTCCCTGCCATC-3' (primer efficiency 1.93) and GAPDH, forward 5'-GCTCCTCTCGCAAAGGTCA-3' and reverse 5'-GGGCCATCCACTGTCTTGT-3' (primer efficiency 1.98). GAPDH was used as the control housekeeping gene. All primer pairs were intron-spanning. Primer efficiencies were determined by making consecutive dilutions of one cDNA sample and measuring the known amounts with quantitative RT-PCR to establish a standard curve; the slope of the curve was used to calculate the primer efficiency (10<sup>-1</sup>/slope).

Optimum cycling temperature was 95 °C for 10 minutes, which was followed by 40 reaction cycles at 95 °C for 15 seconds and at 60 °C for 1 minute, by using a 7500 Real Time PCR System (Applied Biosystems). For each mRNA, the cycle threshold (*C<sub>t</sub>*) was determined as the cycle number needed to reach an arbitrary fluorescence value where *C<sub>t</sub>*-values of all mRNAs were within the exponential phase of their amplification. To correct for possible variations in melanotrope cell content among different NIL samples, the *C<sub>t</sub>*-values of BDNF transcript IV, POMC and CRHr1 mRNA were subtracted from the *C<sub>t</sub>*-value of GAPDH of the corresponding sample, giving the  $\Delta C_t$ . The relative amount of mRNA of the experimental groups were compared to the control group by first subtracting the  $\Delta C_t$  of the control group from the  $\Delta C_t$  of the experimental group, giving the  $\Delta\Delta C_t$  and putting this at 2-  $\Delta\Delta C_t$  (control group set as 1) (Livak & Schmittgen, 2001).

#### 2.2.4 Statistical analysis

Statistical analysis was performed on the  $\Delta C_t$  values and analyzed by means of Student t-test ( $\alpha = 5\%$ ) for the anti-BDNF versus control data; and ANOVA with Dunnett post-hoc test ( $\alpha = 5\%$ ) for the anti-BDNF and anti-MSH versus control data, using SPSS V.15.0 software (SPSS Inc., Chicago, IL, USA).

### 2.3. Dynamic Ca<sup>2+</sup> imaging

#### 2.3.1 Melanotrope cell isolation

Seventeen fully black-adapted animals were anesthetized by immersion in tap water containing

1 g/L ethyl-m-aminobenzoate methane sulfonic acid (MS222, ICN biomedicals Inc., Aurora, OH, USA) and 1.5 g/L NaHCO<sub>3</sub>, and transcardially perfused with *Xenopus* perfusion Ringer's solution (112 mM NaCl, 15 mM Hepes, 2 mM KCl, 2 mM CaCl<sub>2</sub>·2H<sub>2</sub>O, 2 g/L glucose, 250 mg/L MS222, pH 7.4, diluted in Milli Q water), to remove blood cells. The animals were decapitated; NILs were dissected and rinsed three times in XLL15 medium. After incubating the NILs for 45 minutes at 22 °C in a 0.25% trypsin solution, enzymatic reaction was stopped with XLL15 medium containing 10% FCS. Cells were dispersed by gentle trituration of the NILs with siliconized Pasteur's pipette. The cell suspension was filtered to remove the undissociated pars nervosa and centrifuged for 10 minutes at 500 rpm. The pellet was resuspended in XLL15 medium (60 µl/ NIL equivalent) and plated on a glass four chambered cover slip (Nalge Nunc International, Rochester, NY, USA) coated with 0.01% poly-L lysine hydrobromide (MW > 300 kD; Sigma-Aldrich Inc., St Louis, MO, USA). After allowing the cells to attach to the cover slip for 1 hour at 22 °C, 750 µl of XLL15 containing 10% FCS was added to each chamber. Cells were kept overnight at 22 °C and incubation medium was refreshed the next day before experimental use.

#### 2.3.2 Ca<sup>2+</sup> measurements

In each chamber, culture medium was removed and cells were loaded for 20 minutes at 22 °C in the dark in 1 ml *Xenopus* Ringer's solution (as described above, except MS222 is replaced by 0.3 g/L bovine serum albumin (BSA)), containing 25 µM pluronic acid F127 (Molecular Probes Inc., Eugene, OR, USA), 3% FCS and 2 µM fura-2/AM (Molecular Probes Inc.). After loading, cells were washed three times with *Xenopus* Ringer's solution to remove excess of non-hydrolyzed fura-2/AM and incubated in 250 µl Ringer's solution for 20 minutes at 22 °C in the dark to allow complete intracellular de-esterification of the probe. The incubation chamber was placed on an inverted microscope (Axiovert 135 TV; Zeiss, Göttingen, Germany) and cells were studied using a 40x oil-immersion objective (Zeiss Fluar, N.A. 1.30). Data were collected and analyzed with Metafluor Imaging V.6.2 (Universal Imaging Corporation, Downingtown, PA, USA). Individual cells were selected using region of interest. Fura-2 was excited at 340 and 380 nm and fluorescent emission was monitored by collecting wavelengths above 460 nm. Ca<sup>2+</sup> oscillations were measured with a sample interval of 6 seconds and were expressed as ratio of

the 340 nm/380 nm fluorescence intensity.

During measurements, test substances (diluted in *Xenopus* Ringer's solution) were added to the chamber with a Pasteur's pipette. The substances used were: 100 ng/ml BDNF (Promega), 5 mM ethylene glycol tetraacetic acid (EGTA) (Sigma), 50  $\mu\text{M}$  2-aminoethoxydiphenyl borate (2-APB) (Tocris) and 1  $\mu\text{M}$  thapsigargin (Calbiochem). EGTA was dissolved in *Xenopus* Ringer's solution and the pH was set at 7.4. In the experimental conditions that involved addition of EGTA to the chamber, substances in following applications were diluted in *Xenopus* Ringer's solution containing 5 mM EGTA.

### 2.3.3 Data analysis

Analysis of frequency and amplitude of the  $\text{Ca}^{2+}$  oscillations were performed with Origin V.6.1 (OriginLab Corp., Northampton, MA, USA) and

Microsoft Excel V.2007 software (Microsoft Corp., USA).

The effect of BDNF on  $\text{Ca}^{2+}$  oscillations was investigated by adding BDNF to the medium 15 minutes after the start of the measurements. For this group of cells ( $n = 7$ ), frequency and amplitude of the  $\text{Ca}^{2+}$  oscillations were studied before and after addition of BDNF. For each cell, its frequency (before and after BDNF) was obtained by determining the time between peaks (seconds). The amplitude was determined as the difference between maximum and minimum of each oscillation, and then averaged for each cell (before and after BDNF). Statistical analysis on frequency and amplitude before and after addition of BDNF for all cells was performed with the Wilcoxon matched-pairs signed-rank test ( $\alpha = 5\%$ ), using SPSS V.15.0 software. Data are expressed as the average of the percentages difference in frequency and amplitude.

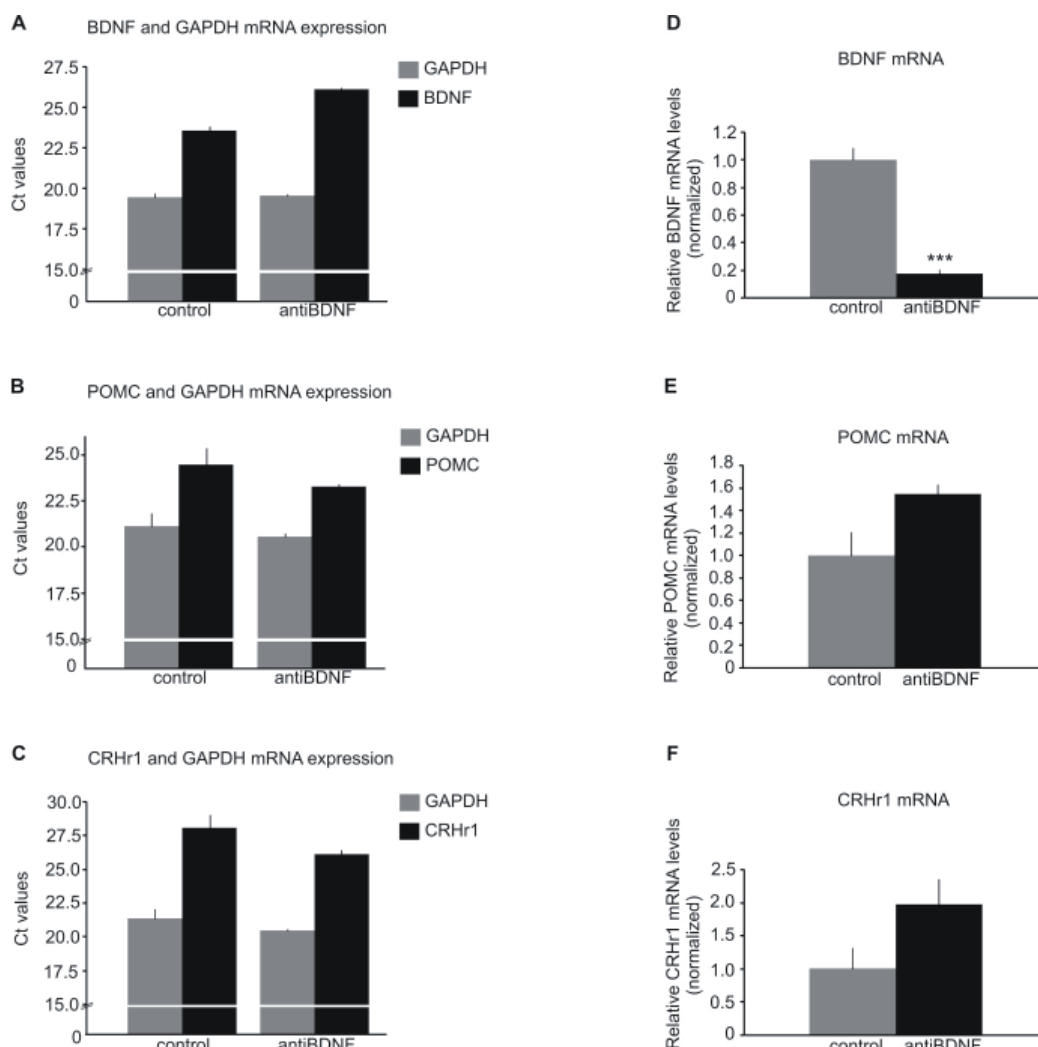


**Figure 1.** BDNF transcript IV, POMC and CRHr1 mRNA expression. The mRNA levels were determined with quantitative RT-PCR indicated by as the cycle number (Ct-values) above threshold. **A-C.** Ct-values  $\pm$  S.E.M. for (A) BDNF transcript IV, (B) POMC and (C) CRHr1; and the respective GAPDH levels. **D-F.** Relative mRNA levels normalized to the control group (set as 1)  $\pm$  S.E.M.; using GAPDH as housekeeping gene. (D) BDNF transcript IV mRNA levels (\*\* p < 0.001). (E) POMC mRNA levels (not significant). (F) CRHr1 mRNA levels (not significant).

The data on effect of BDNF in intracellular  $\text{Ca}^{2+}$  stores was analyzed by observing if the addition of BDNF to the medium induced a  $\text{Ca}^{2+}$  transient.

### 3. Results

#### 3.1 Quantitative RT-PCR on lobes treated with anti-BDNF

The effect of BDNF on gene expression in the melanotrope cells of the pituitary pars intermedia of *Xenopus laevis* was studied by culturing neurointermediate lobes of fully black-adapted animals for three days in medium (control group) or in medium containing [1:50] polyclonal rabbit anti-BDNF serum (anti-BDNF group), and subsequently quantifying the messenger RNA (mRNA) levels of BDNF transcript IV, POMC, CRHr1 and GAPDH (housekeeping gene) using quantitative RT-PCR.  $C_t$ -values were determined as described in the materials and methods.

$C_t$ -values for BDNF transcript IV were  $23.56 \pm 0.28$  ( $n = 4$ ) for the control group and  $26.14 \pm 0.10$  ( $n = 4$ ) for the anti-BDNF group (Figure 1A). The housekeeping gene GAPDH presented  $C_t$ -values of  $19.42 \pm 0.26$  and  $19.52 \pm 0.13$  for control and anti-BDNF groups, respectively. The resulting  $\Delta C_t$ -values (BDNF IV minus GAPDH) were significantly different between the anti-BDNF group and the control group ( $6.61 \pm 0.23$  versus  $4.13 \pm 0.11$ , respectively;  $p < 0.001$ ). Normalizing the control group to 1, the relative BDNF IV mRNA level in the anti-BDNF group is  $0.18 \pm 0.03$ , reflecting a 5.6-fold decrease (Figure 1D).

For POMC,  $C_t$ -values were  $24.42 \pm 0.87$  ( $n = 4$ ) for the control group and  $23.21 \pm 0.12$  ( $n = 4$ ) for the anti-BDNF group (Figure 1B). In this case,  $C_t$ -values for GAPDH were  $21.08 \pm 0.71$  and  $20.50 \pm 0.17$ , respectively. Calculated  $\Delta C_t$ -values (POMC minus GAPDH) were  $3.34 \pm 0.26$  for the control group

and  $2.71 \pm 0.75$  for the anti-BDNF group. The small increase in POMC mRNA levels in the anti-BDNF group relative to the control group ( $1.5 \pm 0.08$  versus  $1.0 \pm 0.21$ , respectively; Figure 1E) was not significant.

For CRHr1,  $C_t$ -values were  $28.06 \pm 1.03$  ( $n = 4$ ) for the control group and  $26.13 \pm 0.35$  ( $n = 4$ ) for the anti-BDNF group (Figure 1C).  $C_t$ -values for GAPDH were  $21.39 \pm 0.68$  and  $20.44 \pm 0.11$  for control and anti-BDNF groups, respectively. Calculated  $\Delta C_t$ -values (CRHr1 minus GAPDH) were  $6.67 \pm 0.47$  for the control group and  $5.69 \pm 0.30$  for the anti-BDNF group. The small increase in CRHr1 mRNA levels in the anti-BDNF group relative to the control group ( $1.97 \pm 0.38$  versus  $1.0 \pm 0.32$ , respectively; Figure 1F) was not significant.

To investigate whether addition of antibody serum to the incubation medium would have any aspecific effect on gene expression, neurointermediate lobes of fully black-adapted animals were incubated for three days in medium containing [1:50] rabbit anti-MSH serum (anti-MSH group) and compared to neurointermediate lobes incubated in medium (control group) or in medium containing [1:50] rabbit anti-BDNF serum (anti-BDNF group). Levels of mRNA of BDNF transcript IV, POMC, CRHr1 and GAPDH were determined using quantitative RT-PCR.

For BDNF transcript IV,  $C_t$ -values were  $24.29 \pm 0.09$  ( $n = 3$ ) for the control group,  $27.05 \pm 0.29$  ( $n = 3$ ) for the anti-BDNF group and  $23.64 \pm 0.26$  ( $n = 3$ ) for the anti-MSH group. The respective  $C_t$ -values for GAPDH were  $20.33 \pm 0.31$  for the control group,  $20.83 \pm 0.006$  for the anti-BDNF group and  $20.02 \pm 0.22$  for the anti-MSH group; resulting in  $\Delta C_t$ -values of  $3.96 \pm 0.39$  for the control group,  $6.22 \pm 0.29$  for the anti-BDNF group and  $3.63 \pm 0.051$  for the anti-MSH group. The 4.7-fold decrease seen in BDNF transcript IV mRNA levels in neurointermediate lobes treated with anti-BDNF serum ( $0.21 \pm 0.04$ ) relative to the control group

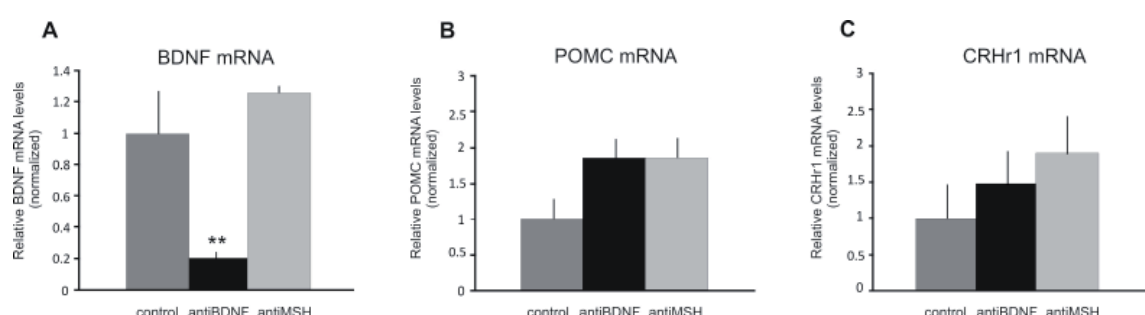


**Figure 2.** Effect of antibody serum. Relative mRNA levels of BDNF transcript IV, POMC and CRHr1. Relative mRNA levels normalized to control group (set as 1)  $\pm$  S.E.M. are shown. **A.** BDNF transcript IV mRNA levels (\*\*  $p < 0.01$ ). **B.** POMC mRNA levels (not significant). **C.** CRHr1 mRNA levels (not significant).

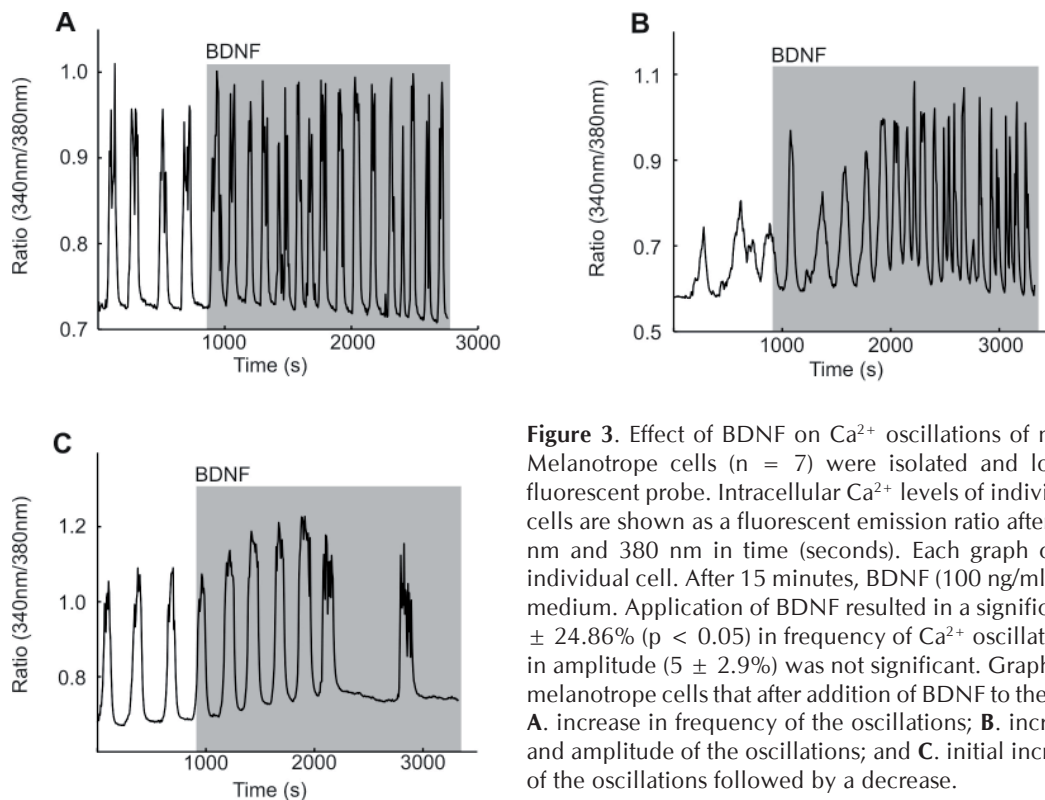


**Figure 3.** Effect of BDNF on  $\text{Ca}^{2+}$  oscillations of melanotrope cells. Melanotrope cells ( $n = 7$ ) were isolated and loaded with fura-2 fluorescent probe. Intracellular  $\text{Ca}^{2+}$  levels of individual melanotrope cells are shown as a fluorescent emission ratio after excitation at 340 nm and 380 nm in time (seconds). Each graph corresponds to an individual cell. After 15 minutes, BDNF (100 ng/ml) was added to the medium. Application of BDNF resulted in a significant increase of  $55 \pm 24.86\%$  ( $p < 0.05$ ) in frequency of  $\text{Ca}^{2+}$  oscillations. The increase in amplitude ( $5 \pm 2.9\%$ ) was not significant. Graphs are examples of melanotrope cells that after addition of BDNF to the medium showed: **A.** increase in frequency of the oscillations; **B.** increase in frequency and amplitude of the oscillations; and **C.** initial increase of frequency of the oscillations followed by a decrease.

( $1.0 \pm 0.27$ ) was not present in the anti-MSH group ( $1.26 \pm 0.04$ ) (Fig. 2A). These results indicate that the approximate 5-fold decrease in BDNF transcript IV mRNA expression in the anti-BDNF group is the result of the specific action of the anti-BDNF serum ( $F(2,6) = 24.25$ ,  $p < 0.001$ ; post hoc  $p < 0.01$ ).

For POMC mRNA levels (Fig. 2B), there was a small nonsignificant increase in the anti-BDNF and anti-MSH group ( $1.86 \pm 0.26$  and  $1.85 \pm 0.29$ , respectively;  $n = 3$  each) when compared to the control group ( $1.0 \pm 0.29$ ,  $n = 3$ ;  $F(2,6) = 3.01$ ). A similar small, nonsignificant increase holds for the CRHr1 mRNA expression (Fig. 2C) in the anti-BDNF and anti-MSH group ( $1.48 \pm 0.45$  and  $1.9 \pm 0.53$ , respectively;  $n = 3$  each) when compared to the control group ( $1.0 \pm 0.48$ ,  $n = 3$ ;  $F(2,6) = 0.86$ ).

### 3.2 Effect of BDNF on $\text{Ca}^{2+}$ dynamics

The effect of BDNF on  $\text{Ca}^{2+}$  dynamics in the melanotrope cells of the pituitary pars intermedia of *Xenopus laevis* was investigated by measuring  $\text{Ca}^{2+}$  oscillations of isolated cells using dynamic video imaging with fura-2 as fluorescent probe. After a control period of fifteen minutes, 100 ng/ml BDNF was added to the medium.

The frequency of the  $\text{Ca}^{2+}$  oscillations during the control period was  $0.0037 \pm 0.0004$  Hz ( $n = 7$ ). Application of BDNF resulted in a frequency of  $0.0057 \pm 0.001$  Hz. This represents an increase of

$55 \pm 24.86\%$  ( $p < 0.05$ , Fig. 3A and B). Interestingly in two cells, after an initial increase in  $\text{Ca}^{2+}$  oscillations frequency, this frequency drastically reduced (Fig. 3C).

The average amplitude of the  $\text{Ca}^{2+}$  oscillations before addition of BDNF to the medium was  $0.21 \pm 0.04$  ratio units ( $n = 7$ ), and after BDNF  $0.26 \pm 0.06$  ratio units, representing a nonsignificant increase of  $5 \pm 2.9\%$  in the amplitude of the oscillations, even though some cells displayed a clear increase (Fig. 3B).

To investigate whether the effect of BDNF seen on the  $\text{Ca}^{2+}$  oscillations involves intracellular  $\text{Ca}^{2+}$  stores, extracellular  $\text{Ca}^{2+}$  was buffered using EGTA (5 mM). Without extracellular  $\text{Ca}^{2+}$ ,  $\text{Ca}^{2+}$  oscillations of melanotrope cells stop (Fig. 4A-C). Approximately five minutes after application of EGTA, BDNF (100 ng/ml) was added to the medium. The addition of BDNF evoked a  $\text{Ca}^{2+}$  transient in 63% of the cells (17 of the 27 cells measured; Fig. 4A);  $\text{Ca}^{2+}$  transients were clearly visible as a small increase in the ratio 340 nm/380 nm after BDNF application.

In order to establish whether these intracellular  $\text{Ca}^{2+}$  stores contain InsP<sub>3</sub> receptors, 2-APB (50  $\mu$ M), an InsP<sub>3</sub> receptor antagonist, was added to the medium under EGTA treatment, prior to BDNF (100 ng/ml) application (Figure 4B;  $n = 12$ ). Under these conditions, no BDNF-induced  $\text{Ca}^{2+}$  transient was observed. To evaluate the involvement of a SERCA, its inhibitor thapsigargin (1  $\mu$ M) was added to the medium under EGTA treatment. Application

of thapsigargin leads to the depletion of the SERCA-dependent  $\text{Ca}^{2+}$  store resulting in a small transient increase in intracellular  $\text{Ca}^{2+}$  levels in all cells measured (Figure 4C, n = 14). After complete depletion of the endoplasmic reticulum  $\text{Ca}^{2+}$  store, BDNF (100 ng/ml) was applied. In this situation, no BDNF-induced  $\text{Ca}^{2+}$  transient was observed.

## 4. Discussion

BDNF can initiate diverse intracellular signaling pathways upon binding to its receptors TrkB and p75NTR. Three pathways have been described for the Trk receptors: the ERK/MAPK, the PI3K/Akt and PLC pathway (For review see Huang & Reichardt, 2001). These pathways eventually lead to regulation of gene expression and translation; additionally Trk receptors may affect intracellular  $\text{Ca}^{2+}$  signaling via the PLC/InsP3 pathway (Bramham & Messaoudi, 2005; Chao, 2003; Kovalchuk et al., 2004). Melanotrope cells of the pituitary pars intermedia of *Xenopus laevis* express BDNF (Kramer et al., 2002) and mRNA for its receptors, namely the TrkB (full-length and truncated) and the p75NTR (Kidane et al., 2007). In addition, BDNF is co-localized with  $\alpha$ -MSH in secretory granules of these cells (Wang et al., 2004). As such, melanotrope cells provide a good model to study the role of endogenous BDNF in cellular plasticity. It has been previously shown that BDNF is able to stimulate POMC biosynthesis in neurointermediate lobes of *Xenopus laevis* (Kramer et al., 2002) and cell size growth (Kuribara and Scheenen, unpublished data). In the present study, the role of BDNF in melanotrope cells of *Xenopus laevis* was investigated in respect of regulation of gene expression and  $\text{Ca}^{2+}$  dynamics. Our results show that BDNF regulates its transcript IV gene expression, but no evidence was found for a regulation of POMC or CRHr1 mRNA. Furthermore, BDNF has a stimulatory effect on the frequency of the  $\text{Ca}^{2+}$  oscillations and the ability to release  $\text{Ca}^{2+}$  from InsP3- and SERCA-dependent intracellular  $\text{Ca}^{2+}$  store. To our knowledge this is the first evidence for the presence of the BDNF/InsP3 pathway in melanotrope cells of *Xenopus laevis*.

### 4.1 BDNF stimulates the gene expression of BDNF transcript IV, but not POMC and CRHr1 genes

Among the numerous factors that change in melanotrope cells during adaptation of the animals

to a black background (For review, see Jenks et al., 2007) are increased levels of BDNF mRNA and of precursor protein of BDNF (proBDNF) when compared to white-adapted animals (Kramer et al., 2002). Of all BDNF transcripts, background adaptation regulates transcript IV in melanotrope cells more drastically. Therefore, in this study only BDNF transcript IV was analyzed. Apart from BDNF, also POMC mRNA and CRH receptor 1 mRNA are differentially expressed (Jenks et

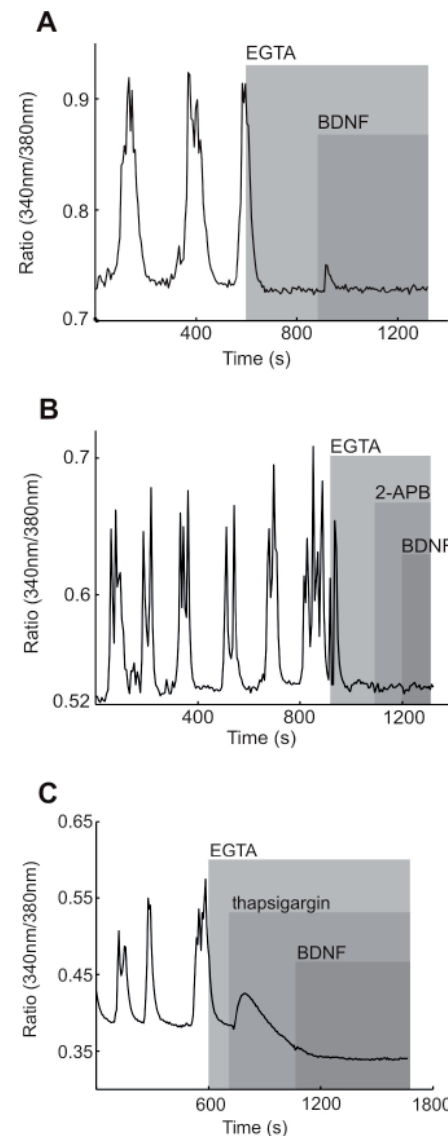


**Figure 4.** Effect of BDNF on intracellular  $\text{Ca}^{2+}$  stores. Melanotrope cells were isolated and loaded with fura-2 fluorescent probe. Intracellular  $\text{Ca}^{2+}$  levels of individual melanotrope cells are shown as a fluorescent emission ratio after excitation at 340 nm and 380 nm in time (seconds). Each graph corresponds to an individual cell. **A.** BDNF evokes  $\text{Ca}^{2+}$  transient in the absence of extracellular  $\text{Ca}^{2+}$  ( $\text{Ca}^{2+}$  free medium is a result of addition of EGTA) in 17 cells (n = 27). **B.** Inhibition of InsP3 receptors by 2-APB abolished the BDNF-induced  $\text{Ca}^{2+}$  transient under EGTA (n = 12). **C.** Depletion of endoplasmic reticulum (intracellular  $\text{Ca}^{2+}$  store) by thapsigargin abolished the BDNF-induced  $\text{Ca}^{2+}$  transient under EGTA (n = 14).

al., 2007): in black background adapted situation, POMC mRNA is upregulated (Martens et al., 1987) while CRHr1 is down-regulated (Calle, 2006).

Using antibodies against BDNF, we now determined whether endogenous BDNF affects the expression of such genes that are differentially expressed in black- versus white-adapted animals, specifically of BDNF transcript IV, POMC and CRHr1 genes. The idea is that the antibody will bind specifically to BDNF decreasing the amount of free BDNF available to bind to the membrane receptors and initiate the intracellular signaling pathways (Ghosh et al., 1994). Our quantitative RT-PCR results revealed that the decrease in BDNF transcript IV mRNA levels is specific for this antibody serum since it is not present in lobes incubated with anti-MSH serum. This specific reduction in BDNF transcript IV mRNA indicated that BDNF, acting through its membrane receptors, is necessary to maintain the high levels of BDNF transcript IV mRNA seen in melanotrope cells of black-adapted animals. We therefore conclude that BDNF is regulating its transcript IV expression. These data are in agreement with the idea of a positive feedback loop in the regulation of BDNF expression (Saarelainen et al., 2001; Wu et al., 2004).

We found no effect of anti-BDNF treatment on POMC mRNA or CRHr1 mRNA levels in neurointermediate lobes. The absence of an effect on POMC mRNA is in contrast with the BDNF stimulation on POMC biosynthesis (Kramer et al., 2002). Moreover, treatment with anti-BDNF inhibits POMC biosynthesis (Scheenen and Jenks, unpublished data). Taken these facts together with the absence of an effect on gene expression, it can be hypothesized that BDNF instead regulates the translation of POMC. It has been previously demonstrated that BDNF can regulate the translation of specific mRNAs, including calmodulin kinase-II $\alpha$  (Aakalu et al., 2001; Bramham & Messaoudi, 2005; Schratt et al., 2004; Takei et al., 2001). Moreover, regulation of translation of pre-existing mRNAs allows for faster protein availability than regulation of gene expression, which is important for plasticity of a cell or during adaptation of an animal to the environment. *Xenopus laevis* is able to adjust its skin colour to the environment in a matter of hours, whereas full adaptation is a slow process taking days. Pigment dispersion in dermal melanophore is regulated by  $\alpha$ -MSH released from melanotrope cells of the pituitary pars intermedia (Jenks et al., 2007). Therefore, the idea that regulation of POMC in melanotrope cells of *Xenopus laevis*, the precursor

for  $\alpha$ -MSH, is a tight process with fast and slow time kinetics, taking place on translation as well as transcription during adaptation (Martens et al., 1987) is very plausible. Our results indicate that regulation of transcription and translation might not be coupled one-to-one to a regulatory factor since BDNF appears to be regulating POMC translation but not transcription.

#### **4.2 BDNF stimulates the frequency of $\text{Ca}^{2+}$ oscillations and releases $\text{Ca}^{2+}$ from an InsP3-dependent $\text{Ca}^{2+}$ store**

Intracellular  $\text{Ca}^{2+}$  oscillations in *Xenopus* melanotrope cells are the driving force for  $\alpha$ -MSH secretion (For review, see Jenks et al., 2003), as well as POMC biosynthesis (van den Hurk et al., 2005). In general, these oscillations are stimulated (frequency and/or amplitude) by the same stimulatory inputs and inhibited by inhibitory inputs that regulate the  $\alpha$ -MSH secretion, or POMC biosynthesis (Scheenen et al., 1994b; Shibuya & Douglas, 1993; for review, see Jenks et al., 2003). To further understand the role of BDNF in the *Xenopus laevis* model, the effect of BDNF on  $\text{Ca}^{2+}$  dynamics in the melanotrope cells was investigated. Our results showing that BDNF stimulates the frequency of  $\text{Ca}^{2+}$  oscillations is in agreement with other stimulatory inputs that stimulate the frequency of  $\text{Ca}^{2+}$  oscillations in *Xenopus* melanotrope cells, and with the stimulatory effect of BDNF on the frequency of spontaneous  $\text{Ca}^{2+}$  oscillations in cultured hippocampal (Sakai et al., 1997) and cortical (Numakawa et al., 2002) rat developing neurons. Sakai et al. (1997) also reported a stimulatory effect on the amplitude of the oscillations.

The fact that, in the majority of melanotropes, BDNF induced a  $\text{Ca}^{2+}$  transient in the absence of extracellular  $\text{Ca}^{2+}$  implies that BDNF stimulates  $\text{Ca}^{2+}$  release from intracellular stores. For other cell types, it has been described that BDNF might cause the hydrolysis of phospholipase C resulting in the generation of InsP3 and subsequently release of  $\text{Ca}^{2+}$  from InsP3-sensitive intracellular stores (Kovalchuk et al., 2004; Li et al., 1998). However, the presence and activation of the BDNF/InsP3 pathway is dependent on cell type and condition (Gottschalk et al., 1999; Li et al., 1998). In *Xenopus* melanotropes, the rate of inositol metabolism is higher in cells of black-adapted animals compared to white-adapted (Jenks et al., 2003), although to date no role of the InsP3-sensitive  $\text{Ca}^{2+}$  stores in the regulation by first messengers has been demonstrated (For review, see

Jenks et al., 2003). Since 2-APB is known to affect other targets such as the mitochondria, besides the InsP<sub>3</sub> receptor (Bootman et al., 2002), the effect of the SERCA inhibitor thapsigargin was also tested. Our results showing that both blocking the InsP<sub>3</sub> receptor and SERCA abolished the BDNF-induced Ca<sup>2+</sup> transient provides strong evidence that BDNF in *Xenopus* melanotropes acts through Ca<sup>2+</sup> release from InsP<sub>3</sub>-sensitive ER stores. As such, it is the first evidence that the InsP<sub>3</sub>-sensitive Ca<sup>2+</sup> store is regulated by a first messenger in *Xenopus* melanotropes.

The importance of the involvement of an intracellular Ca<sup>2+</sup> store in the overall effect of BDNF seen in the Ca<sup>2+</sup> oscillations requires further investigation since studies in other cell types show that BDNF might also exert an effect on membrane channels influencing the influx of extracellular Ca<sup>2+</sup>, consequently affecting the Ca<sup>2+</sup> oscillations. Two examples are the transient receptor potential canonical channel (TrpC) and sodium channel: studies suggest that BDNF activation of PLC/InsP<sub>3</sub> pathway could lead to a store-operated influx of extracellular Ca<sup>2+</sup> through TrpC channels; and also there is evidence that TrkB might directly activate sodium channels causing a membrane depolarization which in turn could activate voltage-operated Ca<sup>2+</sup> channels (VOCC) resulting in an influx of Ca<sup>2+</sup> (For review see Blum & Konnerth, 2005). A pilot patch-clamp study done in our Department in melanotrope cells indicated that BDNF can affect sodium and potassium currents (Zhang and Scheenen, unpublished data). The results of this study suggest a potential effect of BDNF on Ca<sup>2+</sup> dynamics independent of intracellular Ca<sup>2+</sup> stores. Thus, further investigation is necessary to clarify the importance of intracellular Ca<sup>2+</sup> stores versus influx of extracellular Ca<sup>2+</sup> for the observed effect of BDNF on the frequency of the Ca<sup>2+</sup> oscillations.

Previous studies with *Xenopus* melanotrope cells showed that sensitizing InsP<sub>3</sub> receptors with thimerosal increased the speed of the cytoplasmic Ca<sup>2+</sup> wave (Scheenen et al., 1996). Therefore, it would be interesting to investigate whether BDNF affects the propagation kinetics of the Ca<sup>2+</sup> waves into the nucleus. If the latter is the case it would suggest that BDNF might regulate gene expression through modulation of intracellular Ca<sup>2+</sup>. A possible candidate for the BDNF-Ca<sup>2+</sup> mediated regulation of gene expression is the BDNF gene itself since it has been demonstrated that Ca<sup>2+</sup> can regulate BDNF expression (Mellström et al., 2004; Tao et al., 2002; West et al., 2001). Moreover, three potential responsive elements with high homology to human

and rat promoter IV where identified in the promoter for BDNF transcript IV of *Xenopus*, namely two Ca<sup>2+</sup> responsive elements (CaREs) and one calcium/cAMP responsive element (CRE); a downstream regulatory element (DRE) sequence which is Ca<sup>2+</sup>-dependent was also identified (Kidane et al., 2008).

### 4.3 Conclusion

In conclusion, our results indicate that BDNF is regulating its own transcript IV mRNA expression in the melanotrope cells, but not POMC or CRHr1 mRNA. Our results also show a stimulatory effect of BDNF on the frequency of Ca<sup>2+</sup> oscillations, and the ability of BDNF to release Ca<sup>2+</sup> from InsP<sub>3</sub>- and SERCA-dependent intracellular Ca<sup>2+</sup> stores. To our knowledge this is the first evidence for the presence of the BDNF/InsP<sub>3</sub> pathway in melanotrope cells of *Xenopus laevis*. Further investigation is required to determine the importance of this pathway for *Xenopus* melanotrope cells. Possibly, the effect of BDNF on its gene expression and on Ca<sup>2+</sup> oscillations are coupled; we hypothesize that BDNF is regulating its own transcript IV expression by affecting the kinetics of intracellular Ca<sup>2+</sup> oscillations or properties of Ca<sup>2+</sup> entry into the nucleus.

### Acknowledgments

I would like to thank my supervisor Wim J.J.M. Scheenen, my daily supervisor Miyuki Kuribara and Bruce G. Jenks for the teaching, valuable discussions and great support throughout the project; Debbie T.W.M. Tilburg-Ouwens and Peter M.J.M. Cruijsen for technical assistance; Ron J.C. Engels for animal care; and Eric W. Roubos for his input for my poster presentation and discussions.

### References

- Aakalu, G., Smith, W.B., Nguyen, N., Jiang, C. & Schuman, E.M. (2001). Dynamic visualization of local protein synthesis in hippocampal neurons. *Neuron* 30, 489-502.
- Aid, T., Kazantseva, A., Piirsoo, M., Palm, K. & Timmusk, T. (2007). Mouse and rat BDNF gene structure and expression revisited. *Journal of Neuroscience Research* 85, 525-535.
- Bekinschtein, P., Cammarota, M., Katche, C., Slipczuk, L., Rossato, J., Goldin, A., Izquierdo, I. & Medina, J.H. (2008). BDNF is essential to promote persistence of long-term memory storage. *PNAS* 105, 2711-2716.

- Blum, R., Kafitz, K.W. & Konnerth, A. (2002). Neurotrophin-evoked depolarization requires the sodium channel NaV1.9. *Nature* 419, 687-693.
- Blum, R. & Konnerth, A. (2005). Neurotrophin-mediated rapid signaling in the central nervous system: mechanisms and functions. *Physiology* 20, 70-78.
- Bootman, M.D., Collins, T.J., Mackenzie, L., Roderick, H.L., Berridge, M.J. & Peppiatt, C.M. (2002). 2-Aminoethoxydiphenyl borate (2-APB) is a reliable blocker of store-operated  $\text{Ca}^{2+}$  entry but an inconsistent inhibitor of InsP3-induced  $\text{Ca}^{2+}$  release. *The FASEB Journal* 16, 1145-1150.
- Bramham, C.R. & Messaoudi, E. (2005). BDNF function in adult plasticity: the synaptic consolidation hypothesis. *Progress in Neurobiology* 76, 99-125.
- Calle, M. (2006). Integrative physiology and communication in the amphibian brain. Thesis, Radboud University, Nijmegen.
- Chao, M.V. (2003). Neurotrophins and their receptors: a convergence point for many signaling pathways. *Nature Reviews Neuroscience* 4, 299-309.
- Clapham, D.E. (2007). Calcium signaling. *Cell* 131, 1047-1058.
- Ghosh, A., Carnahan, J. & Greenberg, M.E. (1994). Requirement for BDNF in activity-dependent survival of cortical neurons. *Science* 263, 1618-1623.
- Gottschalk, W.A., Jiang, H., Tartaglia, N., Feng, L., Figurov, A. & Lu, B. (1999). Signaling mechanisms mediating BDNF modulation of synaptic plasticity in the hippocampus. *Learning and Memory* 6, 243-256.
- Heinrich, G. & Pagtakhan, C.J. (2004). Both 5' and 3' flanks regulate Zebrafish brain-derived neurotrophic factor gene expression. *BMC Neuroscience* 5, 19.
- Huang, E.J. & Reichardt, L.F. (2001). Neurotrophins: roles in neuronal development and function. *Annual Review of Neuroscience* 24, 677-736.
- Jenks, B.G., Roubos, E.W. & Scheenen, W.J.J.M. (2003).  $\text{Ca}^{2+}$  oscillations in melanotropes of *Xenopus laevis*: their generation, propagation and function. *General and Comparative Endocrinology* 131, 210-219.
- Jenks, B.G., Kidane, A.H., Scheenen, W.J.J.M. & Roubos, E.W. (2007). Plasticity in the melanotrope neuroendocrine interface of *Xenopus laevis*. *Neuroendocrinology* 85, 177-185.
- Kidane, A.H., van Dooren, S.H.J., Roubos, E.W. & Jenks, B.G. (2007). Expression and physiological regulation of BDNF receptors in the neuroendocrine melanotrope cell of *Xenopus laevis*. *General and Comparative Endocrinology* 153, 176-181.
- Kidane, A.H., Heinrich, G., Dirks, R.P.H., De Ruyck, B.A., Lubsen, N.H., Roubos, E.W. & Jenks, B.G. (2008). Differential neuroendocrine expression of multiple brain-derived neurotrophic factor transcripts. *Endocrinology* doi:10.1210/en.2008-0993.
- Kovalchuk, Y., Holthoff, K. & Konnerth, A. (2004). Neurotrophin action on a rapid timescale. *Current Opinion in Neurobiology* 14, 558-563.
- Kramer, B.M.R., Cruijsen, P.M.J.M., Ouwens, D.T.W.M., Coolen, M.W., Martens, G.J.M., Roubos, E.W. & Jenks, B.G. (2002). Evidence that brain-derived neurotrophic factor acts as an autocrine factor on pituitary melanotrope cells of *Xenopus laevis*. *Endocrinology* 143, 1337-1345.
- Li, Y.X., Zhang, Y., Lester, H.A., Schuman, E.M. & Davidson, N. (1998). Enhancement of neurotransmitter release induced by brain-derived neurotrophic factor in cultured hippocampal neurons. *The Journal of Neuroscience* 18, 10231-10240.
- Liu, Q.R., Walther, D., Drgon, T., Polesskaya, O., Lesnick, T.G., Strain, K.J., de Andrade, M., Bower, J.H., Maraganore, D.M. & Uhl, G.R. (2005). Human brain derived neurotrophic factor (BDNF) genes, splicing patterns, and assessments of associations with substance abuse and Parkinson's disease. *American Journal of Medical Genetics Part B (Neuropsychiatric Genetics)* 134B, 93-103.
- Livak, K.J. & Schmittgen, T.D. (2001). Analysis of relative gene expression data using real-time quantitative PCR and the  $2^{-\Delta\Delta Ct}$  method. *Methods* 25, 402-408.
- Martens, G.J.M., Weterings, K.A.P., van Zoest, I.D. & Jenks, B.G. (1987). Physiologically-induced changes in proopiomelanocortin mRNA levels in the pituitary gland of the amphibian *Xenopus laevis*. *Biochemical and Biophysical Research Communications* 143, 678-684.
- Mellström, B., Torres, B., Link, W.A. & Naranjo, J.R. (2004). The BDNF gene: exemplifying complexity in  $\text{Ca}^{2+}$ -dependent gene expression. *Critical Reviews in Neurobiology* 16, 43-49.
- Numakawa, T., Yamagishi, S., Adachi, N., Matsumoto, T., Yokomaku, D., Yamada, M. & Hatanaka, H. (2002). Brain-derived neurotrophic factor-induced potentiation of  $\text{Ca}^{2+}$  oscillations in developing cortical neurons. *The Journal of Biological Chemistry* 277, 6520-6529.
- Rizzuto, R. & Pozzan, T. (2006). Microdomains of intracellular  $\text{Ca}^{2+}$ : molecular determinants and functional consequences. *Physiological Reviews* 86, 369-408.
- Roubos, E.W., Scheenen, W.J.J.M. & Jenks, B.G. (2005). Neuronal, neurohormonal, and autocrine control of *Xenopus* melanotrope cell activity. *Annals of the New York Academy of Sciences* 1040, 172-183.
- Saarelainen, T., Vaittinen, S. & Castrén, E. (2001). TrkB-receptor activation contributes to the kaianate-induced increase in BDNF mRNA synthesis. *Cellular and Molecular Neurobiology* 21, 429-435.
- Sakai, N., Yamada, M., Numakawa, T., Ogura, A. & Hatanaka, H. (1997). BDNF potentiates spontaneous  $\text{Ca}^{2+}$  oscillations in cultured hippocampal neurons. *Brain Research* 778, 318-328.
- Scheenen, W.J.J.M., Jenks, B.G., Roubos, E.W. & Willemse, P.H.G.M. (1994a). Spontaneous calcium oscillations in *Xenopus laevis* melanotrope cells are mediated by  $\omega$ -conotoxin sensitive calcium channels. *Cell calcium* 15, 36-44.
- Scheenen, W.J.J.M., Jenks, B.G., Willemse, P.H.G.M. & Roubos, E.W. (1994b). Action of stimulatory and

- inhibitory  $\alpha$ -MSH secretagogues on spontaneous calcium oscillations in melanotrope cells of *Xenopus laevis*. European Journal of Physiology 427, 244-251.
- Scheenen, W.J.J.M., Jenks, B.G., van Dinter, R.J.A.M. & Roubos, E.W. (1996). Spatial and temporal aspects of  $\text{Ca}^{2+}$  oscillations in *Xenopus laevis* melanotrope cells. Cell calcium 19, 219-227.
- Schratt, G.M., Nigh, E.A., Chen, W.G., Hu, L. & Greenberg, M.E. (2004). BDNF regulates the translation of a select group of mRNAs by a mammalian target of rapamycin-phosphatidylinositol-3-kinase-dependent pathway during neuronal development. The Journal of Neuroscience 24, 7366-7377.
- Shibuya, I. & Douglas, W.W. (1993). Spontaneous cytosolic calcium pulsing detected in *Xenopus* melanotrophs: modulation by secreto-inhibitory and stimulant ligands. Endocrinology 132, 2166-2175.
- Takei, N., Kawamura, M., Hara, K., Yonezawa, K. & Nawa, H. (2001). Brain-derived neurotrophic factor enhances neuronal translation by activating multiple initiation processes. The Journal of Biological Chemistry 276, 42818-42825.
- Tao, X., West, A.E. & Chen, W.G. (2002). A calcium-responsive transcription factor, CaRF, that regulates neuronal activity-dependent expression of BDNF. Neuron 33, 383-395.
- Tapia-Arancibia, L., Rage, F., Givalois, L. & Arancibia, S. (2004). Physiology of BDNF: focus on hypothalamic function. Frontiers in Neuroendocrinology 25, 77-107.
- Timmusk, T., Palm, K., Metsis, M., Reintam, T., Paalme, V., Saarma, M. & Persson, H. (1993). Multiple promoters direct tissue-specific expression of the rat BDNF gene. Neuron 10, 475-489.
- Van den Hurk, M.J.J., Scheenen, W.J.J.M., Roubos, E.W. & Jenks, B.G. (2005). Calcium influx through voltage-operated calcium channels is required for pro-opiomelanocortin protein expression in *Xenopus* melanotropes. Annals of the New York Academy of Sciences 1040, 494-497.
- Wang, L.C., Meijer, H.K., Humbel, B.M., Jenks, B.G. & Roubos, E.W. (2004). Activity-dependent dynamics of coexisting brain-derived neurotrophic factor, pro-opiomelanocortin and  $\alpha$ -melanophore-stimulating hormone in melanotrope cells of *Xenopus laevis*. Journal of Endocrinology 16, 19-25.
- West, A.E., Chen, W.G., Dalva, M.B., Dolmetsch, R.E., Kornhauser J.M., Shaywitz, A.J., Takasu, M.A., Tao, X. & Greenberg, M.E. (2001). Calcium regulation of neuronal gene expression. PNAS 98, 11024-11031.
- Wu, X., Zhu, D., Jiang, X., Okagaki, P., Mearow, K., Zhu, G., McCall, S., Banaudha, K., Lipsky, R.H. & Marini, A.M. (2004). AMPA protects cultured neurons against glutamate excitotoxicity through a phosphatidylinositol 3-kinase-dependent activation in extracellular signal-regulated kinase to upregulate BDNF gene expression. Journal of Neurochemistry 90, 807-818.

# **Self-other representation and differentiation in children with autism spectrum disorders**

Madelon Riem<sup>1</sup>, Astrid Stoit<sup>2</sup>, Hein van Schie<sup>3</sup>, Ruud Meulenbroek<sup>1</sup>, Roger Newman-Norlund<sup>1</sup>, Jan Buitelaar<sup>4</sup>

<sup>1</sup>Donders Institute for Brain, Cognition and Behaviour, Nijmegen, The Netherlands

<sup>2</sup>Karakter, Institute for Child Psychiatry, Zwolle, The Netherlands

<sup>3</sup>Behavioural Science Institute, Radboud University Nijmegen, Nijmegen, The Netherlands

<sup>4</sup>Department of Psychiatry, University Medical Center, St. Radboud, Nijmegen, The Netherlands

Recent findings indicate that two different neural networks might be impaired in autism spectrum disorders (ASD) and might cause the problems in social interaction children with this disorder experience. First, abnormalities in cortical midline structures (CMS) might lead to difficulty in attributing mental states to other people and problems in differentiation of action contributions of the self and the other. It has been shown that CMS become activated during joint-tasks; goal-directed tasks that can not be accomplished alone and thus require cooperation of a co-actor. Another neural network that becomes activated in joint-action and has been shown to be impaired in ASD is the mirror neuron system. Abnormalities in this system could explain difficulty in representing actions of other people in autism. Successful joint action requires representation of the actions of the co-actor in order to form an internal model of the task. This internal model enables anticipations to the actions of the co-actor. The present study investigated whether children with ASD have difficulty with self-other differentiation and with forming an internal model of the timing of the actions of the co-actor. The participants performed a virtual bar-balancing task in which the lift of the bar was controlled with two hands in a solo condition and with two or four hands in joint conditions. The results show larger distribution for lift of children with ASD in the joint-action condition in which the participants used four hands and difficulty in anticipating the movement onset of the co-actors in the most demanding joint-action condition. This suggests that children with ASD indeed have difficulty in differentiation of the action contributions of the self and the other and in building an internal model of the timing of the co-actor.

*Key words:* autism, mirror neuron system, cortical midline structures, sense of, agency, joint action

---

Corresponding author of thesis: Madelon Riem, Nijmegen Institute for Cognition and Information, PO Box 1904, 6500 HE Nijmegen, The Netherlands, m.riem@student.ru.nl

## 1. Introduction

Autism is a neurodevelopmental disorder characterized by impairments in communication and social interaction, executive functioning, the lack of empathy and emotional engagement of others and repetitive, stereotyped behaviour (DSM-IV, American Psychological Association, 2000). Most children with Autism Spectrum Disorders (ASD) find it difficult to understand people's actions, emotions and beliefs. To be an autistic child means to be incapable to establish meaningful social relations, to share attention with others or to imitate the behaviour of other people (D'Entremont & Yazbek, 2007). ASD have been associated with deficits in different aspects of social cognition, for example joint attention or gaze following (Baron-Cohen 1997; Leekam 2000).

Recent studies suggest that abnormalities in two different neural networks might cause the social problems in autism. First, impairments in the mirror neuron system (MNS) might be responsible for these problems. The MNS consists of neurons in the premotor cortex and parietal cortices that fire when somebody performs an action, but also when the same person observes someone else performing that action. It has been suggested that the MNS provides a link between self and other, and that it enables the understanding of the actions of others through the automatic simulation of the actions and associated mental states of the self (Gallese, 2006). It provides a common substrate for action observation and execution that supports our ability to infer the goals and intentions of others (Fogassi et al., 2005; Iacoboni et al., 2005). The MNS is also involved in imitation learning (Buccino et al. 2004) and empathy (Iacoboni et al., 2005). Impairment of the mirror neuron system might explain why children with autism find it difficult to understand motor intentions of others (Pierno et al., 2006) and to imitate (Williams, 2006). Support for dysfunction of the MNS in autism comes from Hadjikhani et al. (2005) who found smaller volumes of grey matter in areas belonging to the MNS than in a control group. This cortical thinning of the MNS was correlated with the severity of social problems. Another example of a study that supports the role of the MNS in autism is an fMRI study by Dapretto et al. (2005) in which individuals with ASD showed less mirror neuron activation in the inferior frontal gyrus during imitation and observation of facial expressions compared to control participants. Furthermore, TMS data show reduced corticospinal facilitation during action

observation (Théoret et al., 2005) and Cattaneo et al (2007) showed that children with autism lack the mechanism for understanding intentions of others experientially using electromyographic recordings.

Whereas frontoparietal mirror-neuron areas provide the basis for bridging the gap between the physical self and others through motor-simulation mechanisms, cortical midline structures (CMS) (dorsal and ventral medial prefrontal cortex and the precuneus) and lateral structures such as the temporoparietal junction are involved in the processing of self-referential stimuli and in processing information about the self and others in more abstract, evaluative terms (Uddin, 2007). These areas are components for the neural system for Theory of Mind, the ability to attribute mental states such as beliefs, intents, desires, pretending and knowledge to another person (Premack & Woodruff, 1978). A similar distinction between the mirror neuron area's and Theory of Mind area's is made by Iacoboni (2006) who suggests that internally oriented processes that focus on one's own or others' mental states rely on CMS and lateral structures, whereas externally focused processes based on one's own or others' visible actions rely on mirror neurons in frontoparietal networks. CMS are activated during tasks of a social nature (Iacoboni et al., 2004). Besides processing information of mental states of the self and others, CMS and lateral structures are involved in sense of agency, which requires differentiation between one's own and other people's actions. The precuneus is suggested to be part of a network in which personal identity and experiences (Cavanna & Trimble, 2006), and sense of agency (Vogely et al., 2001, Vogeley & Fink, 2003) are processed. Moreover, it has been shown that the temporoparietal junction is important in determining agency in situations where one must distinguish between actions generated by oneself and another agent (Chaminade & Decety, 2002; Blakemore et al., 2003). Several studies indicate that children with autism have difficulty with processes that rely on CMS and lateral structures. They have impaired recognition memory for potential agents and superior memory for objects that clearly do not have agency (Blair et al., 2002). Other studies show limitations in mentally representing themselves in relation to others (Lee & Hobson, 1998). Neuro-imaging evidence for abnormalities in CMS comes from Kennedy et al. (2006) who found that children with autism fail to reduce activity of the 'default network': cortical areas that show high metabolic activity at rest and typically reduced activity while

subjects are engaged in laboratory tasks designed to investigate classical cognitive functions. This network has been associated with self-oriented thoughts. Abnormalities in children with autism are also found in the precuneus (Rojas et al. 2006) and temporoparietal junction (Barnea-Goraly, 2004).

So, there is support for the idea that the MNS is impaired in subjects with ASD and that this leads to poor representation of the actions. In addition, impaired CMS leads to poor sense of agency. This could explain their problems in communication and relationships with other people. Therefore, an interesting question is how children with autism perform on tasks which require self-other representation and sense of agency in order to successfully cooperate with other people, i.e. joint-action tasks.

### 1.1 The MNS and CMS in joint action

Many situations require the cooperation of people, e.g. during a football game the players have to take into account the movements of their team mates or when two persons carry a heavy suitcase together, they have to walk at the same speed. These joint actions are shared co-operative activities that require the integration of intention, goal and action (Bratman, 1992). In order to complete such a joint-action task successfully, people have to process the effects of their own actions on the environment but also the effects of the actions of the other person with whom we cooperate. They have to be willing to correct the mistakes made by the co-actor, hence to allow for modifications of their own actions in response to others' errors or failed actions (Pacherie & Dokic, 2006). Research has shown that actors form an internal model of the joint-dynamics of the action of which they are part (Jordan, 1994). This makes it possible to learn to make accurate behavioural predictions (Dizio & Lackner, 1995). Other studies indicate that individuals form shared representations of tasks automatically, even when it is more effective to ignore one another (Sebanz, 2003). Sebanz et al. (2005) showed that in a joint-action situation, actors know what the other should do and that the other's task was represented in a functionally equivalent way to one's own.

Given the role of mirror neurons in action observation and action execution, it has been suggested that mirror neurons in the inferior frontal and inferior parietal areas might be a critical component in joint action (Newman-Norlund et al., 2007). Processing of goals is important in joint

action because in order to cooperate, actors must have the same goal. Knowledge about the actions that somebody else can perform and the underlying intentions of his or her actions can be integrated into the internal model of the task on which our own actions are based. Other support for the role of the MNS in joint action comes from Newman-Norlund et al. (2007) who found greater activity in the MNS when participants executed complementary movements compared to imitative movements. This suggests that the MNS may be essential in dynamically coupling action observation to action execution. Recent evidence for the involvement of the MNS in joint action comes from an fMRI-study of Newman-Norlund et al. (2008). They showed that when participants performed a virtual lift and balance task in which they had to lift a bar into a target area, brain areas with mirror neurons implicated in simulation (left inferior parietal lobule, left inferior frontal gyrus, and left superior temporal sulcus) were more active in the joint-action condition compared to a solo condition. These data suggest that participants were engaging more motor simulation of others' actions, or in other words that there was more activation of the MNS during the joint-action condition. In addition, there was more activity in the joint action condition that was the most demanding and required close cooperation. This indicates that tasks in which people have to cooperate in order to reach a common goal require motor simulation supported by activation of the MNS.

Newman-Norlund et al. (2008) also found evidence that CMS and lateral structures areas play an important role in joint-action tasks. They found an increase in brain activity in the precuneus and the temporoparietal junction compared to a single condition. These areas are probably activated because this task requires sense of agency: actors had to disambiguate their actions from those of their co-actor and they were required to devote more effort to monitoring their actions. Disambiguation is not required to successfully perform the task, however it is likely that it would help in determining action patterns of the co-actor and anticipated these actions.

Hence, joint action relies on two different neural networks that are assumed to be impaired in autism. Therefore, it is likely that children with autism have difficulty performing joint action. Due to abnormalities in the MNS they might have problems representing the actions of the co-actor. As a consequence, the internal model of the task is not complete and it is difficult to predict and

anticipate the actions of the co-actor that are based on this model. Therefore, behaviour can not be adapted. In addition, due to impairment of CMS and lateral structures, children with autism could have poor sense of agency which will result in difficulty differentiating the action contributions of the self and the other in a joint action task.

## 1.2 Experimental paradigm and predictions

To test these hypotheses we designed a study 1) to investigate whether children with ASD indeed have difficulty with differentiating the action contribution of the self and the other 2) to investigate whether children with ASD have problems with building an internal model of the timing of actions of the co-actor that could help them to anticipate to actions of others. We exploited a virtual bar-balancing task with three conditions similar to ones used by Newman-Norlund, Bosga, Meulenbroek and Bekkering (2008).

To examine whether there is a difference in motor performance between the ASD participant group and the control group on the bar-balancing task when no cooperation is required, participants performed the task alone with two hands in a single condition first. Group differences were not expected, although motor impairments in children with ASD could have an influence (Green et al., 2002; Johansen-Berg et al. 2007). In a second condition, the actors performed the task together with four hands. In this condition, it was particularly difficult to disambiguate the action contributions of the self and the other. To examine whether children with ASD have difficulty with self-other differentiation, the lift distribution was examined in this condition. Children with ASD were expected to avoid the ambiguous situation by lifting the bar with the hand that was compatible with their position: the left actor was predicted to primarily use his/her left hand that controlled the left end of the bar, the right actor was predicted to primarily use his/her right hand that controlled the right end of the bar. As a consequence of the difficulty in self-other differentiation, children with ASD were predicted to have poor overall performance in this condition. To examine whether children with ASD are impaired in building an internal model of the actions of the co-actor, temporal synchronization of the movement onset of the actors was measured in a third condition in which participants had to lift the bar together with two hands. Short reaction times of the ASD participant group were expected because

they have difficulty waiting at the other participant. This was expected to result in poor anticipation to the actions of the co-actor and poor temporal synchronization, as expressed in long inter-individual reaction time differences.

## 2. Methods

### 2.1 Participants

The experimental group consisted of 28 children with ASD from Karakter Zwolle, a psychiatric institute for children. The control group consisted of 28 children from regular primary schools and students from the Radboud University. The children's age ranged between 8 and 18 years. The intelligence of both groups was estimated with the subtests block design, picture completion similarities and arithmetic of the WISC-III. Participants with an IQ lower than 80 were excluded. Autism spectrum diagnoses were made by a psychologist who had considerable experience with autistic spectrum diagnoses. Data on each child was gathered using the Autism Diagnostic Interview-Revised (ADI-R; Lord, Rutter, & LeCouter, 1994) and the Autism Diagnostic Observation Schedule (ADOS; Lord et al., 1989). All children with ASD showed impairments in social interaction, communication or stereotyped behaviour. Normal behavioural functioning in the control group was screened using Dutch versions of the Parent form of the Child Behavior Checklist (Achenbach, 1991) and the Children's Social Behaviour Questionnaire, the VISK (Luteijn et al., 1998). None of the control participants was reported to have behavioural problems. All participants had normal vision or corrected to normal vision. The parents of all children gave their informed consent as well as children above the age of twelve years. The children were rewarded with a gift voucher.

### 2.2 Apparatus

Participants were paired with another child of the same age (less than an age difference of one year) from the same experimental group. They were seated comfortably on adjustable chairs side by side in front of a table. The virtual bar-balancing task was realized using Presentation software (<http://nbs.neuro-bs.com>) and displayed on a monitor (refresh rate 75 Hz; 1024 by 768 pixels) that was placed on eye level. The participants were able to control the bar

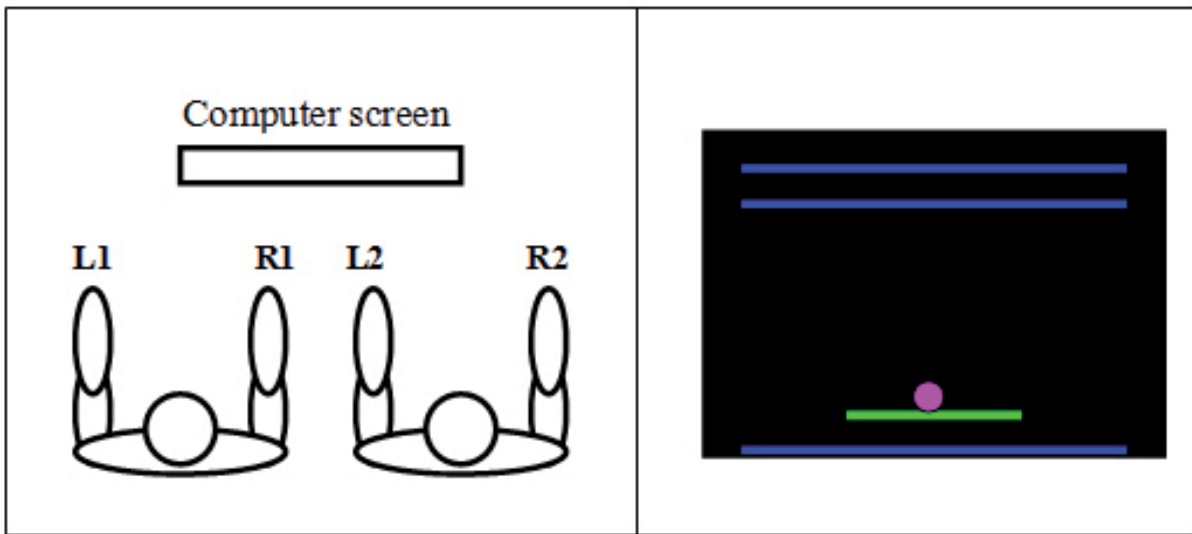


**Figure 1.** A top view of the experimental setup (left panel). The bar (right panel) was controlled by L1, R1, L2, R2 in the J4-condition and by L1 and R2 in the J2-condition.

by vertically rotating four joy-sticks (Logitech Dual Action), one joy-stick for each hand (see figure 1). Lateral rotations of the joy-sticks did not affect the position of the bar, only forward-backward motion did. The visual effects of the joy-stick rotations on the computer screen were linked. The output signals of the left-hand joy-sticks of each participant, i.e. L1 and L2, were combined and the output signals of the right-hand joy-sticks R1 and R2 were also summated. Output signals of the gamepad were sampled at a rate of 75 Hz and smoothed by running-average technique with a window -size of 30 samples. Then, the output signal was multiplied by a gain factor of 3.5 to produce positional output of the bar in pixels.

### 2.3 Task and procedure

Before the experiment started, instructions were given to the participants and they were asked not to communicate with each other during the task. The participants were allowed to become familiar with the task during three practice trials before each condition. At the start of each trial there was a countdown of three seconds before each trial visible on the screen and the children were asked to wait during that countdown. If they started moving the joy-sticks before the countdown was finished, the Dutch words 'Valse Start ('false start') were displayed on the screen and the countdown was started over again. After the countdown, a horizontal green bar with a pink ball on top was displayed on the monitor (see Figure 1). The angles of joy-sticks L1 and L2 together determined the height of the left-hand side of the bar and the angles of joy-sticks R1 and

R2 determined the height of the right-hand side of the bar. Participants were not able to change the horizontal position of the bar.

The dyads, i.e. participant pairs, had to lift the bar in 30 trials into a target area which consisted of two horizontal lines in the upper part of the screen (see the top two horizontal lines in Fig. 1). To complete a trial successfully they had to hold the bar between the horizontal lines for two seconds without dropping the ball. Participants received feedback whether the bar was positioned correctly in the target area by the colour of the bar which changed from green to white when it was positioned in the target area. When the bar was two seconds in target area, the colour changed to purple. The maximum duration of a trial was 15 seconds.

In the single condition (S), one participant lifted the bar on his/her own with both hands. This condition was always performed first in order have a baseline measure of bimanual motor performance of the experimental and the control group. Sometimes more practice trials (maximum 9 trials) were required before the single condition because some children didn't understand the task. In the joint-action condition with four hands (J4) participants lifted the bar together with four hands (L1, R1, L2, R2), the right hands controlling the right end of the bar and the left hands controlling the left end. The joint-two hands (J2) condition required more explicit cooperation because each participant controlled one side of the bar. Participants sitting on the right side used their right hand (R2) to control the right end of the bar and participants on the left side used their left hand (L1) to control the left end of the bar. By distributing the joy-stick rotation

evenly both with respect to space (left versus right) and time (the trial duration) they could keep the bar in a horizontal orientation while it was being lifted. The J2 and J4-conditions were randomly assigned as second and third condition.

## 2.4 Data analyses

The overall performance of the two groups, as expressed in success rates and time in target area (ms), was measured in order to evaluate Group differences in the outcome of the joint-action task. Overall performance was also expressed in height of ball drop to examine whether children with ASD lost the ball in an earlier stage of the task. In addition, rotation of the bar was derived to assess overall performance because poor inter- and intrapersonal coordination was expected to lead to instability of the bar orientation during the task.

To investigate whether there were group differences in the time domain, reaction times were measured. A zero joy-stick rotation measurement just before the start of the experiment was obtained to calibrate the zero point. Reaction times were derived by an algorithm that measured when the joy-stick rotation was larger than the zero measurement plus a constant (equal to 1 degree change of the rotation of the joy-stick). Inter-individual reaction time differences were measured in order to assess action adaptation.

Furthermore, in the spatial dimension in the J4-condition, the lift distribution of L1, R1, L2 and R2 was examined by calculating the contribution to the lift of the bar of each hand:

$$\text{Outer hands: } \%L1 = L1 / (L1+R1) *100 \\ \%R1 = R1 / (L1+R1) *100$$

$$\text{Inner hands: } \%L2 = L2 / (L2+R2) *100 \\ \%R2 = R2 / (L2+R2) *100$$

Distribution of lift can occur when the participant on the left rotates primarily his left joy-stick and the participant on the right primarily his right joystick. Then, the percentage lift of the outer hands (L1 and R2, see fig. 1) will be larger than the percentage lift of the inner hand (R1 and L2). A typical example of a lift distribution is depicted in figure 2.

## 2.5 Statistical evaluation

First, t-tests were applied to test whether there were differences in Group characteristics. Then, overall performance as expressed in success rates, time of the bar in target area, bar rotation, and height of ball drop was examined. Sign tests were used to test the effects of Condition and Group on the success rate in the J2 and J4 condition. A Mann-Whitney test was used to evaluate the effect of Group on success rate in the single condition, which was not compared with the J2 and J4 condition because it was always performed first. Mann-Whitney tests were also used to examine Group effects on the success rates in the single, J2 and J4 condition. For the evaluation of effects of Group and Condition on time of the bar in target area, bar rotation and height of ball drop in the J2 and J4 condition Repeated Measures ANOVAs were used. T-tests were used to examine whether there were group differences in time in target area, bar rotation and height of ball drop in the single condition. T-tests were also used for post hoc comparisons to evaluate effects of Group on time in target area, bar rotation and height of ball drop within the J2 and J4 condition. In addition, paired sample t-tests were used as post hoc comparison to examine effects of Condition (J2, J4) on time in target area, bar rotation and height of ball drop within the experimental and control group.

To examine the time domain, mean reaction

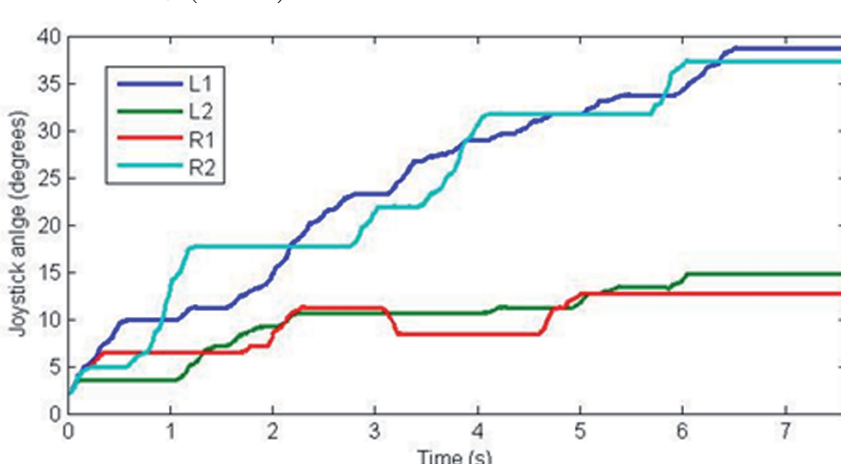


Figure 2. Example of a typical lift distribution of a dyad from the ASD participant group in a trial of the J4-condition.

**Table 1.** Mean percentage success rates, mean and standard deviation of Time in Target Area (TTA) (ms), Bar Rotation (BR) (degrees), height of ball drop (HBD) (pixels).

Group	Condition	%Success	TTA (SD)	BR (SD)	HBD (SD)
Children with ASD	S	16.0%	574 (108)	18 (1)	270.5 (39.1)
	J4	28.7%	904 (216)	20 (2)	482.0 (44.2)
	J2	23.7%	703 (247)	22 (2)	145.8 (59.9)
Control Group	S	24.7%	691 (123)	14 (2)	291.0 (42.0)
	J4	43.3%	1385 (155)	16 (1)	467.8 (40.2)
	J2	29.0%	976 (131)	17 (1)	371.6 (50.5)

times were calculated after exclusion of reaction times longer or shorter than 3 \* standard deviation of the reaction times within one trial, as well as reaction times shorter than 100 ms and longer than 1000 ms. Repeated Measures ANOVAs and paired sample t-tests were used to test effects of Condition and Group on reaction time. T-tests were used as post hoc comparison to examine Group differences in reaction time within the single, J2 and J4 condition. T-tests were also applied to evaluate the effect of Group on inter-individual reaction time difference in the J2-condition in order to assess action adaptation.

To examine the spatial dimension, lift percentages of outer hands (L1, R2) and inner hands (R1, L2) were calculated in order to examine the distribution of lift. The lift percentages were transformed to the normally distributed variable z by means of Fisher's z transform. ANOVAs were used to test the effects of Group, Hands (outer, inner) and sequence of condition (J2,J4 and J4,J2) on lift percentage. For post hoc comparison t-tests were used to test the effects of Hands and Group within each sequence of conditions. Pearson correlations between lift percentages outer hands, inter-individual reaction time differences and rotation of the bar were calculated to evaluate the influence of lift distribution on action adaption and overall performance. Bonferroni corrections were applied whenever multiple tests were conducted.

## 3. Results

### 3.1 Group characteristics

Autism and control subjects did not differ significantly in age,  $t(54)=-.4$ , ns, but did differ in Full Scale IQ, with the control group having a higher Full Scale IQ (mean=111.9) than the experimental group (mean=100.3),  $t(54)=-3.7$ ,  $p<.01$ .

## 3.2 Overall performance

### 3.2.1 Success rate

Overall performance was assessed by determining the dyads' success rates. The mean success rates are displayed in table 1. There was no significant difference in success rate between the groups in the single condition (Mann-Whitney test,  $N=56$ , ns). Neither was there a significant group difference in success rate in the J4-condition (Mann-Whitney test,  $N=28$ , ns) or J2-condition, (Mann-Whitney test,  $N=28$ , ns). However, nineteen of the twenty-eight pairs had a lower success rate in the J2-condition than in the J4-condition (sign test,  $N=28$ ,  $p<.01$ ). This effect of condition was only significant, however, for the control group (sign test,  $N=14$ ,  $p<.05$ ), but not for children with ASD (sign test,  $N=14$ , ns).

### 3.2.2 Time in target area

Another measure of overall performance was the duration that the bar was positioned in the target area (see Table 1). T-tests did not show a significant Group difference in time in target area in the single condition,  $t(54)=-.7$ , ns. The analysis of the J2 and J4-conditions did not show a significant Group difference,  $F(1,26)=2.3$ , ns. However, the mean time in the target area was significantly shorter in the J2-condition than in the J4-condition,  $F(1,26)=7.7$ ,  $p<.05$ . There was no significant Group\*Condition interaction,  $F(1,26)=.9$ , ns. In the control group, t-tests showed that time in target area was significantly longer in the J4-condition,  $t(13)=3.8$ ,  $p<.01$  compared to the J2-condition, whereas in the experimental group this effect was not significant,  $t(13)=1.05$ , ns.

### 3.2.3 Bar rotation

We also determined the mean bar rotation per trial as an index of overall task performance, the reason being that lifting the bar horizontally, i.e., without

any rotation, reflected ideal performance because only then the ball on top of the bar would remain on the bar. The mean bar rotation for each group and condition are displayed in table 1. The experimental group had a significantly larger mean bar rotation in the single condition compared to the control group,  $t(54)=2.6$ ,  $p<.05$ . Also the analysis of the J2 and J4-conditions showed that the experimental group had significantly larger bar rotation compared to the control group,  $F(1,26)=4.6$ ,  $p<.05$ . However, t-tests showed that this effect was only significant in the J2-condition,  $t(26)=2.2$ ,  $p<.05$ , not in the J4-condition,  $t(26)=1.8$ , ns). There was no significant effect of condition (J2, J4),  $F(1,26)=2.8$ , ns, and no Group\*Condition interaction,  $F(1,26)<1$ , ns.

### 3.2.4 Height of ball drop

For unsuccessful trials in each group, the height of the bar in pixels was measured at the moment that the ball dropped (see table 1). There was no significant difference between the experimental and the control group in the single condition,  $t(54)=-.4$ , ns. Neither was there a significant group difference in the joint conditions,  $F(1,26)=2.9$ , ns. However, pairs lost the ball at significantly lower height (maximum height is 768 pixels) in the J2-condition than in the J4-condition,  $F(1,26)=48.3$ ,  $p<.001$ . In addition, there was a significant Group\*Condition interaction,  $F(1,26)=14.9$ ,  $p<.01$ . T-tests showed that the experimental group lost the ball at significantly lower height in the J2-condition compared to the control group,  $t(26)=-2.9$ ,  $p<.01$ . This effect of Group was not significant in the J4-condition,  $t(26)=.2$ , ns. The effect of Condition was only significant for the experimental group,  $t(13)=7.9$ ,  $p<.001$ , but not for the control group,  $t(13)=2.1$ , ns.

### 3.2.5 Summary overall performance

The control group had higher success rates and more time in the target area in the J4-condition than in the J2-condition, whereas the performance of children with ASD did not differ between the joint conditions. In addition, children with ASD had a higher mean bar rotation in the single, as well as in the J2-condition compared to the control group . They also lost the ball at significantly lower height in the J2-condition compared with control children. Overall, this reflects that the children with autism investigated in the present study had difficulties with both joint conditions.

## 3.3 The time domain

### 3.3.1 Reaction time

The mean reaction time of the experimental group did not differ significantly from the mean reaction time of the control group in the single condition,  $t(54)=-1.5$ , ns. There was no significant effect of Condition (J4, J2) on reaction time,  $F(1,54)=2$ , ns, and no significant effect of Group,  $F(1,54)=2.8$ , ns. However, there was a significant Group\*Condition interaction,  $F(1,54)=5.06$ ,  $p<.05$ . Group differences in reaction time were not significant in the J4-condition,  $t(54)=-.3$ , ns, whereas the control group had significantly longer reaction times in the J2-condition compared to the experimental group,  $t(54)=-2.6$ ,  $p<.05$ , (see Fig. 3). In the experimental group there was no significant difference in reaction time between the J4 and J2-conditions,  $t(27)=.8$ , ns, whereas the control group had a significantly longer reaction time in the J2-condition than in the J4-condition,  $t(27)=-2.14$ ,  $p<.05$ .

### 3.3.2 Absolute inter-individual reaction time differences

The absolute inter-individual reaction time differences were measured in the J2-condition in order to evaluate whether the increase in reaction time in the control group was the consequence of an adaption process that led to smaller timing differences between actors. There were no significant group differences in the J2-condition,  $t(27)=-1$ , ns. However, the experimental group anticipated the start of the action of the co-actor in this condition significantly less compared to the control group. The control group had inter-individual timing differences

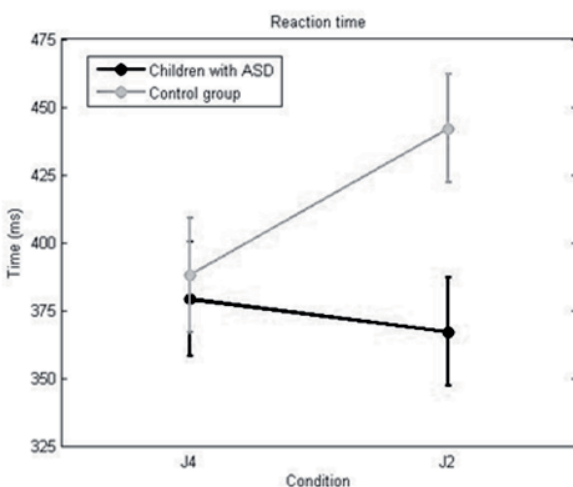


**Figure 3.** Mean reaction time for each group and condition.

below 100 ms in 20% of the trials whereas children with ASD only in 10% of the trials,  $t(26)=-2.5$ ,  $p<.05$ .

### 3.3.3 Summary time domain

Children with ASD had significantly shorter reaction time in the J2-condition compared with the control group. The control group showed a significant increase in reaction time in the J2-condition compared to the J4-condition, which might reflect an adaption process that takes into account the actions of the co-actor. This increase in reaction time is not present in children with ASD. This hypothesis that children with ASD find it difficult to adapt their actions to the actions of the co-actor is supported by the finding that they anticipated significantly less to the reaction time of the co-actor in the J2-condition compared to the control group.

## 3.4 The spatial dimension

In the comparison of the lift percentages of inner and outer hands, the Sequence of conditions (J4,J2 and J2,J4) was included as factor because the result could be influenced by biased outer hands due to experience that is acquired when the J2-condition is performed before the J4-condition. There was no significant effect of Group,  $F(1,104)<1$ , ns, and no effect of Sequence,  $F(1,104)<1$ , ns, on lift percentage. However, there was a significant effect of Hands,  $F(1,104)=10.0$ ,  $p<.01$ , a significant Group\*Hands interaction,  $F(1,104)=4.0$ ,  $p<.05$ , and a significant Sequence\*Hands interaction,  $F(1,104)=4.8$ ,  $p<.05$ . The 3-way Group\*Hands\*Sequence interaction however was not significant,  $F(1,104)=2.4$ , ns. The mean lift percentages inner and outer hands for each group are displayed in Figure 4a and 4b.

Then, the lift distribution was separately examined in each sequence of condition. First, the effects

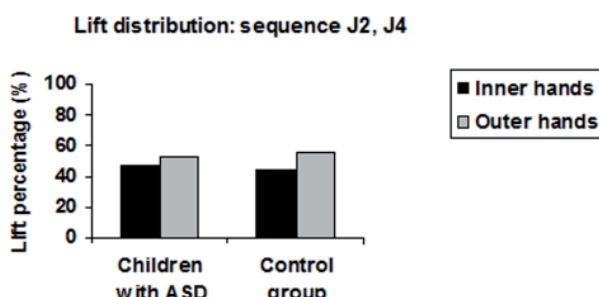


**Figure 4a.** Lift percentage inner and outer hands within total lift of one actor in the J4-condition when this condition was performed after the J2-condition.

**Lift distribution: sequence J4, J2**

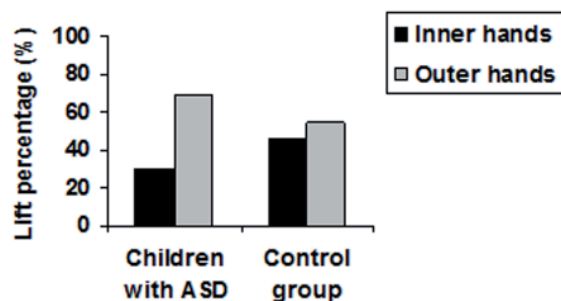


**Figure 4b.** Lift percentage inner and outer hands within total lift of one actor in the J4-condition when this condition was performed before the J2-condition.

of Group and Hands were analysed when the J4 condition was performed first. In this analysis there was no significant effect of Group,  $F(1,52)=1.1$ , ns. However, there was a significant effect of Hands,  $F(1,52)=13.0$ ,  $p<.01$ , and a significant Group\*hands interaction  $F(1,52)=7.1$ ,  $p<.05$ ). Post hoc comparisons showed that the lift percentage of the outer hands of the experimental group was significantly larger than the lift percentage of the inner hands,  $t(26)=3.3$ ,  $p<.01$ . This effect of Hands was not significant in the control group,  $t(26)=1.4$ , ns.

The analysis of the lift percentages when the J4 condition was performed after the J2 condition did not show an effect of group  $F(1,52)=1.1$ , ns. Neither was there an effect of Hands,  $F(1,52)=.3$ , ns, and no significant Group\*Hands interaction  $F(1,52)<1$ , ns.

These results indicate that children with autism rotate significantly more with the joy-stick that is compatible with their position when the J4-condition is performed before the J2-condition, whereas control children do not. To test whether children with autism made more corrections with their outer hands as well, the covariation coefficient was calculated by dividing the standard deviation of the angle of each joy-stick by the mean angle of each joystick. There was no significant effect of Group, ( $F(1,104)<1$ , ns), Hands ( $F(1,104)<1$ , ns), Sequence ( $F(1,104)=1.5$ , ns). Neither was there a significant Group\*Hands interaction ( $F(1,104)=1.6$ , ns), significant Sequence\*Hands interaction ( $F(1,104)=1.2$ , ns), Group\*Sequence ( $F(1,104)=1.6$ , ns) or Group\*Sequence\*Hands interaction ( $F(1,104)<1$ , ns).

To test whether distribution of lift was an effective strategy for children with ASD to deal with ambiguous self-other contribution, the correlation between lift percentage outer hands and bar rotation in the J4 condition was calculated. There was a significant negative correlation in the experimental

group (Pearson  $r=-.56$ ,  $p<.01$ ), whereas there was no correlation in the control group (Pearson  $r=-.24$ , ns). The relation between lift percentage outer hands and bar rotation was also evaluated by comparison of a group of children with ASD with small distribution of lift ( $N=14$ , lift percentage outer hands < 58%) and a group of children with ASD with larger distribution of lift ( $N=14$ , lift percentage outer hands > 58%). Children with ASD who had larger distribution of lift had marginal significant smaller mean bar rotation in the J4-condition ( $M=19.4$  degrees) than children with ASD who had less distribution of lift ( $M=23.9$ ) ( $t(26)=2.01$ ,  $p=.072$ ). In the control group, lift percentage did not have effect on bar rotation ( $t(26)=1.5$ , ns).

There is a possibility that children with ASD who distribute lift are better in representing the actions of the other person compared to children who do not distribute lift. As a consequence, children who distribute lift could have smaller inter-individual reaction time differences. Therefore, the correlation between lift percentage outer hands and absolute inter-individual reaction time difference in the J4-condition was calculated. There was a significant negative correlation in the experimental group (Pearson  $r=-.48$ ,  $p<.01$ ), whereas in the control group there was no significant correlation between lift percentage outer hands and absolute inter-individual reaction time difference (Pearson  $r=-.08$ , ns). The analysis with the group who had large distribution of lift the group who had small distribution of lift showed that children with ASD who had larger distribution of lift had smaller absolute inter-individual reaction time difference in the J4-condition ( $M=187.9$  ms) than children with ASD who had less distribution of lift ( $M=236.6$ ) ( $t(26)=-5.9$ ,  $p<.001$ ).

### *3.4.1 Summary spatial dimension*

Children with ASD lift the bar more with their outer hands (L1, R2) compared to their inner hands (R1, L2) in the J4-condition when this condition is performed first. The negative correlation between lift percentage outer hands of children with ASD and rotation of the bar in the J4-condition and the marginally significant group difference between children with ASD who show lift distribution and those children who do not distribute lift, indicates that distribution of lift leads to better performance. In addition, the negative correlation between lift percentage outer hands and absolute inter-individual reaction time difference in the J4-condition indicates

that distribution of lift is an effective strategy for children with ASD. Children with ASD who distribute lift have smaller absolute inter-individual reaction time differences in the J4-condition. This indicates that children with ASD who distribute lift are better in representing the actions of the co-actor.

## 4. Discussion

Because joint action relies on two different neural networks that are assumed to be impaired in autism, we hypothesized that children with ASD have difficulty performing joint action. First, due to impairment of CMS and lateral structures, children with ASD were expected to have difficulty differentiating the action contributions of the self and the other in a joint action task. To test this hypothesis, children had to perform the bar-balancing task with another actor with four hands. As expected, we found that children with ASD distribute the lift of the bar by rotating the joy-stick more with their outer hands than with their inner hands and that this distribution of lift leads to improved performance. Second, due to impairment of the MNS, children with ASD were expected to have problems representing the actions of the co-actor. This was expected to lead to problems in building an internal model of the joint action and to problems in anticipating the actions of the co-actor. As expected, children with ASD anticipated the movement onset of the co-actor less compared to the control group. These findings will be discussed below after a discussion of the possible influence of motor impairments. Another variable that could have influence on the results is IQ. The children with ASD that participated in the present study have a lower IQ than the control children.

### **4.1 Influence of motor impairments on overall performance**

Because it is likely that children with autism have motor impairments (Green et al., 2002), the single condition was included in the present study in order to have a baseline measure of motor performance of children with ASD and control children. Although the success rates did not differ in this condition, the bar rotation was larger in children with ASD compared to the control group. It seems that it is difficult for them to make accurate movements in order to stabilize and to maintain the horizontal orientation of the bar. An explanation for this problem might be abnormalities

in the corpus callosum. Vidal et al. (2006) reported a significant reduction in both the splenium and genu of the corpus callosum, reflecting decreased interhemispheric connectivity. Johansen-Berg et al. (2007) showed that variation in white matter integrity in the body of the corpus callosum is associated with variation in performance of a bimanual co-ordination task. Because the bar-balancing task that was used in the present study requires bimanual coordination, it is likely that corpus callosum deficits have influence on overall performance. Corpus callosum deficits could also explain more general motor impairment that has been reported in children with autism. Motor impairment in autism has been shown by behavioural neurological assessment (Teitelbaum et al., 1998), gait analyses (Vernazza-Martin et al., 2005) and analyses of movement kinematics during reach-and grasp experimental tasks (Hughes, 1996). Hence, due to the importance of the corpus callosum in bimanual co-ordination (Marion et al., 2003) it is likely that the abnormalities that are found in children with autism will have influence on the rotation of the bar in the bar-balancing task that was used. However, motor impairment can not explain other findings in the present study.

#### **4.2 Self-other differentiation in autism**

Due to impairment of CMS and lateral structures, children with ASD were expected to have difficulty differentiating the action contributions of the self and the other in a joint action task. Therefore, we expected to find poor performance in children with ASD in the J4-condition in which self-other differentiation was particularly difficult. As opposed to our expectations, we did not find poor overall performance of children with ASD in this condition. So, although children with ASD might have difficulty with self-other differentiation, this does not lead to poor overall performance on a joint action task in which action contributions are ambiguous.

The finding that children with ASD do not have poor overall performance in this condition might be the result of lift distribution in the spatial dimension. The ASD participants lift more with the hand that is compatible with their position relative to the co-actor. This finding supports the hypothesis that children with ASD have difficulty with self-other differentiation. They are not able to disambiguate the action contributions of the self and the other and they try to avoid the ambiguous movements of the bar that are composed of actions of both actors by rotating the joy-sticks more with

their outer hands. The lift distribution can not be the result of biased outer hands due to experience that is acquired when the J2-condition is performed before the J4-condition because it only occurs when the J4-condition is performed first. An explanation for the absence of this effect when the J4-condition was administered second might be that children with ASD had practiced and learned to cooperate in the J2-condition and are therefore better in representing the other in the J4-condition. As a consequence, lift distribution is no longer necessary to disambiguate the actions of the self and the other.

So, in the J4-condition, problems with self-other differentiation do not lead to poor overall performance for children with ASD because they develop their own disambiguation strategy. They were able to compensate for difficulty with self-other differentiation by lift distribution. This is supported by the negative correlation between distribution of lift and rotation of the bar. For children with ASD who did not distribute lift, difficulty with self-other differentiation led to larger bar rotation. In addition, children with ASD who distribute lift had smaller inter-individual reaction time differences compared to children who did not. This means that these children were better in representing the action of the co-actor.

#### **4.3 The internal model of the timing of the joint action**

Due to impairment of the MNS, children with ASD were expected to have problems in representing the actions of the co-actor. This was expected to lead to problems in building an internal model of the joint action and to problems in anticipating the actions of the co-actor. This hypothesis was tested in the J2-condition that required close cooperation, in particular anticipation of the movement onset of the co-actor. Evidence that the control group adapts their reaction time is the finding that they increase their reaction time in the J2-condition compared to the J4-condition. These findings are surprising because Kelso et al. (1979) and Ohtsuki (1994) showed that unilateral movements such as in the J2-condition are normally initiated faster than simultaneous bilateral actions that are carried out by two hands because of the interhemispheric inhibition in the latter condition. This could mean that in the J2-condition participants take into account the actions and the preparation for the task of the other. The finding that children with ASD do not increase their reaction times means that they take the

actions of the co-actor less into account than the control group.

Our finding is similar to the results of a study by Bosga and Meulenbroek (2007) in which participants had to lift a virtual bar in a single condition with both hands or with one hand or two hands in two joint action conditions. They found that both individuals and dyads in the two-handed conditions were equally fast in preparing and initiating the movement. A difference is that we found an increase in reaction time in the control group in the J2-condition, whereas Bosga and Meulenbroek did not find an increase in healthy participants. This could be explained by the fact that participants in the present study had to balance a ball on top of the bar whereas there was no ball in the study of Bosga and Meulenbroek. Adaptation of reaction time is more important in this study because poor adaptation leads to ball drop.

The hypothesis that difficulty with building an internal model of the joint action leads to problems in anticipating the actions of the co-actor was also supported by the finding that children with ASD made less anticipations to the start of the movement of the co-actor. This could be caused by difficulty with representing the reaction times of the co-actor over time, and the inability to use this information for aligning the response onsets in accordance with their co-actor in subsequent trials. Successful adaption, which is based on an internal model of the task, will not be acquired when this model is incomplete due to poor representation of the actions of the co-actor. The poor adaptation and anticipation of the reaction times in children with ASD leads to a larger bar rotation and lower height of ball drop in the J2-condition.

#### 4.4 Conclusion

In the present study we examined whether children with ASD have difficulty with self-other differentiation of action contributions in a joint action task. Problems with self-other differentiation are likely because CMS and lateral structures, which are involved in sense of agency and self-other differentiation, have shown to be impaired in ASD. The results of the J4-condition showed that children with ASD distribute lift by rotating more with their outer hands than with their inner hands. This distribution of lift is not present in the control group and supports the hypothesis that children with ASD have difficulty in differentiating between the action contributions of the self and the other. However,

because they have their own disambiguation strategy, difficulty with self-other differentiation does not lead to poor performance in this task. The present study also aimed to investigate whether children with ASD have difficulty forming an internal model of the timing of the actions of the co-actor due to impairments in the MNS. The results of the J2-condition showed that this indeed is the case. Children with ASD take the movement onset of the co-actor less into account and anticipated less to the actions of the co-actor compared to the control group. This is probably caused by difficulty with representing the actions of the other. As a consequence, the internal model of the task is incomplete and this leads to poor anticipation. In addition, we also found that motor impairments in ASD might have influenced the performance of the bar-balancing task. Future experiments involving joint action in children with autism might explore the role of motor impairments in joint action, for example by comparison with a group of children with developmental coordination disorder. Neuro-imaging studies might contribute to the understanding of the different roles of impairments in the MNS and CMS in joint action.

#### References

- Achenbach, T. M. (1991). Integrative Guide to the 1991 CBCL/4-18, YSR, and TRF Profiles. Burlington, VT: University of Vermont, Department of Psychology.
- Barnea-Goraly, N., Kwon, H., Menon, V., Eliez, S., Lotspeich, L., Reiss, A.L. (2004). White matter structure in autism: preliminary evidence from diffusion tensor imaging. *Biological Psychiatry*, 55(3), 323-6.
- Baron-Cohen, S., Baldwin, D.A., Crowson, M. (1997). Do children with autism use the speaker's direction of gaze strategy to crack the code of language? *Child Development*, 68(1), 48-57.
- Baron-Cohen, S., Jolliffe, T., Mortimore, C., Robertson, M. (1997). Another advanced test of theory of mind: evidence from very high functioning adults with autism or asperger syndrome. *Journal of Child Psychology and Psychiatry, and allied disciplines*. Oct 38(7), 813-822.
- Blair, R.J.R., Frith, U., Smith, N., Abell, F., Cipolotti, L.(2002). Fractionation of visual memory: agency detection and its impairment in autism. *Neuropsychologia*, 40, 108–118.
- Blakemore, S.J., Oakley, D.A., Frith, C.D. (2003). Self-awareness and action. *Current Opinion in Neurobiology*, 13, 219–222.
- Bosga, J., Meulenbroek, R.G.J. (2007). Joint-action coordination of J4 force contributions in a virtual lifting task. *Motor-Control*, 11(3), 235-258.
- Bratman, M. (1992). Shared cooperative activity. *The*

- Philosophical Review, 101.2, 327-341.
- Buccino, G., Binkofski, F., Fabbri-Destro, M., Rizzolatti, G. (2004). The mirror neuron system and action recognition. *Brain and Language*, May 89(2), 370-376.
- Cattaneo, L., Fabbri-Destro, M., Boria, S., Pieraccini, C., Monti, A., Cossu, G., Rizzolatti, G. (2007) Impairment of actions chains in autism and its possible role in intention understanding. *Proceedings of the National Academy of Sciences of the United States of America*, 104(45), 17825-17830.
- Cavanna, A.E., Trimble, M.R. (2006). The precuneus: a review of its functional anatomy and behavioral correlates. *Brain*, 129, 564-583
- Chaminade, T., Decety, J. (2002). Leader or follower? Involvement of the inferior parietal lobule in agency. *NeuroReport* 13, 1975-1978.
- Dapretto, M., Davies, M.S., Pfeifer, J.H., Scott, A.A., Sigman, M., Bookheimer, S.Y., Iacoboni, M. (2006) Understanding emotions in others: mirror neuron dysfunction in children with autism spectrum disorders. *Nature Neuroscience*, Jan 9(1), 28-30.
- D'entremont, B., Yazbek, A. (2007). Imitation of intentional and accidental action by children with autism. *Journal of Autism and Developmental Disorders*, Oct 37(9), 1665-1678.
- Dizio, P., & Lackner, J. R. (1995). Motor adaptation to coriolis force perturbations of reaching movements: Endpoint but not trajectory adaptation transfers to the nonexposed arm. *Journal of Neurophysiology*, 74, 1787-1792.
- Fogassi, L., Ferrari, P.F., Gesierich, B., Rozzi, S., Chersi, F., Rizzolatti, G. (2005). Parietal lobe: From action organization to intention understanding. *Science*, 29, 662-667.
- Gallese, V. (2006). Intentional attunement: a neurophysiological perspective on social cognition and its disruption in autism. *Brain Research*, 1079, 15-24.
- Green, D., Baird G., Barnett, A.L., Henderson, L., Huber, J., Henderson, S.E. (2002). The severity and nature of motor impairments in Asperger's syndrome: a comparison with specific developmental disorders of motor function. *Journal of child psychology and psychiatry*, 43(5), 655-688.
- Hadjikhani, N., Joseph, R.M., Snyder, J., Tager-Flusberg, H. (2006). Anatomical differences in the mirror neuron system and social cognition network in autism. *Cerebral Cortex* 16, 1276-1282.
- Hamilton, A.F., Wolpert, D. M., Frith, U., Grafton, S.T. (2006). Where does your own action influence your perception of another person's action in the brain? *NeuroImage*, Jan 29(2), 524-535
- Hill, E.L. (2004), Executive dysfunction in autism. *Trends in Cognitive Science*, 8, 26-32.
- Hughes, C. (1996). Brief Report: planning problems in autism at the level of motor control. *Journal of autism and developmental disorders*, 26, 99-108.
- Iacoboni, M., Woods, R.P., Brass, M., Bekkering, H., Mazziotta, J.C., Rizzolatti, G. (1999). Cortical mechanisms of human imitation. *Science*, 286, 2526-2528.
- Iacoboni, M., Lieberman, M.D., Knowlton, B.J., Molnar-Szakacs, I., Moritz, M., Throop, C.J., Fiske, A.P. (2004). Watching social interactions produces dorsomedial prefrontal and medial parietal BOLD fMRI signal increases compared to a resting baseline. *Neuroimage*, 21, 1167-1173
- Iacoboni, M., Molnar-Szakacs, I., Gallese, V., Buccino, G., Mazziotta, J. C., & Rizzolatti, G. (2005). Grasping the intentions of others with one's own mirror neuron system. *PLOS Biology*, 3, 529-535.
- Iacoboni, M. (2006). Failure to deactivate in autism: the co-constitution of self and other. *Trends in Cognitive Science*, Oct 10(10), 431-433.
- Johansen-Berg, H., Della-Maggiore, V., Behrens, T.E., Smith, S.M., Paus, T. (2007). Integrity of white matter in the corpus callosum correlates with bimanual coordination skills. *Neuroimage*, 36 Suppl 2: T16-21.
- Jordan, M.I. (1994). Computational motor control. In M.S. Gazzaniga (Ed.). *The cognitive neurosciences* (pp. 597-609). Cambridge, MA: MIT Press.
- Kelso, J.A., Southard, D.L., Goodman, D. (1979). On the coordination of two-handed movements. *Journal of Experimental Psychology: Human Perception and Performance*, 5, 229-238.
- Kennedy, D.P., Redcay, E., Courchesne, E. (2006). Failing to deactivate: resting functional abnormalities in autism. *Proceedings of the National Academy of Sciences of the United States of America*. May 103(21), 8275-80.
- Lee, A., Hobson, R.P. (1998). On developing self-concepts: a controlled study of children and adolescents with autism. *Journal of Child Psychology and Psychiatry*, Nov 39(8), 1131-1144.
- Leekam, S.R., Lopez, B., Moore, C. (2000). Attention and joint attention in preschool children with autism. *Developmental Psychology*, Mar 36(2), 261-273.
- Lord, C., Rutter, M., & Le Couteur, A. (1994). Austin Diagnostic Interview-Revised. *Journal of Autism and Developmental Disorders*, 24, 659-686.
- Lord C, Risi S, Lambrecht L, Cook EH Jr, Leventhal BL, DiLavore PC, Pickles A, Rutter M (2000). The autism diagnostic observation schedule-generic: a standardized observation of communicative and social behavior associated with the spectrum of autism. *Journal of Autism and Developmental Disorders*, 3, 205-223.
- Luteijn, E.F., Jackson, A.E., Volkmar F.E., Minderaa, R.B. (1998) The development of the Children's Social Behavior Questionnaire: Preliminary data. *Journal of Autism and Developmental Disorders*, 28(6), 559-565.
- Marion, S.D., Kilian, S.C., Naramor, T.L., Brown, W.S. (2003). Normal development of bimanual coordination: visuomotor and interhemispheric contributions. *Developmental Neuropsychology*, 23(3), 399-421.

- Newman-Norlund, R.D., Noordzij, M.L., Meulenbroek, R.G.J., Bekkering, H. (2007). Exploring the brain basis of joint action: Co-ordination of actions, goals and intentions. *Social-Neuroscience*, Mar 2(1), 48-65.
- Newman-Norlund RD, van Schie HT, van Zuijlen AM, Bekkering, H. (2007). The mirror neuron system is more active during complementary compared with imitative action. *Nature Neuroscience*, Jul 10(7), 817-818.
- Newman-Norlund, R.D., Bosga, J., Meulenbroek, R.G.J., Bekkering, H. (2008). Anatomical substrates of cooperative joint-action in a continuous motor task: virtual lifting and balancing. *Neuroimage*, May 41(1), 169-77.
- Uddin, L.Q., Iacoboni, M., Lange, C., Keenan, J.P. (2004) The self and social cognition: the role of cortical midline structures and mirror neurons. *Trends in Cognitive Science*, Apr 11(4), 153-157.
- Ohtsuki, T. (1994). Changes in strength, speed, and reaction time induced by simultaneous bilateral muscular activity. In S.P. Swinnen, H. Heuer, J. Massion, & P. Casaer (Eds.), *Interlimb coordination: neural, dynamical and cognitive constraints* (259-274). San Diego, CA: Academic Press.
- Pacherie, E., Dokic, J. (2006). From mirror neurons to joint action. *Cognitive Systems Research*, Jun. 7(2-3), 101-112.
- Pierro, A.C., Mari, M., Glover, S., Georgiou, I., Castiello, U. (2005) Failure to read motor intentions from gaze in children with autism. *Neuropsychologia*, 44(8), 1483-1488.
- Premack, D. G. & Woodruff, G. (1978). Does the chimpanzee have a theory of mind? *Behavioral and Brain Sciences*, 1, 515-526.
- Rojas, D.C., Peterson, E., Winterrowd, E., Reite, M.L., Rogers, S.J., Tregellas, J.R. (2006). Regional gray matter volumetric changes in autism associated with social and repetitive behavior symptoms. *BMC Psychiatry*, Dec 13, 6-56.
- Sebanz, N., Knoblich, G., Prinz, W. (2003). Representing others' actions: just like one's own? *Cognition*, 88, B11-B21.
- Sebanz, N., Knoblich, G., Stumpf, L., Prinz, W. (2005) Far from action blind: representation of others' actions in individuals with autism. *Cognitive Neuropsychology*, 22, 433-454.
- Sebanz, N., Knoblich, G., Prinz, W. (2005). How two share a task: co-representing stimulus-response mappings. *Journal of Experimental Psychology. Human Perception and Performance*, 3, 1234-1246.
- Teitelbaum, P., Teitelbaum, O., Nye, J., Fryman, J., Maurer, R.G. (1998). Movement analysis in infancy may be useful for early diagnosis of autism. *Proceedings of the national academy of science: psychology*, 95, 13982-13987.
- Théoret, H., Halligan, E., Kobayashi, M., Fregni, F., Tager-Flusberg, H., Pascual-Leone, A. (2005). Impaired motor facilitation during action observation in individuals with autism spectrum disorder. *Current Biology*, 15, R84-R85.
- Uddin, L.Q., Kaplan, J.T., Molnar-Szakacs, I., Zaidel, E., Iacoboni, M. (2005). Self-face recognition activates a frontoparietal "mirror" network in the right hemisphere: an event-related fMRI study. *Neuroimage*. Apr 25(3), 926-935.
- Uddin, L.Q., Iacoboni, M., Lange, C., Keenan, J.P. (2007). The self and social cognition: the role of cortical midline structures and mirror neurons. *Trends in Cognitive Science*, Apr 11(4), 153-157.
- Vernazza-Martin, S., Martin, N., Vernazza, A., Lepellec-Muller A., Rufo, M., Massion, J., Assaiante, C. (2005). Goal Directed Locomotion and Balance Control in Autistic Children. *Journal of Autism and Developmental Disorders*, 35, 91-102.
- Vidal, C.N., Nicolson, R., DeVito, T.J., Hayashi, K.M., Geaga, J.A., Drost, D.J., Williamson, P.C., Rajakumar, N., Sui, Y., Dutton, R.A., Toga, A.W., Thompson, P.M. (2006). Mapping corpus callosum deficits in autism: an index of aberrant cortical connectivity. *Biological Psychiatry*, 60, 218-225.
- Vogeley, K., Fink, G.R. (2003). Neural correlates of the first-person-perspective. *Trends in Cognitive Science*, 7, 38-42.
- Vogeley, K., Bussfeld, P., Newen, A., Herrmann, S., Heppe, F., Falkai, P., Maier, W., Shah, N.J., Fink, G.R., Zilles, K. (2001). Mind reading: neural mechanisms of theory of mind and self-perspective. *NeuroImage*, 14, 170-181.
- Williams, J.H., Waiter, G.D., Gilchrist, A., Perrett, D.I., Murray, A.D., Whiten, A. (2006). Neural mechanisms of imitation and 'mirror neuron' functioning in autistic spectrum disorder. *Neuropsychologia* 44(4), 610-21.

# Differences in resting state functional connectivity related to learning a new language

Kim Veroude<sup>1</sup>, David Norris<sup>1</sup>, Peter Indefrey<sup>1,2</sup>

<sup>1</sup>*Donders Institute for Brain, Cognition and Behaviour, Nijmegen, The Netherlands*

<sup>2</sup>*Max Planck Institute for Psycholinguistics, Nijmegen, The Netherlands*

Functional connectivity, temporal correlations between neurophysiological activity of distinct areas, provides information about interactive processing in the brain. Previous studies have shown that correlations in the fMRI time courses of functionally related regions can be observed during rest. The aim of the current experiment was to investigate if differences in resting state functional connectivity can be related to exposure to a new language. We hypothesized that learning of novel word forms might be associated with stronger functional connectivity of regions that are involved in phonological processing. A naturalistic movie of a weather report in Mandarin Chinese was presented twice to Dutch native speakers, interleaved with three resting state periods during which the subjects closed their eyes and relaxed. Afterwards, a word recognition task was performed and the participants were divided into two groups, learners and non-learners, based on the results. The learners were able to recognize Chinese target words from the weather report, while the non-learners were not. In order to investigate functional connectivity of areas involved in phonological processing during rest, partial correlations were calculated. In the first resting state period, we found stronger functional connectivity for the learners compared to the non-learners for two region pairs, the left supplementary motor area and the left precentral gyrus as well as the left insula and the left rolandic operculum. In addition, after exposure to the weather report, functional connectivity between the left and right supramarginal gyrus was stronger for learners than for non-learners. These findings are interpreted as pre-existing and learning-induced differences between the two groups and are further discussed with respect to the functional role of these regions.

*Keywords:* functional connectivity, resting state, learning, language, phonology

---

Corresponding author of thesis: Kim Veroude, Donders Institute for Brain, Cognition and Behaviour: Centre for Cognitive Neuroimaging, P.O. Box 9101, 6500 HB, Nijmegen, The Netherlands, e-mail: kim.veroude@donders.ru.nl

## 1. Introduction

Neurocognitive research aims at revealing the underlying brain mechanisms of cognitive functions such as perception, language and memory. Hemodynamic methods, primarily functional Magnetic Resonance Imaging (fMRI) and Positron Emission Tomography (PET), are used for establishing correspondence between cognitive states or processes and changes in local blood flow. Traditionally, this is done by contrasting a condition of interest with a control condition, such as a lower-level baseline or rest. A blocked or event-related design specifying the time course of the conditions is used and the hemodynamic-response data are analyzed with a statistical model that takes into account the temporal order and duration of conditions. An increase in neural activity, measured indirectly as an increase in blood flow, indicates that a region is involved in the experimental task.

Findings from brain imaging studies have provided insight into which areas play a role in different cognitive functions. However, this type of research provides little information on how brain regions work together. Coactivation of areas during a specific task does not prove that these regions form a functional network. If one wants to investigate the coupling between areas, a possible approach is to look at low frequency ( $<0.08$  Hz) temporal fluctuations in the hemodynamic BOLD response. Functional connectivity is defined as correlations between the neurophysiological time courses of spatially distinct areas (Friston, Frith, Liddle, & Frackowiak, 1993). This constitutes a model-free analysis for hemodynamic-response data. In contrast, effective connectivity, the influence of one neural system on another, requires a priori specification of connections of interest.

Several studies have found that during rest, functionally related brain regions display correlations in the fMRI time courses. This was first demonstrated in the motor system (Biswal, Yetkin, Haughton, & Hyde, 1995). Functional connectivity has also been shown between other areas, for instance in the visual cortex (Lowe, Mock, & Sorenson, 1998), the language system (Cordes et al., 2000) and in the so-called default mode network (Greicius, Krasnow, Reiss, & Menon, 2003), a set of regions that show deactivations during task performance (Raichle et al., 2001). Recently, Damoiseaux et al. (2006) identified ten functionally relevant resting state networks by Independent Component Analysis (ICA) which were found to be consistent across subjects and across

sessions. These findings suggest that functional connectivity reflects true interaction between brain regions, although there is also some evidence for an effect of physiological noise, such as low frequency changes in respiration (Birn, Diamond, Smith, & Bandettini, 2006).

Other researchers have demonstrated that dependent on the state of the brain, the strengths of correlations in functional networks can differ. In patients suffering from schizophrenia, decreases in connectivity have been observed which may reflect disrupted functional integration in the brain (Liang et al., 2006). Altered functional connectivity is present in other disorders as well, including autism (Cherkassky, Kana, Keller, & Just, 2006) and ADHD (Tian et al., 2006). More subtle, temporary changes in correlations between brain regions also occur and can be the result of task performance. For example, functional connectivity between Broca's area and Wernicke's area was observed during rest and increased during continuous listening (Hampson, Peterson, Skudlarski, Gatenby, & Gore, 2002). In resting state after performance of a language task, stronger correlations were found between regions involved in that task (Waites, Stanislavsky, Abbott, & Jackson, 2005).

Functional and effective connectivity has been related to associative learning. In a study by Büchel, Coull and Friston (1999), subjects performed a task in which line drawings of objects were paired with locations. Over time, activation decreased in the ventral and dorsal visual stream, which indicates repetition suppression. In contrast, effective connectivity between these areas increased. These changes were correlated with individual task performance which shows that interactions between brain regions play a role in learning. Others have demonstrated comparable findings (McIntosh, Rajah, & Lobaugh, 1999; Toni, Rowe, Stephan, & Passingham, 2002).

In the current exploratory study we investigate differences in functional connectivity related to the learning of novel words. First exposure to a new language usually occurs in a complex real world situation. Nonetheless, previous experiments on vocabulary acquisition have used standard word-by-word presentation (Breitenstein & Knecht, 2002; Breitenstein et al., 2005; Mei et al., 2008; Wong, Perrachione, & Parrish, 2007). Other studies have correlated structural changes in the brain with language learning (Golestani, Molko, Dehaene, LeBihan, & Pallier, 2007; Lee et al., 2007). Looking at functional connectivity before and after natural language input

might provide additional information on aspects of vocabulary learning in a real world context.

A recent study investigated the behavioural effects of naturalistic exposure to a new language (Gullberg, Dimroth, Roberts, & Indefrey, in prep.). Dutch native speakers were presented with a movie of a weather report in Mandarin Chinese, a typologically unrelated language that was unknown to the participants. Afterwards, an auditory word recognition task had to be performed. The subjects were able to recognize words from the weather report that had occurred frequently and were highlighted by a gesture. Mean accuracy for these words was 64% (with a 50% chance level) after one exposure to the movie (6:14 minutes) and increased to 71% after two exposures. These results show that acoustic or phonological units can be segmented from the continuous speech stream during minimal exposure to a new language. In the current experiment, we use the materials from this study and combine it with resting state fMRI to investigate functional connectivity of brain regions involved in phonological processing.

There is considerable evidence that the phonological loop, a component of working memory, plays a role in acquiring novel word forms (Baddeley, 1986; Baddeley, Gathercole, & Papagno, 1998). The phonological loop consists of a subvocal rehearsal system and a phonological store. Neuroimaging research suggests that the pars opercularis (Brodmann area (BA) 44, part of Broca's area) and the left supplementary motor area (BA 6) are involved in phonological rehearsal while the left supramarginal gyrus (BA 40) mediates the storage of novel phonological forms (Paulesu, Frith, & Frackowiak, 1993; Smith, Jonides, Marshuetz, & Koeppe, 1998).

Indeed, several studies have found these brain regions to be important for word learning. The magnitude of activation in left inferior prefrontal cortex and bilateral parietal regions was shown to be greater for new than for familiar words and positively correlated with memory for these items (Clark & Wagner, 2003). Breitenstein et al. (2005) demonstrated increased activity in the left supramarginal gyrus during learning of a novel lexicon, in addition to modulations of the left hippocampus and fusiform gyrus. A positive correlation between vocabulary knowledge and grey matter density in bilateral supramarginal gyri has also been observed (Lee et al., 2007).

Another brain area that has been implicated in phonological recognition of words is the left insula (Bamiou, Musiek, & Luxon, 2003). On a phonological

working memory task, increasing load resulted in increased activation in the middle frontal gyrus, the insula, superior temporal gyrus and inferior parietal cortex. Of these areas, the left insula showed greater activation for balanced compared to unbalanced bilinguals (Chee, Soon, Lee, & Pallier, 2004).

The posterior superior and middle temporal regions also play a role in vocabulary acquisition. Stronger activation in the left posterior superior temporal region was found for successful learners while less successful learners displayed increased activation in areas involved in nonlinguistic pitch processing, working memory and attention (Wong, Perrachione, & Parrish, 2007). The activity in the superior temporal cortex differed between the two groups even before language training. Mei et al. (2008) also observed pre-existing differences between good and poor learners with the former having more activation in left middle temporal gyrus and superior temporal sulcus and less activation in right inferior frontal gyrus.

In summary, brain regions that appear to be involved in phonological acquisition of a new language are the left supramarginal gyrus, the pars opercularis, the left supplementary motor area, the insula and the posterior superior and middle temporal gyri.

We propose that learning of novel words is related to functional connectivity of these areas. The recruitment of a phonological network might manifest itself as stronger correlations between regions reflecting interactive processing. Therefore, we predict stronger functional connectivity for subjects that are able to extract phonological information compared to subjects that do not learn new word forms. These differences in functional connectivity between the two groups might be pre-existing or learning-induced.

## 2. Methods

### 2.1 Participants

Thirty-one healthy volunteers participated in the study (21 females, mean age 22, range 18 - 24) after giving written informed consent. They received money or course credit for their collaboration. All were native Dutch speakers without any knowledge of Chinese or a related language, according to their answers on a language background questionnaire (Gullberg & Indefrey, 2003). The participants were right-handed, had normal or corrected-to-normal

vision and no hearing problems. Three other subjects were discarded based on the behavioural results. Their D-prime values on a word recognition task were negative which indicates that they showed sensitivity to the stimuli but gave incorrect responses.

## 2.2 Materials

We used the materials of the experiment by Gullberg et al. (in prep.). A movie of a weather report in Mandarin Chinese was recorded in a controlled, but naturalistic manner. Six weather charts were presented with a verbal description by a native Mandarin Chinese speaker. The movie lasted 6:14 minutes and contained 24 target words in four conditions of six target words (two verbs, two nouns, two function words) each: frequent (eight occurrences) or infrequent (two occurrences) and highlighted (yes or no) by a gesture forming a deictic link to the referential context, the icons on the weather chart. In a subsequent auditory word recognition task the 24 target words and 72 filler words were presented randomly. Participants had to indicate by button press whether they had heard the word in the weather report or not. Two versions of this task were created using Presentation software ([www.neurobs.com](http://www.neurobs.com)) and counterbalanced across subjects to avoid order effects.

## 2.3 Experimental paradigm

The fMRI session consisted of five parts. First, there was a resting state period of five minutes, followed by the first presentation of the weather report, then another resting state period, the second presentation of the weather report and finally a third resting state period. Before each part, the instructions were presented onto a back-projection screen that could be seen through a tilted mirror. Participants were instructed to close their eyes and relax during rest and to attentively watch and listen to the movie. A piece of music was played after five minutes of rest which indicated that the subjects could open their eyes. An eye tracker was used to verify that the eyes were closed during rest and open during presentation of the weather report. The sound level was adjusted for each participant individually at the start of the experiment to make sure they could hear the movie sound against the background scanner noise. After the fMRI session, subjects performed the auditory word recognition task for which they were asked to answer as accurately as possible.

## 2.4 Behavioural data analysis

Participants were divided into two groups based on their performance on the word recognition task. Performance was assessed according to signal detection theory, which takes response bias into account (Macmillan & Creelman, 2005). The D-prime, which is the difference between the normalized hit and false alarm rate, was calculated. Subjects with a D-prime higher than 0.3 showed some sensitivity on the task and were included in the learners group. The participants with a D-prime between -0.3 and 0.3 formed the non-learners group because their scores indicate that they did not distinguish between target and filler words. If the D-prime was below -0.3, the subjects were excluded, since this suggests that they were sensitive to the stimuli but for unknown reasons rejected the target words on the task.

## 2.5 fMRI data analysis

### 2.5.1 Image acquisition

The fMRI data were acquired on a 3 Tesla Trio scanner (Siemens, Erlangen, Germany). A functional T2\* weighted EPI-BOLD sequence was used with the following parameters: TE = 30 ms, TR = 1350 ms, flip angle = 67°, number of slices = 21, interleaved acquisition order, voxel size = 3.5 x 3.5 x 4.0, bandwidth = 1906 Hz/pixel.

### 2.5.2 Preprocessing

Preprocessing of the functional data was carried out using SPM5 ([www.fil.ion.ucl.ac.uk/spm](http://www.fil.ion.ucl.ac.uk/spm)). The images were realigned and normalized to the EPI template. No spatial smoothing was performed. Temporal filtering was applied by using a band pass Butterworth filter with frequency borders between 0.01 and 0.08 Hz.

### 2.5.3 Partial correlation analysis

We used a resting state toolbox (in-house software) in MATLAB (The MathWorks, Inc., Natick, MA) to carry out a whole brain partial correlation analysis based on the method of Salvador et al. (2005). This provides correlation coefficient values between pairs of regions with contributions of other areas cancelled out. The regions that were included in the analysis were defined by the AAL template, consisting of 116 areas (Tzourio-Mazoyer et al.,

2002). For our purposes, the superior and middle temporal gyri in both hemispheres were divided into a posterior third and an anterior two-third. This was done because the posterior parts of these areas in the left hemisphere are known to play an important role in receptive language processing. Hence, the template we used contained 120 regions and we assessed partial correlations between the six regions of interest and all other areas. Our regions of interest were the following: the pars opercularis of the left inferior frontal gyrus, the left supplementary motor area, the left insula, the left supramarginal gyrus, the left posterior superior temporal gyrus and the left posterior middle temporal gyrus.

During the first, second and third resting state periods, the time course of each region in the template was extracted for every subject. Based on this, a sample covariance matrix was constructed which was rescaled to form a partial correlation matrix. Fisher's r to z transformation was carried out to improve normality. At the group level, multiple one sample t-tests ( $p < 0.05$ , FDR corrected) were performed to find partial correlations that were significantly different from zero. For ten region pairs that were significant in the last resting state period, further tests were conducted.

An overall mixed ANOVA ( $p < 0.05$ ) with within-subject factors region pair (1 - 10), period (1, 2, 3) and between-subject factor group (learners, non-learners) was conducted to test for an interaction effect. For all region pairs, a post-hoc one-sided independent samples t-test ( $p < 0.05$ ) was carried out to see whether learners showed stronger functional connectivity compared to non-learners during any of the resting state periods.

**Table 1.** The ten region pairs which were significantly different from zero during the third resting state period. Mean partial correlation coefficients (pcc, z-transformed values) for the entire group are shown for the first resting state period (rs 1), the second resting state period (rs 2) and third resting state period (rs 3).

region 1	region 2	pcc rs 1	pcc rs 2	pcc rs 3
frontal_inf_oper_l	frontal_inf_tri_l	0.31	0.28	0.30
supp_motor_area_l	precentral_l	0.18	0.17	0.21
supp_motor_area_l	supp_motor_area_r	0.38	0.40	0.39
insula_l	frontal_inf_orb_l	0.06	0.09	0.18
insula_l	rolandic_oper_l	0.18	0.13	0.20
insula_l	insula_r	0.31	0.29	0.32
supramarginal_l	supramarginal_r	0.40	0.35	0.48
temporal_sup_post_l	temporal_sup_post_r	0.30	0.29	0.31
temporal_mid_post_l	temporal_mid_ant_l	0.23	0.25	0.22
temporal_mid_post_l	temporal_mid_post_r	0.31	0.28	0.33

### 3. Results

#### 3.1 Behavioural results

Three subjects were excluded because their D-prime value was below -0.3. Fourteen subjects had a D-prime above 0.3 and seventeen scored between -0.3 and 0.3. The participants that scored around zero were included in the non-learners group and those that scored above 0.3 formed the learners group. The mean D-prime of the learners was 0.52 and that of the non-learners was -0.03.

#### 3.2 fMRI results

The ten region pairs that were significantly different from zero during the third resting state period are displayed in Table 1. Results of the overall mixed ANOVA ( $p < 0.05$ ) with within-subject factors region pair (1 - 10), period (1, 2, 3) and the between-subject factor group (learners, non-learners) showed a significant region pair \* period \* group interaction ( $F = 4.26, p < 0.05$ ).

Further post-hoc tests revealed that during the first resting state period, the partial correlation between the left supplementary motor area and the left precentral region was significantly higher for the learners than for the non-learners (mean learners = 0.29, mean non-learners = 0.09,  $t(29) = 3.38, p < 0.05$ ). There was also a significant difference between the groups for the region pair consisting of the left insula and left rolandic operculum (mean learners = 0.28, mean non-learners = 0.11,  $t(29) = 2.63, p < 0.05$ ). These results are visualized in Figure 1. No other

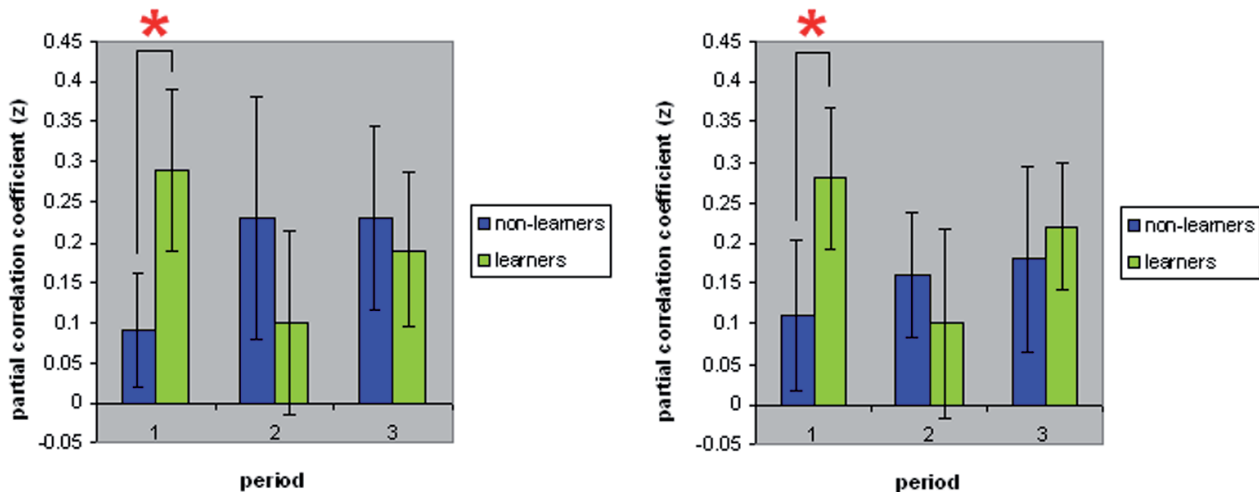


**Figure 1.** Partial correlation coefficients (z-transformed values) for region pairs that showed stronger functional connectivity for the learners compared to the non-learners during the first resting state period. Left: Partial correlation coefficients for the left supplementary motor area and the left precentral gyrus which showed a significant difference between the two groups ( $t(29) = 3.38, p < 0.05$ ). Right: Partial correlation coefficients between the left insula and left rolandic operculum which were also significantly different ( $t(29) = 2.63, p < 0.05$ ). Error bars  $\pm 2$  SE are shown.

pairs showed differences between the groups in the first resting state period. During the second resting state period, there were no significant differences between learners and non-learners for any of the region pairs.

During the third resting state period, the partial correlation between two regions, namely the left and right supramarginal gyrus, was stronger for learners compared to non-learners (mean learners = 0.55, mean non-learners = 0.41,  $t(29) = 1.81, p < 0.05$ ). This is shown in Figure 2. Partial correlations of other region pairs did not differ significantly between the two groups.

## 4. Discussion

In the current exploratory study we investigated differences in resting state functional connectivity between learners and non-learners of novel words. After exposure to a new language, we expected stronger functional connectivity between regions involved in phonological processing for learners, who were able to segment and recognize phonological information from a continuous speech stream, compared to non-learners. In addition, we tested whether pre-existing differences between the two groups could be observed during rest before natural language input.

A partial correlation analysis was performed for six regions of interest that are known to play a role in phonological processing, namely the left inferior frontal opercular region, the left supplementary motor area, the left insula, the left supramarginal gyrus, the left posterior superior temporal gyrus and the left posterior middle temporal gyrus. For these regions, significant partial correlations were found with neighboring areas, their right hemisphere homologues or regions with a similar function.

During the first resting state period, the left supplementary motor area and left precentral gyrus showed stronger functional connectivity for learners compared to non-learners. The left supplementary motor area is important for phonological rehearsal (Paulesu et al., 1993; Smith et al., 1998) and the left precentral gyrus is involved in articulation of speech, since a lesion of this area produces Broca's aphasia (Mori, Yamadori, & Furumoto, 1989).

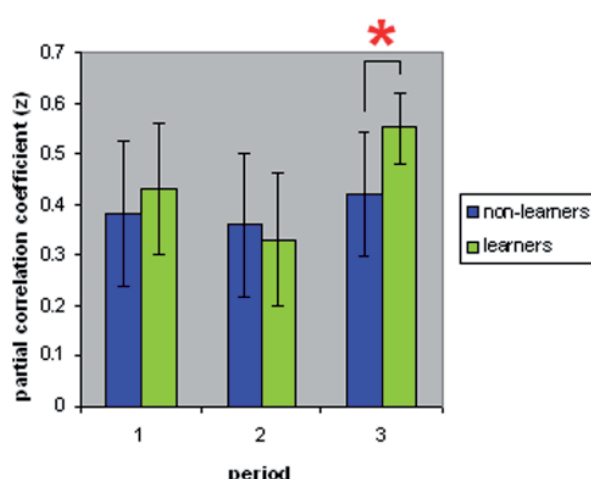


**Figure 2.** Partial correlation coefficients (z-transformed values) between the left and right supramarginal gyrus. Stronger functional connectivity was observed for learners compared to non-learners in the third resting state period ( $t(29) = 1.81, p < 0.05$ ). Error bars  $\pm 2$  SE are shown.

Stronger functional connectivity for learners was also observed between the left insula and the left rolandic operculum. The left rolandic operculum plays a role in speech production, as demonstrated by the finding that lesions of this area are associated with articulatory disorders (Tonkonogy, 1981). The left insula appears to contribute to planning (Dronkers, 1996) or execution of speech (Ackermann & Riecker, 2004). The involvement of the left insula in phonological recognition of words has also been previously shown (Bamiou et al., 2003). Chee et al. (2004) found activation of this region during a phonological working memory task which was greater for balanced than for unbalanced bilinguals.

In summary, although these areas have multiple functions, with respect to language they seem to be predominantly involved in articulation and phonological rehearsal. One possible interpretation might thus be that learners and non-learners differed with respect to the involvement of the speech motor system during perception. However, the aforementioned region pairs showed a dissociation between learners and non-learners only before presentation of the Chinese weather report. Stronger functional connectivity between these areas, and hence possibly an increased readiness for speech motor activation, may thus rather be considered a favorable disposition for the processing of the unknown language input. Note that functional connectivity of these areas was no longer significantly different between the two groups in the second and third resting state periods, i.e. after exposure to the unknown language. This was partly due to an increase in connectivity strength for the non-learners suggesting that also in this group there was motor involvement during speech perception.

One pair of regions, the left supramarginal gyrus and right supramarginal gyrus, showed stronger functional connectivity during the last resting state period for the learners compared to the non-learners. The correlation between these areas was similar for the two groups during the first and second resting state periods. This suggests that there were no pre-existing differences between the learners and non-learners with respect to this region pair, so the stronger functional connectivity is related to exposure to the movie. Our finding that the left and right supramarginal gyrus are the only areas which show stronger functional connectivity for learners after language exposure is consistent with the role of the left supramarginal gyrus as a phonological store (Paulesu et al.; 1993; Smith et al., 1998). However, Clark and Wagner (2003) have provided evidence for the engagement of the left inferior prefrontal cortex

instead of the parietal cortex in encoding novel words into long-term memory.

The interpretation of our result is in accordance with the study by Waites et al. (2005) who found increased functional connectivity during rest after a language task for those areas that were involved in the task. These results indicate that in the resting state, cognitive processing occurs which reflects prior input. This adds to the findings of others who observed increases in connectivity during a task that were related to associative learning (Büchel et al., 1999; McIntosh et al., 1999; Toni et al., 2002). Inverse correlations between areas involved in a function and the posterior cingulate, a region of the default mode network, have previously been demonstrated (Greicius et al., 2003). We did not find such inverse correlations with the phonological areas that were investigated in the current experiment.

There seems to be considerable inter-subject variability in partial correlation values as evident by the large standard deviations in our data. This could explain why we did not get more significant findings. Therefore, one should be cautious when interpreting absence of differences in functional connectivity. We can not exclude that other areas are also involved in learning novel words.

Another important point to note here is that our behavioural scores were lower than those observed by Gullberg et al. (in prep). Although we made sure that the participants were able to hear the movie sound, it is likely that there was some interference from the scanner noise. Thus, our results give a too pessimistic view on how much can be learned during first exposure to a new language. The behavioural results of our experiment indicated small differences between learners and non-learners. If the scores on the word recognition task would have been better separated, we might have found more differences in functional connectivity.

To conclude, the current study provides some evidence for differences in functional connectivity between learners and non-learners of a phonological word recognition task. Additional research is needed to elucidate the effect of task-related activity on functional connectivity during rest. Nonetheless, it was shown here that investigating functional connectivity between different regions can be a useful method when there is no pre-specified design for an experiment, as in the case of naturalistic stimuli. Data-driven techniques provide additional information on how brain regions work together and therefore can complement traditional fMRI research.

## Acknowledgements

I would like to thank David Norris and Peter Indefrey for their supervision. I am also grateful for the support of the MR-methods group and the Multilingualism group, with special thanks to Paul Gaalman, Elena Shumskaya, Huadong Xiang and Frauke Hellwig.

## References

- Ackermann, H., & Riecker, A. (2004). The contribution of the insula to motor aspects of speech production: a review and a hypothesis. *Brain Lang*, 89(2), 320-328.
- Baddeley, A., Gathercole, S., & Papagno, C. (1998). The phonological loop as a language learning device. *Psychol Rev*, 105(1), 158-173.
- Baddeley, A. D. (1986). Working memory. Oxford, England: Oxford University Press.
- Bamiou, D. E., Musiek, F. E., & Luxon, L. M. (2003). The insula (Island of Reil) and its role in auditory processing. Literature review. *Brain Res Brain Res Rev*, 42(2), 143-154.
- Birn, R. M., Diamond, J. B., Smith, M. A., & Bandettini, P. A. (2006). Separating respiratory-variation-related fluctuations from neuronal-activity-related fluctuations in fMRI. *Neuroimage*, 31(4), 1536-1548.
- Biswal, B., Yetkin, F. Z., Haughton, V. M., & Hyde, J. S. (1995). Functional connectivity in the motor cortex of resting human brain using echo-planar MRI. *Magn Reson Med*, 34(4), 537-541.
- Breitenstein, C., Jansen, A., Deppe, M., Foerster, A. F., Sommer, J., Wolbers, T. (2005). Hippocampus activity differentiates good from poor learners of a novel lexicon. *Neuroimage*, 25(3), 958-968.
- Breitenstein, C., & Knecht, S. (2002). Development and validation of a language learning model for behavioral and functional-imaging studies. *J Neurosci Methods*, 114(2), 173-179.
- Büchel, C., Coull, J. T., & Friston, K. J. (1999). The predictive value of changes in effective connectivity for human learning. *Science*, 283(5407), 1538-1541.
- Chee, M. W., Soon, C. S., Lee, H. L., & Pallier, C. (2004). Left insula activation: a marker for language attainment in bilinguals. *Proc Natl Acad Sci U S A*, 101(42), 15265-15270.
- Cherkassky, V. L., Kana, R. K., Keller, T. A., & Just, M. A. (2006). Functional connectivity in a baseline resting-state network in autism. *Neuroreport*, 17(16), 1687-1690.
- Clark, D., & Wagner, A. D. (2003). Assembling and encoding word representations: fMRI subsequent memory effects implicate a role for phonological control. *Neuropsychologia*, 41(3), 304-317.
- Cordes, D., Haughton, V. M., Arfanakis, K., Wendt, G. J., Turski, P. A., Moritz, C. H., et al. (2000). Mapping functionally related regions of brain with functional connectivity MR imaging. *AJNR Am J Neuroradiol*, 21(9), 1636-1644.
- Damoiseaux, J. S., Rombouts, S. A., Barkhof, F., Scheltens, P., Stam, C. J., Smith, S. M., et al. (2006). Consistent resting-state networks across healthy subjects. *Proc Natl Acad Sci U S A*, 103(37), 13848-13853.
- Dronkers, N. F. (1996). A new brain region for coordinating speech articulation. *Nature*, 384(6605), 159-161.
- Friston, K. J., Frith, C. D., Liddle, P. F., & Frackowiak, R. S. (1993). Functional connectivity: the principal-component analysis of large (PET) data sets. *J Cereb Blood Flow Metab*, 13(1), 5-14.
- Golestani, N., Molko, N., Dehaene, S., LeBihan, D., & Pallier, C. (2007). Brain structure predicts the learning of foreign speech sounds. *Cereb Cortex*, 17(3), 575-582.
- Greicius, M. D., Krasnow, B., Reiss, A. L., & Menon, V. (2003). Functional connectivity in the resting brain: a network analysis of the default mode hypothesis. *Proc Natl Acad Sci U S A*, 100(1), 253-258.
- Gullberg, M., & Indefrey, P. (2003). Language Background Questionnaire. Developed in The Dynamics of Multilingual Processing. Nijmegen, Max Planck Institute for Psycholinguistics.
- Gullberg, M., Dimroth, C., Roberts, L., & Indefrey, P. (in prep.). What lexical knowledge can adult learners acquire after minimal exposure to a new language?
- Hampson, M., Peterson, B. S., Skudlarski, P., Gatenby, J. C., & Gore, J. C. (2002). Detection of functional connectivity using temporal correlations in MR images. *Hum Brain Mapp*, 15(4), 247-262.
- Lee, H., Devlin, J. T., Shakeshaft, C., Stewart, L. H., Brennan, A., Glensman, J., et al. (2007). Anatomical traces of vocabulary acquisition in the adolescent brain. *J Neurosci*, 27(5), 1184-1189.
- Liang, M., Zhou, Y., Jiang, T., Liu, Z., Tian, L., Liu, H., et al. (2006). Widespread functional connectivity in schizophrenia with resting-state functional magnetic resonance imaging. *Neuroreport*, 17(2), 209-213.
- Lowe, M. J., Mock, B. J., & Sorenson, J. A. (1998). Functional connectivity in single and multislice echoplanar imaging using resting-state fluctuations. *Neuroimage*, 7(2), 119-132.
- Macmillan, N. A., & Creelman, C.D. (2005). Detection Theory: A User's Guide (2 ed.). Mahwah, NJ: Lawrence Erlbaum Associates.
- McIntosh, A. R., Rajah, M. N., & Lobaugh, N. J. (1999). Interactions of prefrontal cortex in relation to awareness in sensory learning. *Science*, 284(5419), 1531-1533.
- Mei, L., Chen, C., Xue, G., He, Q., Li, T., Xue, F., et al. (2008). Neural predictors of auditory word learning. *Neuroreport*, 19(2), 215-219.

- Mori, E., Yamadori, A., & Furumoto, M. (1989). Left precentral gyrus and Broca's aphasia: a clinicopathologic study. *Neurology*, 39(1), 51-54.
- Paulesu, E., Frith, C. D., & Frackowiak, R. S. (1993). The neural correlates of the verbal component of working memory. *Nature*, 362(6418), 342-345.
- Raichle, M. E., MacLeod, A. M., Snyder, A. Z., Powers, W. J., Gusnard, D. A., & Shulman, G. L. (2001). A default mode of brain function. *Proc Natl Acad Sci U S A*, 98(2), 676-682.
- Salvador, R., Suckling, J., Coleman, M. R., Pickard, J. D., Menon, D., & Bullmore, E. (2005). Neurophysiological architecture of functional magnetic resonance images of human brain. *Cereb Cortex*, 15(9), 1332-1342.
- Smith, E. E., Jonides, J., Marshuetz, C., & Koeppe, R. A. (1998). Components of verbal working memory: evidence from neuroimaging. *Proc Natl Acad Sci U S A*, 95(3), 876-882.
- Tian, L., Jiang, T., Wang, Y., Zang, Y., He, Y., Liang, M., et al. (2006). Altered resting-state functional connectivity patterns of anterior cingulate cortex in adolescents with attention deficit hyperactivity disorder. *Neurosci Lett*, 400(1-2), 39-43.
- Toni, I., Rowe, J., Stephan, K. E., & Passingham, R. E. (2002). Changes of cortico-striatal effective connectivity during visuomotor learning. *Cereb Cortex*, 12(10), 1040-1047.
- Tonkonogy, J., & Goodglass, H. (1981). Language function, foot of the third frontal gyrus, and rolandic operculum. *Arch Neurol*, 38(8), 486-490.
- Tzourio-Mazoyer, N., Landeau, B., Papathanassiou, D., Crivello, F., Etard, O., Delcroix, N., et al. (2002). Automated anatomical labeling of activations in SPM using a macroscopic anatomical parcellation of the MNI MRI single-subject brain. *Neuroimage*, 15(1), 273-289.
- Waites, A. B., Stanislavsky, A., Abbott, D. F., & Jackson, G. D. (2005). Effect of prior cognitive state on resting state networks measured with functional connectivity. *Hum Brain Mapp*, 24(1), 59-68.
- Wong, P. C., Perrachione, T. K., & Parrish, T. B. (2007). Neural characteristics of successful and less successful speech and word learning in adults. *Hum Brain Mapp*, 28(10), 995-1006.

## Abstracts web articles

Nijmegen CNS committed to publish all submitted theses. However, due to the number of submissions, we make a selection based on the recommendations by the editors. As a special service to the interested reader, we provide the abstracts of the articles that are published only in the online version on the following pages. The full versions of these articles are available at our web-site <http://www.ru.nl/master/cns/journal>.

### **Noise tagging as a new auditory BCI-paradigm: A pilot study**

J. Blankespoor, J. Farquhar, P. Desain, S. Gielen

Brain Computer Interfaces (BCI) are intended to translate brain activity into computer actions without intervention of any bodily movements. The main challenge in constructing a BCI involves reliable signal detection to be used for single trial classification. In this paper, we focus on developing a BCI using selective auditory attention. Frequency tagging is a way of watermarking a carrier tone, by means of amplitude modulation, and results in an auditory steady state response (ASSR). This paper investigates the use of a novel stimulus type for an auditory BCI paradigm using pseudo-noise codes as amplitude modulators, called noise tagging. This paper's main hypothesis is that noise tagging offers a more robust signal detectability than frequency tagging, which is used as the control condition. Two experimental conditions were used: perceptual and attentional. The experimental results confirmed that the noise tagged stimuli could be extracted successfully from the EEG signal on a single trial basis in the perceptual condition, with averaged performances of 79 %. In the parallel attentional condition the classification results were not consistent across subjects, but comparable to the results of frequency tagging; highest classification results were around 70 %. Some suggestions for improvement will be discussed.

### **The role of cocaine- and amphetamine-regulated transcript and nesfatin-1 in the non-preganglionic Edinger-Westphal nucleus in stress adaptation and suicide**

B. Bloem, L. Xu, B. Gaszner, G. Faludi, M. Palkovits, T. Kozicz, E. Roubos

Adaptation to our ever changing environment is a biological necessity to maintain physical and mental health. Failed adaptation to stress, however, often leads to the development of stress-induced psychopathologies, such as anxiety and major depression. The non-preganglionic Edinger-Westphal nucleus (npEW) and its urocortin 1 (Ucn1)-containing neurons have previously been implicated in stress adaptation. However, these neurons also contain other neuropeptides, such as cocaine- and amphetamine-regulated transcript (CART) and nesfatin-1. CART has been associated with the stress response and appetite regulation whereas nesfatin-1 seems to have anorexigenic properties. This study tested whether CART and nesfatin-1 in the npEW are colocalized with Ucn1 and whether they are involved in stress adaptation, in a gender-specific way. This hypothesis was first tested in rats exposed to acute restraint stress and to chronic variable mild stress. Second, we tested if stress-induced alterations in CART and nesfatin-1 expression could underpin psychopathology seen in major depression, so we analyzed the expression of CART and nesfatin mRNA in discrete microdissected postmortem rostral ventral midbrain samples containing the npEW nucleus of depressed suicide victims. Our results demonstrate that Ucn1, CART and nesfatin-1 are colocalized to a high degree in the npEW and that these neurons are recruited during acute and chronic stress, as shown using immunohistochemistry for cFos. Second, we showed that in rats the levels of mRNA coding for CART and nesfatin-1 remain equal, whereas the peptide levels in the npEW neurons increase, in particular in the situation of chronic stress. These results show that the secretory activity of the npEW neurons containing CART and nesfatin-1 is changed response to acute and chronic stress. Our data from human postmortem microdissected ventral midbrains containing the npEW revealed that depressed suicide victims of both sexes had a significant 4.7X increase in mRNA coding for CART, whereas only male suicide victims had a 1.8X increase in RNA coding for nesfatin. In conclusion, we showed the involvement of CART and nesfatin-1 in stress adaptation response and identified dysregulated expression of CART and nesfatin-1 mRNAs in the npEW of major depressed subjects who committed suicide. These data can contribute to further elucidation of the molecular alterations of stress-induced brain diseases like major depression.

## **Repetition, repair and alignment in natural dialogue**

M. van Dienst, J. P. de Ruiter

The processing of common ground in human dialogue is controversial. Whereas some dialogue models suggest that taking into account common ground is necessary for successful dialogue, other models suggest that common ground is not used in dialogue at all. One of these is the Interactive Alignment Account by Pickering and Garrod (2004), which suggests that only ‘implicit common ground’ is built up and maintained automatically through the processes of priming, percolation and interactive repair. In this study, these three processes and their predictions are tested using both quantitative and qualitative analyses. The results show that natural conversational data do not support the Interactive Alignment Account. Furthermore, the data suggest that repetitions in natural dialogues are mainly used by speakers to display their knowledge of the topic of the conversation.

## **Two-photon excitation microscopy as a research tool for the analysis of the effect of Taxol on axonal transport velocity and microtubular density in SH-SY5Y cells**

S.R. van Eck, J.G. Veening, R.F. De Jongh, R.M. Nuydens, J. van Egmond, K.C.P. Vissers, T.F. Meert

The cytostatic drug Taxol can induce peripheral neuropathy, and recent studies suggest that axonal transport is affected in the process. Our study aims to clarify whether Taxol indeed affects axonal transport, by investigating in vitro the effects of Taxol on axonal transport velocity of mitochondria in a human neuroblastoma cell line. The method of choice is two-photon excitation microscopy, since this promising method has not been applied to this type of study often. Immunocytochemistry was used for investigating the effect of Taxol on microtubule density. In our first experiment, we used a 2-PE microscope to make multi-time series of SH-SY5Y cells in vitro, of which the mitochondria were labeled with a fluorescent marker. The cells were cultured in two different media, treated with various Taxol concentrations, for various periods of time. In the second experiment, SH-SY5Y cells were cultured and treated as in the first experiment, but now tubulin was labeled, and after cell fixation, cells were imaged using a confocal microscope. We determined density of axonal microtubuli by measuring pixel intensity. We found that not Taxol, but only culture medium has an effect on axonal transport velocity of mitochondria. With the proper settings, 2-PE microscopy seems a suitable tool to analyze axonal transport, but it still has some limitations. Our second experiment revealed no effect of Taxol on microtubule density. Our hypothesis on the effect of Taxol on axonal transport velocity was not confirmed. The effect of culture medium could be explained by specific medium additives such as fetal calf serum and B27. Resolving technical limitations of 2-PE microscopy may result in more exact measurements. The effect of Taxol on microtubule density was also not confirmed.

## **The time course of word-form encoding in second language word production: An ERP study**

J. Hamulová, P. Indefrey, D. J. Davidson

When naming pictures in their second language, even proficient L2 speakers generally initiate articulation later than in their L1 (Christoffels, De Groot, & Kroll, 2006). In an electrophysiological study employing the N200 and LRP event related potentials, we investigated whether or not this difference is due to the later accessibility of the L2 word-form. Proficient Dutch-English bilinguals silently named pictures, on which they first performed a dual-choice, go/no-go manual task based on a semantic (man-made/natural) and a phonological (is the first phoneme an “s” or not?) binary decision (van Turennout, Hagoort, & Brown, 1997; Rodriquez-Fornells et al., 2005). In both languages, the N200 and LRP developed earlier when elicited by the semantic decision rather than the phonological decision. We did not find consistent evidence that the duration of word-form encoding differs in the two languages of a bilingual. On the basis of these findings, we suggest that the L2 word-form retrieval is only slower at post-lexical stages of word production. Furthermore, when the phonological decision in the L2 was congruent with the L1 decision, both go and no-go waveforms were more negative (between 300 and 600 ms post-stimulus) than when the two decisions were incongruent, suggesting automatic activation of L1 phonology in L2 naming.

## **Reading Comprehension in flemish deaf children: Exploring the sources of variability in reading comprehension after cochlear implantation**

A. van der Kant, A. Vermeulen, R. Schreuder, L. De Raeve

Recent data on reading comprehension in deaf children have shown a large delay for those without a cochlear implant (CI) and better reading comprehension, although still a little delayed compared to their normal hearing peers, for deaf children fitted with a CI. Some light has been shed on possible causes of the delay and the discrepancy between CI users and non CI users, but the picture is far from complete. In the present study we investigated reading comprehension in 74 Flemish deaf children of which 44 are fitted with a cochlear implant. First, the level of reading comprehension was determined for both CI users and non CI users. Additionally, good and poor readers with cochlear implants were contrasted on phonological encoding during reading, morphosyntactic skills and a number of working memory measures. Flemish deaf children perform significantly better on reading comprehension than Dutch deaf children and overall children with cochlear implants perform better than children without. Phonological encoding cannot dissociate between good and poor readers like in hearing children. In contrast, a dissociation is observed in the morphosyntactic skills and working memory capacity. Additionally, age of implantation effects are found.

## **Schema-dependent hippocampo-prefrontal connectivity during memory encoding and post-encoding rest in humans**

M. T. R. van Kesteren, G. Fernández, D. G. Norris, E. J. Hermans

Integrating novel information into neocortical representations is proposed to involve a process in which the ventromedial prefrontal cortex (vmPFC) progressively takes over the integrative function of the hippocampus. This process of systems consolidation is thought to be promoted by sleep and mediated by replay of memory-related spiking activity in hippocampo-cortical networks. However, recent studies suggest that systems consolidation already initiates during resting periods subsequent to encoding, and may accelerate when novel information better fits the present cortical network, or schema. Recent evidence thus implies a faster, earlier, and more context-dependent nature of systems consolidation mechanisms, possibly dependent on hippocampal-vmPFC transfer. Since the role of hippocampal-vmPFC connectivity during this process is largely unknown, we explored the influence of prior schema on hippocampal-vmPFC connectivity and intersubject synchronization in vmPFC during memory encoding and post-encoding rest. We manipulated prior schema comprehension by presenting the first part of a movie in either the correct (schema) or temporally scrambled (non-schema) order. Then, participants were scanned using fMRI while watching the last, temporally correct part of the movie (encoding). Subsequently, they performed memory tests interleaved by a post-encoding resting period. Schema manipulation was successful while item recognition and memory performance regarding the last part of the movie was equal for both groups. During movie viewing, the non-schema group showed significantly stronger hippocampal-vmPFC connectivity, which furthermore correlated negatively with initial schema comprehension. This effect persisted during rest. Additionally, intersubject synchronization in the vmPFC was higher for the schema group during encoding. These results show that stronger prior schema is associated with more vmPFC synchronization and less hippocampal-vmPFC connectivity during encoding, suggesting that additional connectivity is recruited to compensate for difficulty integrating novel information into neocortical networks. Since this effect persists during rest, this study highlights the potential role of hippocampal-vmPFC crosstalk in early stages of memory integration.

## Cerebral control of motor imagery of gait in Parkinson's disease patients

I. Leunissen, M. Bakker, S. Overeem, I. Toni, B. R. Bloem

The neural mechanisms and circuitry underlying gait problems in Parkinson's disease (PD) remain largely unclear. Here, we aimed at identifying those portions of the motor system supporting gait that are altered in PD patients. More specifically, motor imagery was used as a tool to investigate alterations in neural activity related to planning of gait in PD. We recorded cerebral activity with functional magnetic resonance imaging in 19 PD patients and 21 matched healthy controls. Subjects were instructed to perform a previously validated protocol including a motor imagery of gait task and a matched visual imagery task. We objectively monitored task performance by examining the effects of motor imagery of walking on supports of different width and length on imagery times, and by recording electromyography during scanning. In addition, actual gait parameters were quantified using an electronic pressure-sensitive walkway. During actual walking, patients had a smaller step length than controls. During imagery of walking, patients and controls were equally sensitive to the constraints associated with walking on supports of different width and length. Cerebrally, PD patients showed a relative decrease in motor imagery-related activity in the bilateral supplementary motor area (SMA), in the superior parietal lobule, and in cerebellar lobule IV, as well as a relative increase in the mesencephalic locomotor region. Furthermore, SMA activity was positively correlated with step length, as measured during actual walking. These findings indicate that, in PD patients, both fronto-striatal and parieto-cerebellar circuits fail to support gait-related control mechanisms, while emphasizing altered responses of brainstem locomotor centres in PD. It remains to be seen whether these altered brainstem responses compensate for, or exacerbate gait disturbances in PD.

## Imagined hand tapping: A time-locked paradigm for Brain-Computer Interfaces

M. Lijster, J. Geuze, P. Desain, S. Gielen

Brain-Computer Interfaces (BCIs) can greatly improve the quality of life of 'locked-in' patients, since such a system controls an external device without muscle activity. In present day BCIs, EEG is predominantly used as a recording technique to register brain activity and the most widely used brain signals are sensorimotor rhythms, which can be modulated by imagining movements of hands, feet or tongue. One problem in developing a BCI is the need for prolonged training, which might be reduced by introducing a time-lock to the mental imagery. In the present study, participants imagined hand tapping time-locked to an auditory stimulus. We investigated whether this paradigm could work in a BCI. The experiment consisted of a training session, after which kernel logistic regression determined classification parameters. These were used in a test session, in which the participants received auditory feedback on their performance. In an actual movement pilot, one subject showed an alternating pattern of ERS and ERD in accordance to the alternation of rest and movement and performed with a classification rate of 87 % ( $p < 0.0001$ ) on the training session. In the test session, the performances were 54 % (n.s.), 77 % ( $p < 0.0001$ ), 80 % ( $p < 0.0001$ ) and 74 % ( $p < 0.0001$ ) over blocks. This subject did not show any significant classification rates on imagined movement, whereas another subject did, i.e. 58 % ( $p = 0.0003$ ) in the training session. Two subjects did not show any significant results and were excluded from analysis. The current data do not convincingly show that time-locked imaginary hand tapping works as a paradigm for BCI. Future work should focus on selection of classes, selection of frequency bands, using spatial filters and optimizing the auditory feedback or switching to visual feedback.

## Using multimodal frequency tagging for BCI

I. H. S. Mischner, R. S. Schaefer, S. Gielen, P. Desain

Stimuli that are presented with a constant frequency elicit responses in the brain that oscillate at that same frequency, also known as steady-state responses (SSRs). SSRs promise to be useful brain patterns for brain computer interfaces (BCI), because their amplitudes can be modulated by attention. However, signal-to-noise ratios are relatively low, and stronger brain signals are needed to increase performances. Previous research on crossmodal amplification has demonstrated that stimulation in one modality can amplify brain signals elicited by stimulation in another modality, thereby yielding stronger signals. To investigate the possibilities of crossmodal amplification for use in BCIsystems, an offline EEG experiment based on a frequency-tagging paradigm was carried out, with stimuli presented in three modality condition: an auditory, tactile and audiotactile condition. Frequency tags were 20 and 28 Hz. Stimuli were either presented to one side of the body (passive perception condition) or to both sides, and the participant had to focus attention on one side of his body (selective attention condition). To ensure attention, small time interruptions (phase shifts) were added to the streams, and the participant was instructed to count the number of interruptions at the attended side. Evoked power at the tagging frequencies was then used to make a comparison between the different modalities. The results do not support the added value of combining auditory and tactile stimulation when making use of the effect of attention on the steady-state response to generate brain signals that may drive a BCI-system.

## Virtual lesions of the inferior frontal gyrus abolish imitative response facilitation

S. Ondobaka, R. Newman-Norlund, H. Bekkering

Data from numerous experiments suggest that humans are faster to perform a given action following observation of that same action. Currently, it is unclear whether the underlying mechanism behind this effect is best explained by specialist or generalist theories of imitation. The two opposing views make different predictions about the processes underlying this imitative facilitation effect. Specialist accounts predict a specific role for pars opercularis in matching biological stimuli to the subsequent responses, whereas generalist accounts predict a more general role in stimulus-response (S-R) matching for this area. In the present study, we investigated this issue by disrupting the left and right dorsal pars opercularis, a site thought critical to the phenomenon of imitative facilitation, during the preparation of congruent (imitative) and incongruent (complementary) actions which were cued by either biological (hand) or non-biological (static dot) stimuli. Delivery of TMS to dorsal pars opercularis, but not to TMS control sites, abolished the advantage in reaction times for congruent stimuli. Importantly, this pattern was identical regardless of whether actions were cued by biological or non-biological stimuli. This finding argues in favor of a generalist interpretation of imitative facilitation effects and stresses the notion of the dorsal pars opercularis as a vital centre of general perception-action coupling in the human brain. A new model for general perception-action coupling is proposed in an attempt to unify specialist and generalist accounts of imitative facilitation.

**They know what you feel:  
Increased activity in Theory of Mind related brain regions in violent  
paranoid schizophrenia with comorbid diagnoses**

C. M. Pawliczek, B. Schiffer, I. Tendolkar

A possible underlying factor influencing the relationship between violence and schizophrenia is Theory of Mind (ToM). In order to investigate ToM functioning in violent offenders with schizophrenia and different histories of violence, violent schizophrenic offenders with comorbid diagnoses of antisocial personality disorder (APD) and substance abuse (SubAb) (Sz + APD + SubAb), schizophrenic offenders without comorbid diagnoses (Sz only) and healthy controls were compared on measures of violence and empathy and also on a ToM task using fMRI. It is hypothesized that the group with longer histories of violence (Sz + APD + SubAb) scores higher on measures of violence and lower on empathy compared to the other two groups. Further, this pattern is thought to be reflected in increased brain activation in ToM related brain networks in this group. Results showed increased activations in middle temporal and cingulate gyrus in the Sz + APD + SubAb group compared to the controls. Only one small cluster of higher activation in the middle temporal cortex was found comparing the Sz + APD + SubAb and the Sz only group. It was concluded that the Sz + APD + SubAb group seem to have a profile resembling psychopaths. It is important for them to have a well-functioning ToM in order to manipulate and deceit other people. Further, APD and substance abuse appear to prevent from cognitive and psychosocial dysfunction. The Sz only group seems to constitute a special group of schizophrenia subjects with better mentalizing abilities than non violent schizophrenics. However, due to the small sample sizes and the lack of important control groups the hypotheses and conclusions have to be regarded as preliminary.

**Analysis of the expression of promoter-specific transcripts of BDNF in *Xenopus*  
melanotropes during physiological adaptation**

B. A. de Ruyck, B. G. Jenks, R. P. H. Dirks, A. H. Kidane

This study concerns the regulation of promoter-specific brain-derived neurotrophic factor (BDNF) transcripts during background adaptation in the pituitary melanotrope cells of the amphibian *Xenopus laevis*. The *Xenopus* BDNF gene consists of six untranslated promoter-specific 5' exons, which are spliced to one 3'-protein coding exon, giving rise to at least seven different transcripts with two of these, transcript IV and VII 5' ext, being highly expressed in the melanotropes. In *Xenopus* adapted to a black background there is an increase in both intracellular Ca<sup>2+</sup> and cAMP to drive secretion of the proopiomelanocortin (POMC)-derived peptide α-melanophore stimulating hormone (α-MSH). This is accompanied by an increased production of both POMC mRNA and protein. However, the POMC promoter lacks any cAMP-responsive elements (CREs) or Ca<sup>2+</sup> responsive elements (CaREs) and is thus not regulated directly by cAMP and Ca<sup>2+</sup>. Remarkably, the promoter of BDNF transcript IV, which is dramatically upregulated in black-adapted animals, contains a CRE-like element and two CaREs. We hypothesize that BDNF IV is an effector gene for POMC, by activating intracellular pathways to affect POMC gene expression. To this end we have examined temporal aspects in the expression of POMC and BDNF transcripts during background adaptation and found that BDNF transcript IV expression precedes that of POMC. Furthermore, we established that a CRE-containing immediate early gene (IEG), c-Fos, is also induced before POMC. We propose that in *Xenopus* melanotropes intracellular cAMP and Ca<sup>2+</sup> signals act on the IEG c-Fos and probably on BDNF promoter IV to upregulate POMC expression. This study further shows that the upstream untranslated region (uUTR) of BDNF transcript IV attenuates translation of a downstream reporter gene when translated in a cap-dependent manner.

## **Enhanced secretory activity of midbrain Ucn1 neurons in two different mouse models with reduced alcohol consumption**

R. Shyti, T. Kozicz, E. W. Roubos

To date the neurocircuitry regulating alcohol consumption and dependence is not well understood. Several experimental studies have focused on the role of CRF peptide; however, recent studies also implicate another CRF-related neuropeptide, urocortin 1 (Ucn1) in alcohol consumption. Ucn1 is highly expressed in the nonpreganglionic Edinger-Westphal nucleus (npEW), and our group has previously shown that npEW Ucn1 is involved in various physiological responses including regulation and modulation of food consumption, stress adaptation and depression. In order to understand better the role of this neuropeptide in alcohol consumption and dependence, we used two different models: PKC-epsilon null mice and the chromosome 2 substitution strain (CSS-2) mice. Both lines voluntarily consume less ethanol, because they derive less reward from ethanol and are more sensitive to its aversive effects. Using fluorescence immunocytochemistry and *in situ* hybridization, we measured changes in the secretory activity of npEW Ucn1 neurons in these mice. Compared with wild type mice, PKC-epsilon null mice exhibited increased secretory activity of npEW Ucn1 neurons. Next we compared the secretory activity of npEW Ucn1 neurons between CSS-2 and C57BL/6J mice in a chronic alcohol consumption paradigm (they consumed alcohol for two hours a day for 3 weeks). FosB/deltaFosB immunocytochemistry revealed a similar activation in the npEW of CSS-2 and C57BL/6J mice in response to chronic alcohol consumption. For CSS-2 mice, however, the expression of npEW Ucn1 mRNA was significantly higher than in C57BL/6J mice. Our results further implicate Ucn1 in the modulation of consumption and responses to alcohol, and suggest that Ucn1 plays a role in the neuroadaptive changes driving excessive consumption of alcohol.

## **Non-native phonemes are open to native interpretation: A study on the flexibility of speech perception**

M. J. Sjerps, J. M. McQueen

Three experiments examined flexibility in speech perception. Experiment 1 examined whether Dutch listeners can learn to interpret a non-native phoneme (English [θ], as in 'bath') as an instance of a native category (Dutch [f] or [s]). During an initial exposure phase, two groups of listeners made lexical decisions to words and nonwords. Listeners heard [θ] replacing [f] in 20 [f]-final words (Group 1), or [θ] replacing [s] in 20 [s]-final words (Group 2). At test, using a cross-modal identity priming paradigm, participants were primed with e.g., [doθ], based on the minimal pair doof/doos (deaf/box), and made visual lexical decisions to e.g., doof and doos. Participants in Group 1 were faster on doof decisions after [doθ] than after an unrelated prime, while participants in Group 2 were faster on doos decisions: Participants had learned to interpret [θ] as either [f] or [s], depending on their initial training. Learning had not been hindered by the L2 status of [θ], as the effect was just as large when the exposure sound was an ambiguous digital [fs]-mixture (Experiment 2). Experiment 3 provided a benchmark for Experiment 1 and 2 by determining the size of the priming effect using the natural fricatives [f] and [s]. This priming effect was statistically indistinguishable from the effects obtained in Experiments 1 and 2, showing that learning of these items had been thorough. It can be concluded that perceptual learning in a native language is thorough, and can override years of second-language phonetic learning.

## Meaning mediates labelling effects on perceptual categorisation

A. van Stee, A. Majid

Can labels affect perceptual category learning? A variety of studies suggest a variety of answers, ranging from 'no, they cannot', to 'yes, labels facilitate category learning' to 'yes, labels are detrimental to category learning'. This study addresses the hypothesis that it is not the presence of labels per se that matters, but rather their meaningfulness. Specifically, it looks at an aspect of meaningfulness called referential accessibility, that is, the ease with which label and category can be connected. Referential accessibility of labels was manipulated in two experiments. Participants learned to categorize line drawings into two groups and during feedback, a nonsense label was presented to people in the label condition. When referential accessibility of labels was low, the presence of labels impaired categorization performance as compared to the no-label condition. When referential accessibility of labels was high, however, this effect disappeared. I conclude that the influence labels have on categorization depends crucially on their referential accessibility.

## Metabolic status modulates the activity of npEW-Ucn1 neurons in a gender specific way

L. Xu, B. G. E. W. Roubos, L. T. Kozicz

Urocortin 1 (Ucn1), most abundantly expressed in the non-preganglionic Edinger-Westphal nucleus (npEW), was first identified as an anorectic peptide. Recently, npEW-Ucn1 neurons have also been reported to play a role in stress adaptation. Furthermore, the npEW was found to contain other anorectic peptides, such as cocaine and amphetamine-regulated transcript (CART), cholecystokinin (CCK). One of the major peripheral signal with regard to energy homeostasis is leptin. It is secreted by adipose tissue and, acting through the leptin receptor, ObR. It increases energy expenditure, decreases food intake, and modulates body weight. Here we hypothesized that leptin would modulate the activity of npEW Ucn1 cells. To test this hypothesis, we have aimed at confirming the presence and identifying the type of ObR in Ucn1-containing neurons in the rat npEW, assessing the effect of fasting and intraperitoneal leptin injection on the activity of Ucn1 and whether this effect is gender-specific. Using RT-PCR, we demonstrated that both short (ObRa) and long forms (ObRb) of leptin receptor expressed in the npEW. Using immunocytochemistry, we showed that ObR occurred in npEW-Ucn1 neurons. Two days fasting caused a decreased activity of Ucn1 neurons in females, whereas in males, npEW-Ucn1 neurons seemed to be more active. After peripheral leptin injection, Ucn1 was significantly upregulated in male rats, but no difference was found in females. In this study we have provided evidence for the direct, gender specific regulation of the activity of Ucn1 neurons in the rat npEW by leptin, which may act as a regulatory link between the energy homeostasis and stress response.

## Institutes associated with the Master's Programme in Cognitive Neuroscience



Donders Institute for Brain, Cognition and Behaviour:  
Centre for Cognition  
Montessorilaan 3  
6525 HR Nijmegen

P.O. Box 9104  
6500 HB Nijmegen  
[www.ru.nl/cognition/](http://www.ru.nl/cognition/)



MAX-PLANCK-GESELLSCHAFT

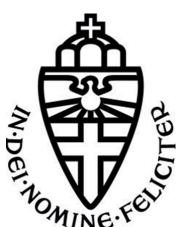
Max Planck Institute for Psycholinguistics  
Wundtlaan 1  
6525 XD Nijmegen

P.O. Box 310  
6500 AH Nijmegen  
<http://www.mpi.nl/>



Donders Institute for Brain, Cognition and Behaviour:  
Centre for Cognitive Neuroimaging  
Kapittelweg 29  
6525 EN Nijmegen

P.O. Box 9101  
6500 HB Nijmegen  
[www.ru.nl/neuroimaging/](http://www.ru.nl/neuroimaging/)



Radboud Universiteit Nijmegen  
Comeniuslaan 4  
6525 HP Nijmegen

P.O. Box 9102  
6500 HC Nijmegen  
<http://www.ru.nl/>



Donders Institute for Brain, Cognition and Behaviour:  
Centre for Neuroscience  
Geert Grootplein Noord 21, hp 126  
6525 EZ Nijmegen

P.O. Box 9101  
6500 HE Nijmegen  
[www.ru.nl/neuroscience/](http://www.ru.nl/neuroscience/)



Universitair Medisch Centrum St Radboud  
Geert Grootplein-Zuid 10  
6525 GA Nijmegen

P.O. Box 9101  
6500 HB Nijmegen  
<http://www.umcn.nl/>

